National Library of Canada
Canadian Theses Service
Ottawa, Canada
K1A 0N4

Bibliothèque nationale du Canada
Service des thèses canadiennes

NOTICE

The quality of this microform is heavily dependent upon the quality of the original thesis submitted for microfilming. Every effort has been made to ensure the highest quality of reproduction possible.

If pages are missing, contact the university which granted the degree.

Some pages may have indistinct print especially if the original pages were typed with a poor typewriter ribbon or if the university sent us an inferior photocopy.

Previously copyrighted materials (journal articles, published tests, etc.) are not filmed.

Reproduction in full or in part of this microform is governed by the Canadian Copyright Act, R.S.C. 1970, c. C-30.

AVIS

La qualité de cette microforme dépend grandement de la qualité de la thèse soumise au microfilmage. Nous avons tout fait pour assurer une qualité supérieure de reproduction.

S'il manque des pages, veuillez communiquer avec l'université qui a conféré le grade.

La qualité d'impression de certaines pages peut laisser à désirer, surtout si les pages originales ont été dactylographiées à l'aide d'un ruban usé ou si l'université nous a fait parvenir une photocopie de qualité inférieure.

Les documents qui font déjà l'objet d'un droit d'auteur (articles de revue, tests publiés, etc.) ne sont pas microfilmés.

La reproduction, même partielle, de cette microforme est soumise à la Loi canadienne sur le droit d'auteur, SRC 1970, c. C-30.

NL-339 (r. 88/04)

Canada

THE UNIVERSITY OF ALBERTA

THE GEOLOGY OF THE BLACKDOME EPITHERMAL DEPOSIT, B.C.

by

Gary J. Vivian

(C)

A THESIS
SUBMITTED TO THE FACULTY OF GRADUATE STUDIES AND RESEARCH
IN PARTIAL FULFILLMENT OF THE REQUIREMENTS FOR THE DEGREE
OF MASTER OF SCIENCE

DEPARTMENT OF GEOLOGY

EDMONTON, ALBERTA
FALL, 1988

Permission has been granted to the National Library of Canada to microfilm this thesis and to lend or sell copies of the film.

L'autorisation a été accordée à la Bibliothèque nationale du Canada de microfilmer cette thèse et de prêter ou de vendre des exemplaires du film.

The author (copyright owner) has reserved other publication rights, and neither the thesis nor extensive extracts from it may be printed or otherwise reproduced without his/her written permission.

L'auteur (titulaire du droit d'auteur) se réserve les autres droits de publication; ni la thèse ni de longs extraits de celle-ci ne doivent être imprimés ou autrement reproduits sans son autorisation écrite.

ISBN 0-315-45535-7

THE UNIVERSITY OF ALBERTA

RELEASE FORM

NAME OF AUTHOR: GARY J. VIVIAN

TITLE OF THESIS: THE GEOLOGY OF THE BLACKDOME EPITHERMAL DEPOSIT, B.C.

DEGREE FOR WHICH THESIS WAS PRESENTED: MASTER OF SCIENCE

YEAR THIS DEGREE GRANTED: FALL, 1988

Permission is hereby granted to THE UNIVERSITY OF ALBERTA LIBRARY to reproduce single copies of this thesis and to lend or sell such copies for private, scholarly or scientific research purposes only.

The author reserves other publication rights, and neither the thesis nor extensive extracts from it may be printed or otherwise reproduced without the author's written permission.

(SIGNED)....Gary J. Vivian....................

PERMANENT ADDRESS :

469 SHUB AVENUE
TIMMINS, ONTARIO
P4N 7N1

DATED ..March 28, 1988..

THE UNIVERSITY OF ALBERTA

FACULTY OF GRADUATE STUDIES AND RESEARCH

The undersigned certify that they have read, and recommend to the Faculty of Graduate Studies and Research, for acceptance, a thesis entitled THE GEOLOGY OF THE BLACKDOME EPITHERMAL DEPOSIT, B.C. submitted by GARY J. VIVIAN in partial fulfillment of the requirements for the degree of MASTER OF SCIENCE.

Supervisor ....

R. St J Lambert ....

R.E. Folinsbee ....

J Gray ....

Date : December 10,1987

DEDICATION

This thesis is dedicated to my wife, Jean, and my children, Krista and Adam. Without their loving support this thesis may not ever have been completed.

ABSTRACT

The Eocene, epithermal Ag-Au (Sb-Cu-Fe-Zn-Pb-S-Se-As) - silica deposits of the Blackdome property in south-central British Columbia, Canada, have been the subject of studies of host-rocks, alteration pattern, vein mineralogy, stable isotope analyses and fluid inclusions. The veins with precious metal mineralogy are hosted within a calc-alkalic volcanic pile. The age dates on this volcanic sequence vary between 24 Ma and 51.5 Ma. The polymetallic deposits were generated when Tertiary meteoric groundwaters penetrated fractures 0.5-1.1 km below surface into the volcanic pile. The hydrothermal fluids were partly vented to surface, resulting in a boiling geothermal system. These hydrothermal fluids effected extreme phyllosilicate and potassium feldspar alteration of the host rocks. Pervasive propylitization into the host rocks characterizes this former geothermal reservoir. The geothermal fluids have low salinities - in the order of 0.21-2.07 wt% NaCl equivalent - densities of 0.720 - 0.810 g/cm^3, $S^{18}O$ values of -6.8 to -8.8^{o}/oo (Smow) and SD values of -125 to -134^{o}/oo (Smow). Hydrative metasomatism caused a positive exchange shift in the $S^{18}O$ value of the fluids, away from the meteoric water line. The minor, positive shift in the SD value of the geothermal fluids away from the parent meteoric water is due to selective hydrogen metasomatism of the wallrocks, to loss of hydrogen from the boiling system, or both. The vein mineralogy is characterized by the open-space fillings of quartz-adularia-sericite (illite) as the major gangue phases along with minor illite. Ore mineralogy comprises pyrite, argentite-acanthite, Ag-sulfosalts, acanthite-aguilarite, electrum, gold, silver and minor base-metals. The Blackdome deposits clearly belong to the adularia-sericite-type group of volcanic-hosted epithermal precious-metal deposits.

ACKNOWLEDGEMENTS

Many thanks to my parents, Bill and Doreen, for their encouragement towards this "late - b[illegible]r".

This study originated from Mr. [illegible]t Reeve, past President, of Blackdome Exploration, and his belief that this deposit should be researched. Many thanks to the Blackdome Mining Corporation, especially Dave Rennie for some of his insights, for the financial assistance to complete this work.

Dr. Roger Morton, my advisor, supervised the project and guided me through many difficult situations with the most valuable advice, insights and constructive criticisms.

Rodger Grover aided me in many conquests of the University of Alberta computing system, or lack of.

Dr. K. Meuhlenbachs and Dr. T. Gray provided lab facilities for the analyses of the oxygen and hydrogen isotopes. Dr. A. Changkakoti and Pierre Maheux carried out the analyses of the hydrogen and oxygen isotopes, respectively. Dr. H. R. Krouse kindly analyzed for the sulfur isotopes at the University of Calgary. Brian Atkin and Peter Harvey of Midland Earth Sciences, U. K., carried out the chemical analyses of the host rocks withan XRFS.

Dr. Dorion Smith and Dave Tomlinson kindly helped in the analyses of some ore mineralogy by allowing me the use of the electron microprobe at the University of Alberta.

George Braybrook supervised the use of the scanning electron microscope in the analyses of the clay mineralogy.

Dr. Fred Longstaffe and Diane Caird were instrumental in guidance and supervision with the XRD.

Graham and Doreen Miller provided food and shelter for me over this 3 1/2 week ordeal.

Doug Bryan originally enticed me into this research and gave me invaluable advice.

Dr. R. Lambert, Dr. R. Folinsbee and Dr. T. Gray all served on my advisory committee.

Danny Pitre, Bathurst, N. B., helped in the drafting of the diagrams.

Loretta Ratchford and Rejeanne Roy (Bathurst, N.B.) and Sharon Gervais (Timmins, Ont.) helped in the typing and the construction of this research.

Brian Groves gave me invaluable insight into the understanding of "Word Perfect".

Finally, and maybe most importantly, my gratitude to Ian Atkinson (Manager, Noranda Expl. Co. Ltd., Timmins, Ont.) for allowing me free reign to complete this research using some Noranda personnel and Noranda time.

TABLE OF CONTENTS

Chapter Page

Dedication iv

Abstract v

Acknowledgements vii

List of Tables xiii

List of Figures xiv

List of Plates xvii

I. INTRODUCTION 1

A. Location and Access 1

B. Topography 2

C. Previous Work 2

D. Geology 5

II. PETROLOGY AND MINERALOGY OF THE HOST ROCKS TO THE BLACKDOME AG-AU VEIN SYSTEM 9

A. Intermediate to Mafic Metavolcanic Rocks: Mineralogy 9

i) Andesite-Basalt Massive Flows 9

ii) Autobrecciated Andesite-Basalt Flows ... 12

B. Felsic Metavolcanic Rocks: Mineralogy 13

i) Rhyolite Flow-Ash Flow Tuff- Ignimbrite . 13

C. Textures 13

D. X-Ray Diffraction Analyses 14

i) Mineralogy 15

ii) Incidentals 18

E. Chemistry 18

i) Alteration and Metamorphism 19

F. Major Element Chemistry 20

G. Trace Element Chemistry 29

i) Trace Element Occurrence 30

ii) Trace Elements as Compositional and Tectonic Classifiers 36

H. Conclusions 42

III. CLAY MINERAL ANALYSES OF THE BLACKDOME NO. 1 AG-AU VEIN SYSTEM 47

A. Clay Mineral Analyses 47

i) Smectite 47

ii) Illite 51

iii) Chlorite 52

iv) Kandite Group 54

v) Mixed-Layer Clays 55

B. Non-Clay Fraction 63

i) Quartz 63

ii) Potassium Feldspar 63

iii) Plagioclase Feldspar 63

C. Discussion 64

D. Conclusions 78

IV. FLUID INCLUSION STUDY 81

A. Methods of Investigation 81

B. Classification of Inclusions 83

C. Types of Inclusions 84

i) Type 1 Inclusions 86

ii) Type 2 Inclusions 86

iii) Type 3 Inclusions 86

D. Salinities of the Hydrothermal Fluids 86

E. Temperatures of the Hydrothermal Fluids 91
F. Conclusions 95
V. SULFUR- OXYGEN- AND HYDROGEN- ISOTOPIC COMPOSITION OF THE ORE FLUIDS AT BLACKDOME 96
A. Experimental Techniques 97
B. Results 98
C. Origin of the Hydrothermal Fluids 99
D. Conclusions 102
VI. VEIN PETROGENESIS, MINERALOGY AND PARAGENESIS .. 105
A. Background and Methods 105
B. Vein Petrogenesis and Mineralogy 106
i) Gangue Minerals 107
a) Quartz 108
b) Adularia 108
c) Carbonate 109
d) Clay Minerals 109
ii) Ore Minerals 110
a) Au-bearing Opaque Minerals 110
1. Native Gold 110
2. Electrum 110
b) Ag-bearing Opaque Minerals 112
1. Acanthite 111
2. Acanthite-Aguilarite 112
3. Native Silver 113
4. Silver Sulfosalts 114
c) Non Au- or Ag- bearing Opaque Minerals 115
1. Pyrite 115

2. Chalcopyrite 115

3. Galena 116

4. Sphalerite 116

5. Marcasite 116

C. Nature of the Ore Fluids as Evidenced by Gangue and Ore Mineralogy at Blackdome 117

D. Discussion 118

VII. BLACKDOME MINE: A MODEL FOR THE FORMATION OF THE EPITHERMAL DEPOSITS 123

A. Geologic Setting 123

B. Hydrothermal Setting 123

C. Oxygen and Hydrogen Isotopic Composition of Ore Fluids 124

D. Salinities, Temperatures and Pressures of Ore Fluids 125

E. Ore Mineralogy 126

F. Nature of the Ore Fluids as Evidenced by Gangue and Ore Mineralogy 127

G. Conclusions 128

i) Blackdome as an Adularia-Sericite Type Deposit 128

VIII. REFERENCES 132

IX. APPENDICES 140

A. Experimental techniques for the Analyses of the Clay Minerals 140

B. Photo-micrographs of the thin sections from Chapter II 143

C. Photo-micrographs and EDA analyses of the Clay Minerals from Chapter III 156

D. Photo-micrographs of Fluid Inclusions from Chapter IV 161

E. Photo-micrographs of the Ore Minerals from Chapter VI 176

LIST OF TABLES

TABLE 2.1 Major Oxide Geochemical Data 21

TABLE 2.2 Irvine and Baragar versus Petrographic Classification 31

TABLE 2.3 Trace Element Geochemical Data 32

TABLE 3.1 Foscolo's Rules for the Identification of Smectite 48

TABLE 3.2 Montmorillonite vs. Beidellite at 54% Humidity and Saturated with K^+ 51

TABLE 3.3 Proper Identification of Clinochlore ... 53

TABLE 3.4 Reflection Characteristics for Kandite Group 54

TABLE 3.5 Compositional Variation of Interstratification of Illite/Smectites . 59

TABLE 3.6 Clay Mineralogy Analyses of the Blackdome No. 1 Vein Zone 61

TABLE 4.1 Temperature and Salinity Data for Hydrothermal Fluids in the Blackdome Silver-Gold Veins, British Columbia, Canada 88

TABLE 5.1 Stable Isotope Data for Host Rocks, Quartz and Hydrothermal Fluids in the Blackdome Ag-Au Deposit, British Columbia, Canada 98

TABLE 6.1 Electron Microprobe Analyses of Some Ore Minerals at Blackdome Mine, British Columbia, Canada 107

LIST OF FIGURES

FIGURE 1.1 Location Map 3

FIGURE 1.2 Geology of the Blackdome Silver-Gold Mine 8

FIGURE 2.1 Geology of the Blackdome Silver-Gold Mine 10

FIGURE 2.2 Identification procedure for reflection peaks of a backpacked sample............ 16

FIGURE 2.3 Blackdome Volcanics: Alkalis vs. SiO_2 22

FIGURE 2.4 Blackdome Volcanics: Alkalis vs. (K_2O / Na_2O K_2O) x 100 24

FIGURE 2.5 Blackdome Volcanics: TiO_2 vs. SiO_2 25

FIGURE 2.6 Blackdome Volcanics: AFM Plot 27

Figure 2.7 Blackdome Volcanics: Al2O3 vs. Normative Plagioclase Composition 28

FIGURE 2.8 Blackdome Volcanics: SiO_2 vs. Zr/TiO_2 37

FIGURE 2.9 Blackdome Volcanics: Zr/TiO_2 vs. Nb/Y 39

FIGURE 2.10 Blackdome Volcanics: Ti - Zr - Yx3 40

FIGURE 2.11 Blackdome Volcanics: FeO vs. Zr/TiO_2 x 10^4 41

FIGURE 2.12 Blackdome Volcanics: Nb/Y vs. Zr/P_2O_5 x 10^4 43

FIGURE 2.13 Blackdome Volcancs: Zr + Y - TiO_2 - Cr 44

FIGURE 3.1 Diffractometer patterns of dioctahedral vs. trioctahedral smectites 49

FIGURE 3.2a Diffractogram of Discrete Illite 50

FIGURE 3.2b Diffractogram of illite/smectite showing the moving 10A peak 50

FIGURE 3.3 Composition of illite/smectite in relation to percent illite 56

FIGURE 3.4 Composition of illite/smectite in relation to percent smectite 57

FIGURE 3.5a 3.5b Identification procedure of reflection peaks 62

FIGURE 3.6 DDH 139 - Clay Mineralogy vs. Depth ... 65

FIGURE 3.7 DDH 84 - Clay Mineralogy vs. Depth 66

FIGURE 3.8 DDH 23 - Clay Mineralogy vs. Depth 67

FIGURE 3.9 DDH 06 - Clay Mineralogy vs. Depth 68

FIGURE 3.10 DDH 01 - Clay Mineralogy vs. Depth 69

FIGURE 3.11 The observed genetic sequence of hydrothermal alteration of silicic groundmass to illite (Steiner, 1967) ... 72

FIGURE 3.12 The observed genetic sequence of hydrothermal alteration from a K$^+$-rich starting composition to a mixed-layer clay (Eberl and Hower, 1977) 74

FIGURE 3.13 Paragenetic sequence of the Clay Phases and other major gangue phases ... 80

FIGURE 4.1 B.C. Epithermal Gold-Silver Deposit Model (Second Approximation) 82

FIGURE 4.2 Weight percent NaCl equivalent vs. Frequency 90

FIGURE 4.3 Homogenization Temperature vs. Frequency 92

FIGURE 4.4 Pressure determinations from Fluid Inclusion Studies 93

FIGURE 5.1 SD vs. S^{18}O Plot of Ore Fluids from the Blackdome Ag-Au Deposit 101

FIGURE 5.2 Range of S^{34}S Values of Sulfides and Sulfates from Various Hydrothermal Ore Deposits 103

FIGURE 6.1 SEM Photo-micrograph of Au vs.Electrum.. 111

FIGURE 6.2 SEM Photo-micrograph of Electrum........ 111

FIGURE 6.3 Paragenetic Sequence of the Blackdome No. 1 Vein System 119

LIST OF PLATES

APPENDIX B. Plates 2.1 to 2.12 Thin section photo-micrographs of the host rocks at Blackdome 143

APPENDIX C. Plates 3.1 to 3.10 Photo-micrographs and EDA analyses of the clay minerals in the No. 1 vein system at Blackdome . 156

APPENDIX D. Plates 4.1 to 4.14 Photo-micrographs of the fluid inclusions within quartz at Blackdome 161

APPENDIX E. Plates 6.1 to 6.10 Photo-micrographs of the ore mineralogy in the No. 1 vein at Blackdome 176

I. INTRODUCTION

Epithermal precious metal veins have become increasingly sought after exploration targets within the last decade. Unfortunately, very few of our Canadian examples have been completely documented.

The Blackdome property in south-central British Columbia hosts one such epithermal Ag-Au vein. It is this epithermal system upon which this thesis concentrates. This deposit will be the subject of host rock, alteration, vein mineralogy and stable isotope analyses along with fluid inclusion studies. This research will allow for the establishment of a working model for the Blackdome Ag-Au deposit.

The Blackdome property covers a large epithermal-precious metal system. Mineralized quartz veins have been found over an area measuring 4500 meters by 1500 meters. It is within the so-called No. 1 vein system that all the present reserves on the property have been documented. Other vein systems do occur on the property, but minimal exploration has been carried out on these to date.

A. LOCATION AND ACCESS

The Blackdome property is located in south-central British Columbia, about 70 km west-northwest of the town of Clinton. It is accessible by 140 km of gravel road leading west from Provincial Highway 97, 18 km north of Clinton.

There is an alternate route west from Williams Lake and south along the Fraser River. This latter distance is 150 km.

The approximate geographic centre of the claim block is at 51° 20' North and 122° 29' West (see location map, Figure 1.1).

B. TOPOGRAPHY

The Blackdome property covers portions of the crest and upper slopes of a prominent north-northeasterly trending ridge, dominated by Blackdome Mountain. The topography is gently rolling along the top of the ridge, but becomes quite steep near the tributaries of Fairless and Porcupine Creeks. The peak of Blackdome Mountain is 2255 meters above sea level and the east and west boundaries of the property are less than 1350 meters above sea level.

Alpine meadows occur above 1800 meters, while thick stands of pine and fir occur on some of the north facing slopes.

The property lies within the interior dry belt of British Columbia and precipitation is generally light. Snow can be expected at scattered intervals throughout the summer but field work can be carried out from June to October.

C. PREVIOUS WORK

Extensive work has been carried out on the Blackdome property dating back to 1947 when it was

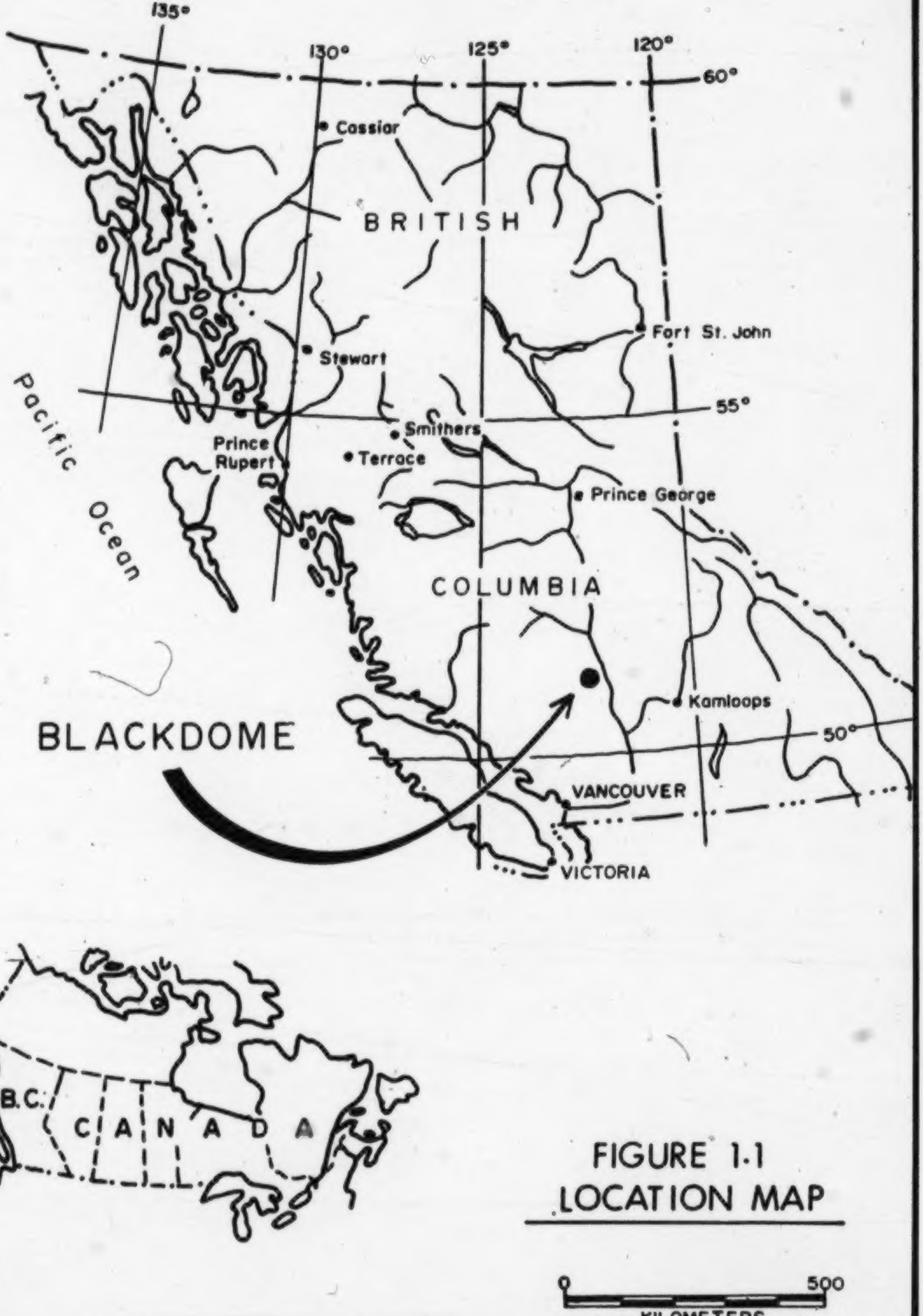

135°
130°
125°
120°
60°
55°
50°
Cassiar
BRITISH
COLUMBIA
Fort St. John
Stewart
Smithers
Prince Rupert
Terrace
Prince George
Pacific Ocean
BLACKDOME
Kamloops
VANCOUVER
VICTORIA
B.C.
CANADA
0
500
KILOMETERS

FIGURE 1.1
LOCATION MAP

discovered by a prospector named Lawrence Frenier.

It was not until 1977, when the Dome claims were staked by Barrier Reef Resources, that extensive work was carried out on the No. 1 vein system. From 1977 to 1983, extensive geological mapping, prospecting, rock geochemistry, geophysics and diamond drilling were performed on the property.

In 1981, underground exploration in the form of 900 meters of drifting and raising delineated 50,000 tons of 0.62 oz gold and 5.6 oz silver per ton along the No. 1 vein zone.

In 1982, Blackdome Exploration (Barrier Reef Resources) and Heath Steele Mines Ltd. (Noranda Exploration Company Limited) made an agreement for further exploration. This work constituted geological mapping, geochemical and geophysical surveying and another 4400 meters of diamond drilling.

In May 1983, Noranda Exploration Company Limited commenced with a drift 762 meters north of the original portal. Approximately 900 meters of drifting were completed by October of 1983. Only limited success resulted.

In 1984, Blackdome promoted their property in order to raise capital for further exploration drifting. A continuation to the south along the No. 1 vein system and an extension to the west was being proposed. The extension west would link the, as yet, untested No. 2 vein system. This drifting was undertaken and completed. An exploration drift at the 1920 m level was initiated in the Fall of 1984. The encouraging results obtained from drifting and raising along the 1920 m level allowed for Blackdome to make a positive decision to go into production. Production began in the Spring of 1986 using a 200 ton per day mill. The first seven and one-half months production to the end of 1986 saw 38,267 tons of ore treated, averaging 174 tons per day with an average grade of 0.86 oz gold and 3.17 oz silver per ton. Approaching the end of March 1987, recovery averaged 92.7% for gold and 72% for silver. Total ore reserves as quoted at the end of 1986 are 276,000 tons averaging 0.72 oz gold and 2.58 oz silver per ton with a cut-off grade of 0.25 oz gold per ton.

D. GEOLOGY

The property is underlain by a sequence of early- to mid- Tertiary volcanic rocks and associated volcaniclastic sediments cut by small intermediate to basic dikes. Age dates obtained on the volcanic sequence range between 51.5 Ma from the dacite to 24 Ma from the plateau basalt. The rocks strike north-northeasterly with shallow, 10-20o, dips to the southeast. Tension fractures are the locus of the epithermal veins. These fractures have apparently been produced by doming. Minor normal faulting effects dislocations of some units and preserves some of the erosional remnants from younger rocks (Dawson, 1983).

Miocene, fine-grained, porphyritic, dark brown to black basalt flows cap Blackdome Mountain. These are the youngest rocks. Basaltic feeder dikes are present across the property.

Underlying the basalt is a uniform sequence of porphyritic andesite flows. When unaltered, they are green-grey in colour, with white, plagioclase phenocrysts. This unit is 150 meters thick. Again, numerous feeder dikes for the andesite have been identified on the property.

A thin, irregular and discontinuous clastic unit underlies the porphyritic andesite. The clastic unit varies from volcaniclastic sandstone to coarse agglomerate with basic bombs up to 40 cm long. This unit can be 30 meters thick but mostly occurs as small, local, erosional remnants.

To the south, a chaotic "rhyolite" unit underlies the porphyritic andesite. This unit is actually a mixture of rhyolitic flows, tuffs and breccias as well as local lenses of volcanic wacke and ash beds. The unit is 60 meters thick and thickens to the south.

Underlying the "rhyolite" and beneath the clastic horizon at the base of the andesite unit, north and northeast of the "rhyolite" are a series of porphyritic dacite flows. They are typically fine-grained, dense, reddish-brown to green-grey with 20% white feldspar phenocrysts. This unit is up to 75 meters thick.

Andesitic flows with propylitic alteration, tuffs and agglomerate underlie the dacite unit. These andesites are light to dark green with various amounts of chlorite and frequent stringers of epidote and calcite. This is the oldest unit on the property and may be over 180 meters thick (Dawson, 1983) (Figure 1.2).

This intermediate- to felsic- volcanic sequence formed within a volcanic-arc type environment which constituted part of Stikinia (Monger et. al., 1982), an allochthonous component of the Canadian Cordillera that was accreted on to the North American continent.

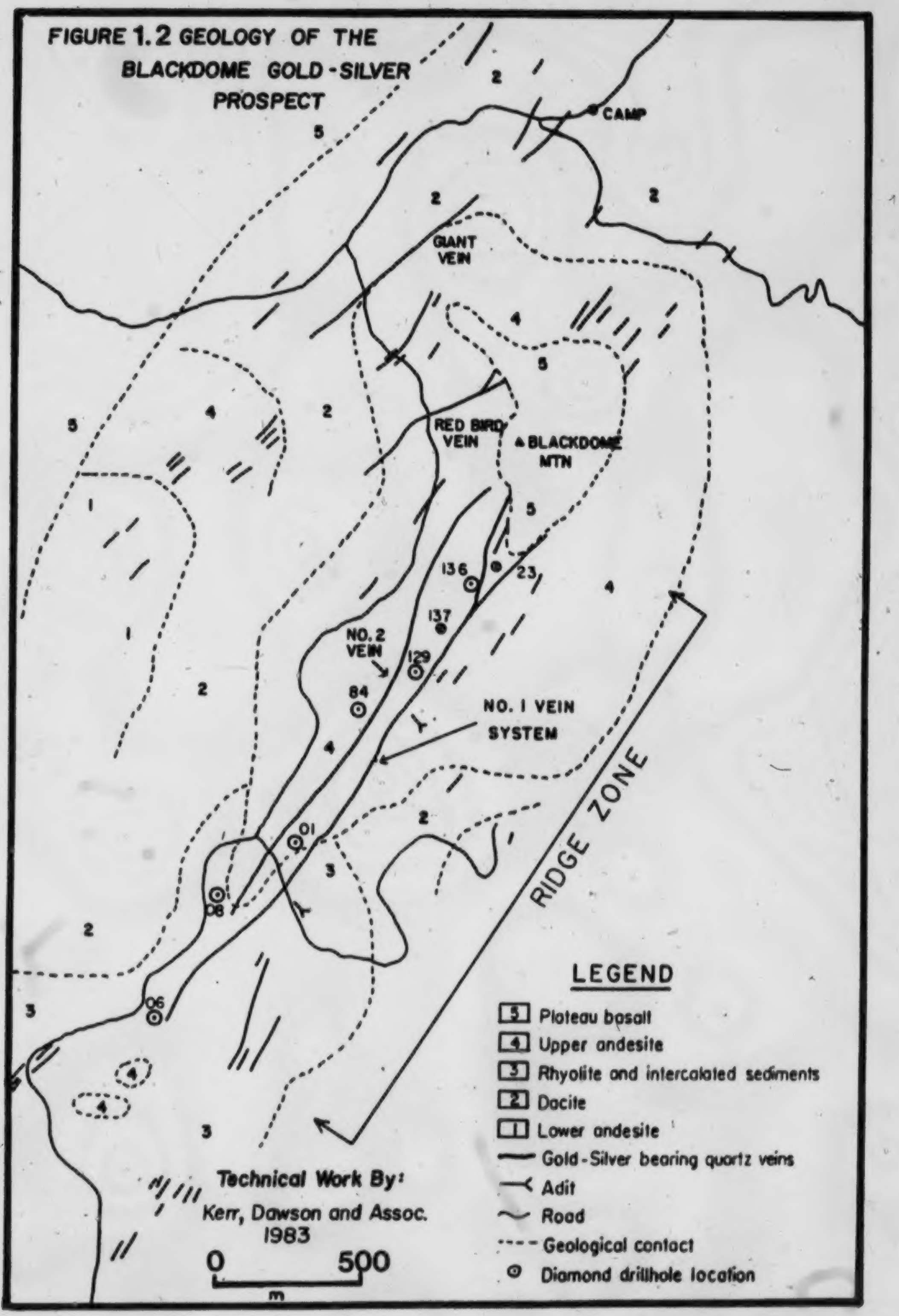

FIGURE 1.2 GEOLOGY OF THE BLACKDOME GOLD-SILVER PROSPECT

CAMP
GIANT VEIN
RED BIRD VEIN
▲ BLACKDOME MTN
NO. 2 VEIN
NO. 1 VEIN SYSTEM
RIDGE ZONE
136
23
137
129
84
01
08
06
1
2
3
4
5
LEGEND
5 Plateau basalt
4 Upper andesite
3 Rhyolite and intercalated sediments
2 Dacite
1 Lower andesite
Gold-Silver bearing quartz veins
Adit
Road
Geological contact
Diamond drillhole location
Technical Work By:
Kerr, Dawson and Assoc.
1983
0
500
m

II. PETROLOGY AND MINERALOGY OF THE HOST ROCKS TO THE BLACKDOME AU-AG VEIN SYSTEM

Representative samples were collected from eight diamond drill holes along the No. 1 vein system of the Blackdome property (see Figure 2.1). Thin sections, representing visually different lithologies, were prepared and observations on these have allowed conclusions to be drawn concerning the environment of deposition. X-Ray Powder diffraction analyses were used to help determine mineralogy and the mineral hosts of certain trace elements.

Chemical analyses were carried out to help classify the host rocks, both tectonically and chemically. The degree of alteration within the Blackdome hydrothermal plumbing system was determined via chemical analyses.

A. INTERMEDIATE TO MAFIC METAVOLCANIC ROCKS: MINERALOGY

i) Andesite-Basalt Massive Flows

Most of the rocks in this section are categorized as andesite flows with one sample (DDH 129-10) being marginal andesite to basalt. These flows are composed of varying amounts of plagioclase, hornblende and pyroxene, with lesser amounts of chlorite, sericite, K-feldspar, quartz, clay, epidote, calcite, magnetite, pyrite, hematite, apatite and sphene. The primary minerals are plagioclase, which can comprise 80% of the mode, hornblende, which may

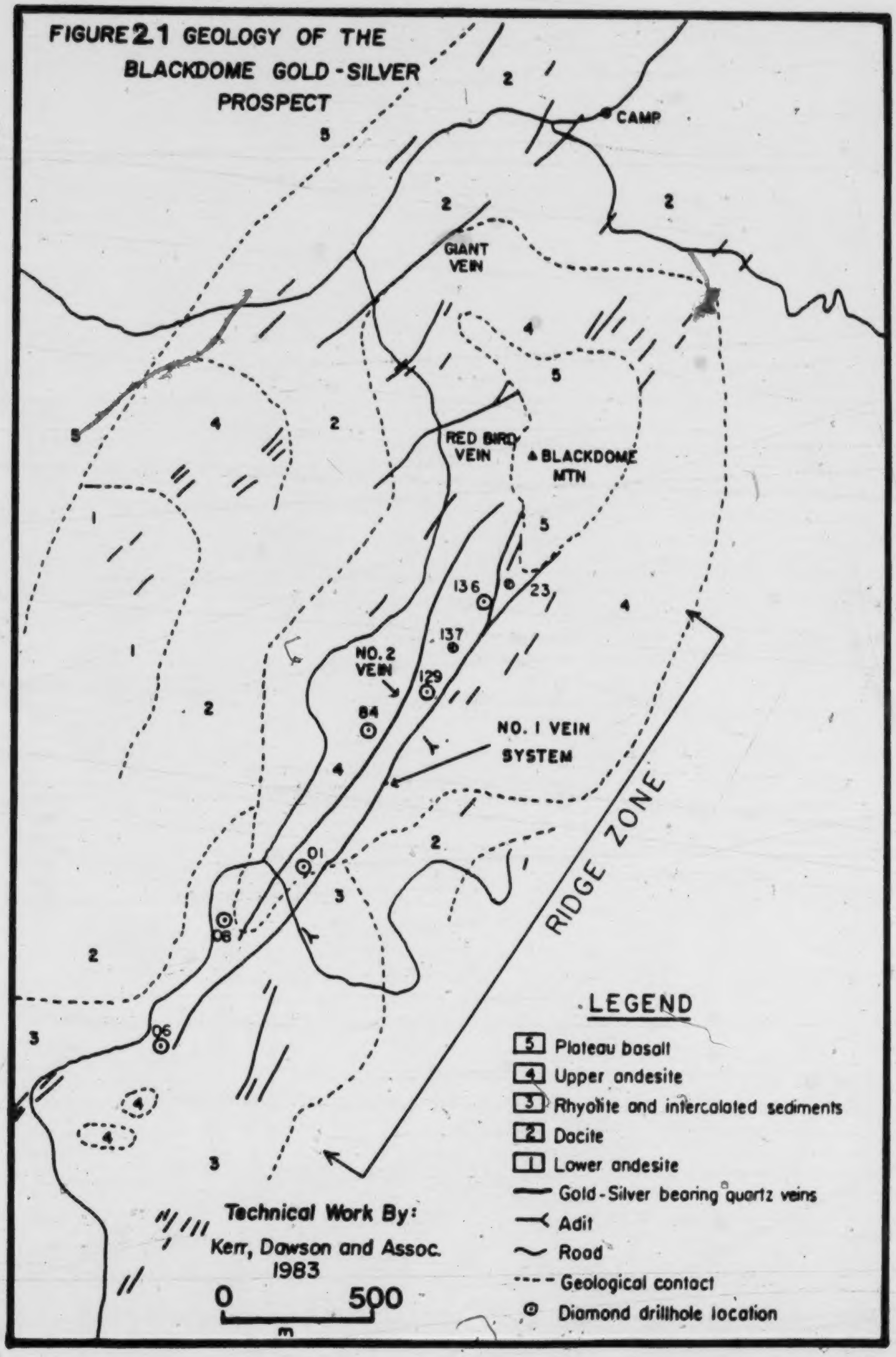

FIGURE 2.1 GEOLOGY OF THE BLACKDOME GOLD-SILVER PROSPECT

CAMP
GIANT VEIN
RED BIRD VEIN
BLACKDOME MTN
NO. 2 VEIN
NO. 1 VEIN SYSTEM
RIDGE ZONE
136
23
137
129
84
01
08
06
5
4
3
2
1
LEGEND
5 Plateau basalt
4 Upper andesite
3 Rhyolite and intercalated sediments
2 Dacite
1 Lower andesite
Gold-Silver bearing quartz veins
Adit
Road
Geological contact
Diamond drillhole location
Technical Work By:
Kerr, Dawson and Assoc.
1983
0
500
m

total 5%,pyroxene (augite, pigeonite) totalling 5%, potassium feldspar (orthoclase) 25% and minor opaque phases (3%). All the above modes are quoted as maxima. The two prominent accessory minerals are apatite and sphene. The remainder of the modes is made up of alteration minerals in these volcanics.

Plagioclase is present as large, tabular crystals (phenocrysts) and as polygonal grains and microlites in the groundmass. The phenocrysts of plagioclase have an An content of 40-60 (i.e. andesine-labradorite). The phenocrysts vary from anhedral to euhedral and severely altered to fairly fresh. Some of the plagioclase crystals show excellent albite twinning, although most of the time it is indistinct. Compositional determinations were impossible on the groundmass plagioclase but it is assumed that this phase will be more Na-rich (possibly oligoclase or lower An content-andesine).

Hornblende is usually tabular and rarely terminated. These hornblendes are very rarely fresh, and usually altered to chlorite or sericite. They usually occur as discrete phenocrysts (up to 0.5 mm) or as a felted aggregate with plagioclase. The hornblende is basaltic hornblende.

Pyroxene occurs as short prismatic crystals with eight- sided cross-sections. The composition is very difficult to determine, for the pyroxenes are severely altered to sericite, calcite and serpentine and/or chlorite.

The pyroxene in the groundmass is possibly pigeonite (the most common pyroxene in volcanic rocks and usually in the groundmass, Kerr 1977), whilst the pyroxene of the phenocrysts appears to be augite. An orthopyroxene (hypersthene) was identified in a couple of sections as primary phenocrysts.

Potassium feldspar occurs as microlites and mosaics in the groundmass. It's exact composition is undeterminable by optical tests. It is assumed that it is orthoclase. Potassium feldspar also occurs as a major alteration product in the form of adularia. It occurs both in veins and in areas along plagioclase grain boundaries.

Quartz appears as a minor component in the groundmass. It occurs as a mosaic with the potassium feldspar. Silicification, in the form of quartz veins and as a replacement along plagioclase and some other phenocrysts' boundaries is common in these intermediate-felsic volcanics.

The remaining minerals occur as alteration products of the phenocrysts and the groundmass. Chlorite, epidote, calcite, clay and sericite were identified.

ii) Autobrecciated Andesite-Basalt Flows

These units are compositionally the same as the above lithologies. The primary difference is textural. In this case fragmented phenocrysts and clasts of host material are found surrounded by a brecciated matrix. The brecciation occurs near the top or bottom of a flow unit. In hand specimen and in thin-section this unit has the appearance of a pyroclastic lithology.

B. FELSIC METAVOLCANIC ROCKS: MINERALOGY

i) Rhyolite Flow - Ash Flow - Ignimbrite

The composition of this unit varies very little on first sight from the more intermediate flows. The difference lies within the abundances of potassium feldspar, plagioclase and quartz. The potassium feldspar increases to about 30-40% of the mode whilst plagioclase shows a decline to 20-45%. The remainder of the mode is comprised of the quartz, up to 40%, and alteration products such as clay and sericite, as well as quartz and potassium feldspar (mostly adularia).

The mineralogy is clearly essentially the same as in the mafic-intermediate volcanic descriptions. One of the foremost problems with these felsic sections lies in determining whether these rocks were originally more mafic and then silicified and K-metasomatized to appear as "pseudo-rhyolites" or dacites.

The outstanding feature of the ignimbrite is the coarser-grained rhyolitic groundmass with fragments of devitrified glass. The glass fragments occur up to 7 mm in size. This ignimbrite may be an autoclastite.

C. TEXTURES

The texture most notable within all these sections is the predominance of flow banding or a trachytic texture and the pilotaxitic texture which is most prominent in the flow volcanics.

The primary phenocrysts, which are assumed to be relatively early magmatic, for the andesite, are the plagioclase, pyroxene and amphibole. These three all show intense alteration, thought to be representative of early autometasomatism, and are ragged and shattered in many instances.

The classic feature which represents a possible Peleen explosive origin for this volcanic sequence is the presence of ash flow/ignimbrite units. The ignimbrites represent nuees ardentes, travelling down the flanks of a stratovolcano or along the surface of the ground. They are produced by the explosive disintegration of viscous lava in a stratovolcanic crater, or by the explosive emission of a gas-charged ash from a fissure or group of fissures. Likely, the emission from fissures is the best explanation considering the tectonic setting of this area.

Note: Photomicrographs, in Appendix II, have been included to illustrate the mineralogy and textures of some of these sections.

D. X-RAY DIFFRACTION ANALYSIS

XRD analyses were carried out, using a Phillips X-ray diffractometer and Cobalt K alpha radiation, on 5 of the 18 host- rock samples to help determine the mineralogy and the theoretical hosts for trace elements within the minerals. Most notably, Ba reaches approximately 1000 ppm in some of the rocks. The common hosts for barium are barite or alkali (K)-feldspar. Barium also substitutes to a minor extent in the plagioclase structure. It is evident from the present study that no discrete barite is present and that the barium ion is being captured or camouflaged within one of the feldspar structures; either K-feldspar or plagioclase. This is revealed by the XRD patterns (Figure 2.2).

Identification of the minerals composing the host-rocks was made easier by the fact that all samples show the exact same reflections as the initial analysis of sample 5. All analyses are, essentially, perfect replicas of one another, save for intensity. Figure 2.2 shows all the labelled peaks with the coinciding d-spacings. The identification of all peaks was carried out using Brown, G. (1961). These are non-oriented samples, so intensity of the reflections may vary significantly from one sample to the next.

i) MINERALOGY

Quartz -Quartz shows up on all the Blackdome

FIGURE 2.2

IDENTIFICATION PROCEDURE FOR REFLECTION PEAKS OF A BACKPACKED SAMPLE

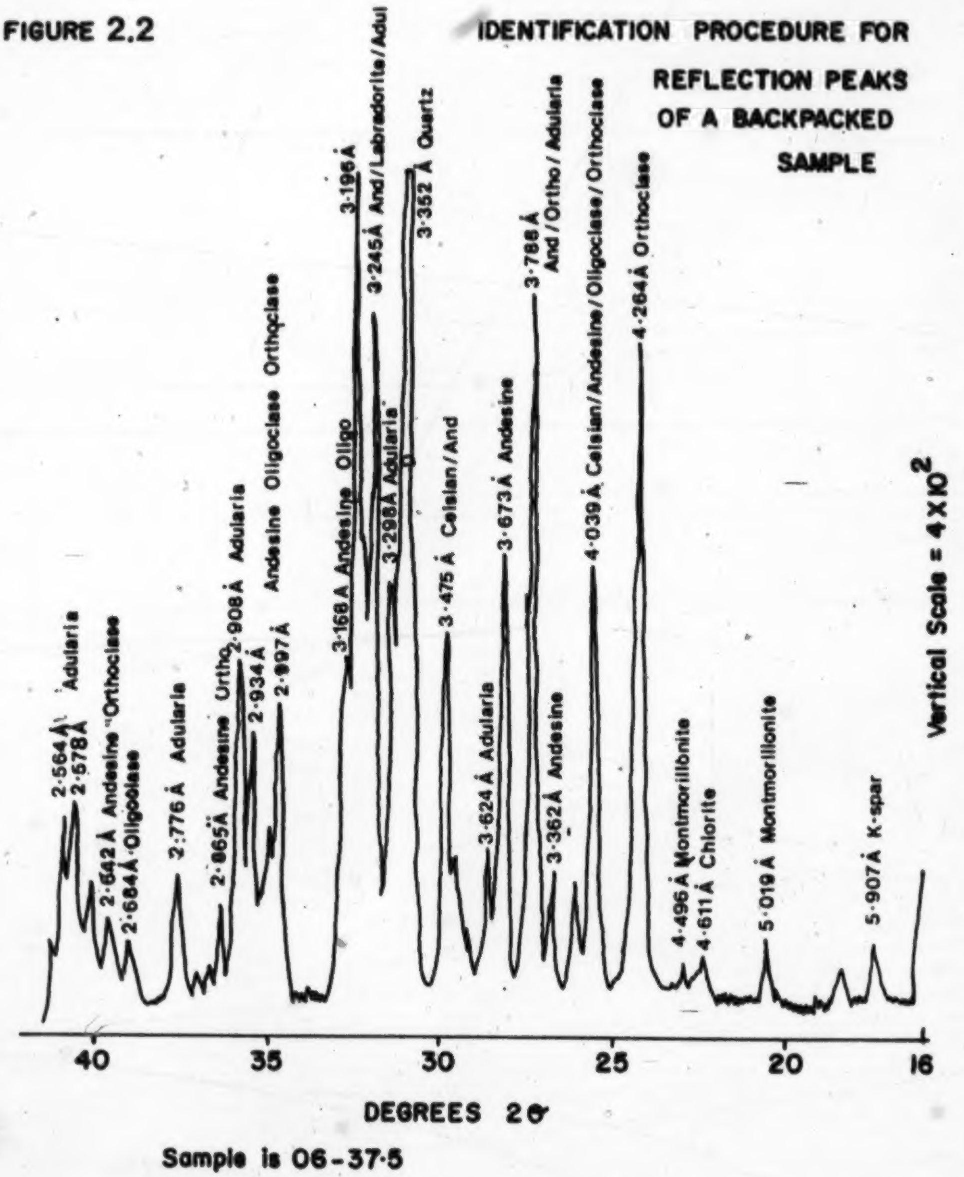

Sample is 06-37·5

Note: Identification of peaks by using J.C.P.D.S. cards analyses and is characteristically identified by the 101 reflection at a d-spacing of 3.343A and an angle of 31°2O.

Plagioclase - Most of the Na-feldspar peaks are characteristic of andesine to labradorite composition, with some oligoclase.

Characteristic andesine peaks are 3.21A, 3.18A, 4.04A, 3.14A, 3.00A and 2.93A.

The characteristic peaks for labradorite are essentially the same (+/- .02A) and it is very difficult, from X-ray charts alone, to discern between andesine and labradorite.

Oligoclase shows the same characteristic d-spacing reflections.

Potassium Feldspar - Most of the remaining peaks can be identified as being due to the presence of K-feldspar. The K-feldspar is contained within the groundmass and also as replacements (fractures, veins and recrystallized rims of phenocrysts). Most of the replacement type K-feldspar is thought to be adularia, while the groundmass material appears to be orthoclase. The most characteristic potassic feldspar peaks are 3.18, 3.8 and 4.02A, while the characteristic peaks for adularia are 3.31, 3.77 and 3.24A.

Clays - The largest underlying problem, in identifying any clay structure in non-oriented (backpacked) samples, arises with the poor reflections which are monitored at angles greater than 16°20. Clay particles are most easily identified within preferred orientation samples and at very low angles ($2^{o}2\theta$-$16^{o}2\theta$).

Montmorillonite was identified by the basal reflection of 003 at 5.019A and the non-basal reflection of the 110 at 4.496A. The montmorillonite is a product of the alteration of the feldspars.

Chlorite was identified from the non-basal 020 reflection at 4.61A. Chlorite is a product of the alteration of the feldspars and mafic minerals.

ii) INCIDENTALS

There are mafic minerals contained within these samples, mostly amphibole (+/- biotite and/or pyroxene), but it is difficult to identify these mafics from the X-ray diffraction analyses. Their characteristic reflections occur at or around 8.4 to 8.6A. Backpacked samples are started at approximately $16^{o}2\theta$ and this places one beyond the best detectable limit for mafic minerals.

E. CHEMISTRY

Eighteen rock samples were analyzed for 10 major oxide elements and 19 trace elements. The ten major oxides were Si, Al, Ti, (Fe2+, Fe3+), Mg, Ca, Na, K, Mn and P. The nineteen trace elements analyzed were As, Ba, Ce, Co, Cr, Cu, La, Mo, Ni, Nb, Pb, Rb, S, Sr, V, W, Y, Zn and Zr. The analyses were performed by Midland Earth Science Associates, Nottingham University, United Kingdom, using X-ray fluorescence spectometry (XRFS).

Classification of volcanic rocks may be carried out using major element contents. The classification of volcanic rocks as outlined by Irvine and Baragar (1971) was employed for the Blackdome suite. However, care must be taken in the interpretation of these data and in the classification of the rocks, as alteration may dramatically alter bulk chemical compositions.

Trace elements were analyzed for certain elements considered relatively immobile (P, Zr, Y and Nb) during mild metasomatism. The Blackdome suite was analyzed for trace elements to permit an investigation of the parent magma series, and the possible tectonic settings. However it should be pointed out that the binary and ternary plots used for classification of the volcanics must be interpreted with care. Pearce et al (1977) suggest that a clear concensus of opinion has not yet been reached as to which elements are truly "immobile".

i) Alteration and Metamorphism

The classification of altered volcanic rocks on the basis of major element chemistry often suffers due to the metasomatic nature of the process being overlooked, or at least downplayed. Significant redistribution of some elements clearly occurs.

Most previous studies on the classification of volcanic rocks have involved suites of mafic volcanics

(Joplin, 1963; Smith, 1968; Condie, 1976). Intermediate volcanics, prevalent at Blackdome, have been analyzed using classification schemes from mafic volcanics.

The Blackdome hydrothermal system has undergone predominant and extensive "propylitic" alteration. Within the Blackdome suite of host rocks, sample number 13 is the least altered rock. Every major element shows depletion except for Si and K. Mn and P appear to be the most stable trace elements.

The metamorphic facies for the Blackdome volcanics is predominantly zeolite facies with possible lower greenschist facies implications.

F. MAJOR ELEMENT CHEMISTRY

The host-rock suite of the Blackdome Ag-Au vein was chemically classified according to Irvine and Baragar (1971). This classification scheme was designed to encompass the large number of chemical analyses of metavolcanic rocks and assumes that the data for severely altered rocks have been omitted. Chemical analyses for the major element oxide data are given in Table 2.1. The prominent elements revealing alteration are silica, calcium and the alkalies indicating silicification and K-metasomatism.

The subalkaline nature of these metavolcanics is clearly demonstrated by the alkali-silica diagram (Figure 2.3). Also evident in this diagram is the variability in

TABLE 2.1 Major Oxide Geochemical Data

(all values are quoted in weight %)

SAMPLE No.	SiO_2	Al_2O_3	TiO_2	Fe_2O_3	MgO	CaO	Na_2O	K_2O	MnO	P_2O_5
06-37.5	68.71	15.06	0.62	3.25	0.22	1.41	3.64	5.84	0.04	0.15
06-45	66.19	15.28	0.64	4.36	0.44	2.04	4.11	4.91	0.06	0.18
06-50	65.37	15.09	0.86	4.91	1.03	2.40	2.64	4.60	0.10	0.22
84-15	62.67	15.71	0.81	4.69	1.65	3.61	3.32	3.90	0.09	0.19
84-50	73.07	14.43	0.13	1.41	0.15	0.12	2.67	7.07	0.02	0.03
84-70	76.21	12.58	0.15	0.98	0.00	0.05	1.87	7.24	0.00	0.03
84-100	75.01	12.76	0.13	1.55	0.00	0.05	0.39	9.56	0.01	0.02
84-120	66.14	14.32	0.60	5.75	0.17	0.69	1.23	9.10	0.15	0.14
129-10	52.11	17.03	2.07	9.71	3.30	4.11	4.69	1.92	0.10	0.38
129-40	60.79	15.51	0.99	5.60	1.65	2.66	1.76	8.16	0.07	0.24
129-60	62.84	14.52	0.98	5.72	1.88	1.74	2.35	6.38	0.09	0.23
129-80	63.01	14.03	0.91	5.11	1.63	3.31	2.05	5.69	0.08	0.23
129-110	62.72	14.39	0.86	5.60	1.64	2.25	2.13	6.82	0.08	0.21
137-20	63.41	14.55	0.98	5.82	1.49	0.65	2.13	5.11	0.13	0.23
137-30	65.90	15.11	0.98	4.28	1.13	0.52	2.11	7.35	0.03	0.22
137-45	61.49	16.68	1.08	7.11	1.72	0.82	3.61	4.13	0.06	0.25
137-55	66.83	13.54	0.87	5.42	1.79	0.60	2.35	6.02	0.08	0.19
137-75	64.64	15.43	1.02	5.70	1.52	0.47	2.03	6.01	0.06	0.23

Note: Fe data are listed as total Fe_2O_3. For the Irvine and Baragar classification of these rocks, FeO was calculated by assuming oxidation ratio = 24. The analyses were done by Midland Earth Science Associates, Nottingham, U.K.

Standard samples were used to check the accuracy of analysis and it was determined by comparing the results of the external standards with Abbey (1977). The analyses are all within experimental error as given.

Oxidation ratio: $(100\ Fe_2O_3)/(Fe_2O_3+FeO) = 24$.

FIGURE 2.3 Blackdome Volcanics:
Alkalis (weight%) vs. SiO_2 (weight%)
(adapted after Irvine and Baragar, 1971)

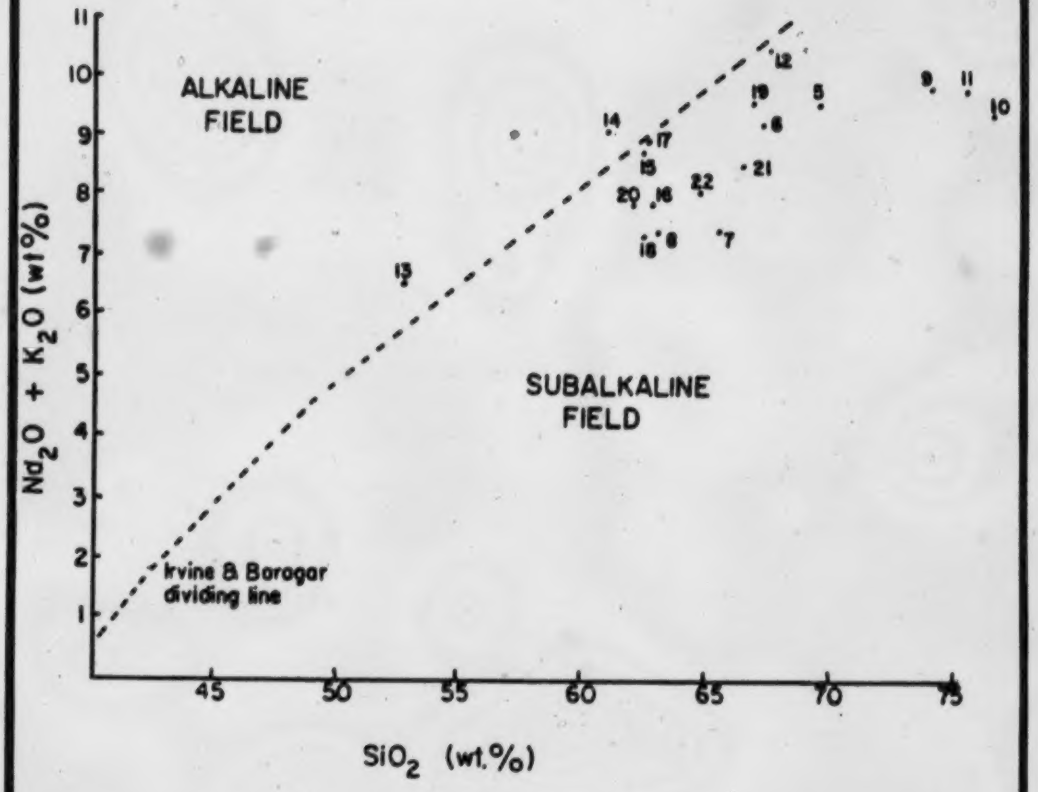

the alkali content within rocks of similar SiO2 content. This demonstrates the distinct probability of alkali metasomatism. Whitehead and Goodfellow (1978) noted a similar case in the volcanic rocks of the Tetagouche group, Bathurst, New Brunswick. Their alkalies diagram was applied to the Blackdome rock suite (Figure 2.4). An erratic distribution of alkali contents is apparent from the spread in 13 of 18 samples lying outside the field of "average igneous rocks" as proposed by Hughes (1973). The diagram indicates that most of the Blackdome suite would be considered as felsic, >62% SiO_2, whilst only one sample, number 13, may be considered to be mafic to intermediate.

Standard samples were used to check the accuracy of analysis. It was determined by comparing the results of the external standards, with Abbey (1977), that the analyses are all within experimental error as given.

Due to the extreme variability of the alkali contents resulting from alteration, a plot using TiO_2 versus SiO_2 (Figure 2.5) was used to classify the host-rocks. This plot employed by MacDonald and Katsura (1964) in a study of Hawaiian volcanic rocks, employs relatively immobile elements and reduces the effect of metasomatism (Whitehead and Goodfellow, 1978). The data from the TiO_2 versus SiO_2 plot closely resemble those from the alkali versus silica plot and the volcanic suite is classified as subalkaline. However, the TiO_2 versus SiO_2 plot clearly depresses the volcanic suite well into the subalkaline region. Only one

FIGURE 2.4 Blackdome Volcanics: Alkalis (weight %) vs. $(K_2O/Na_2O+K_2O) \times 100$ (adapted after Hughes, 1973 and Whitehead et al, 1978)

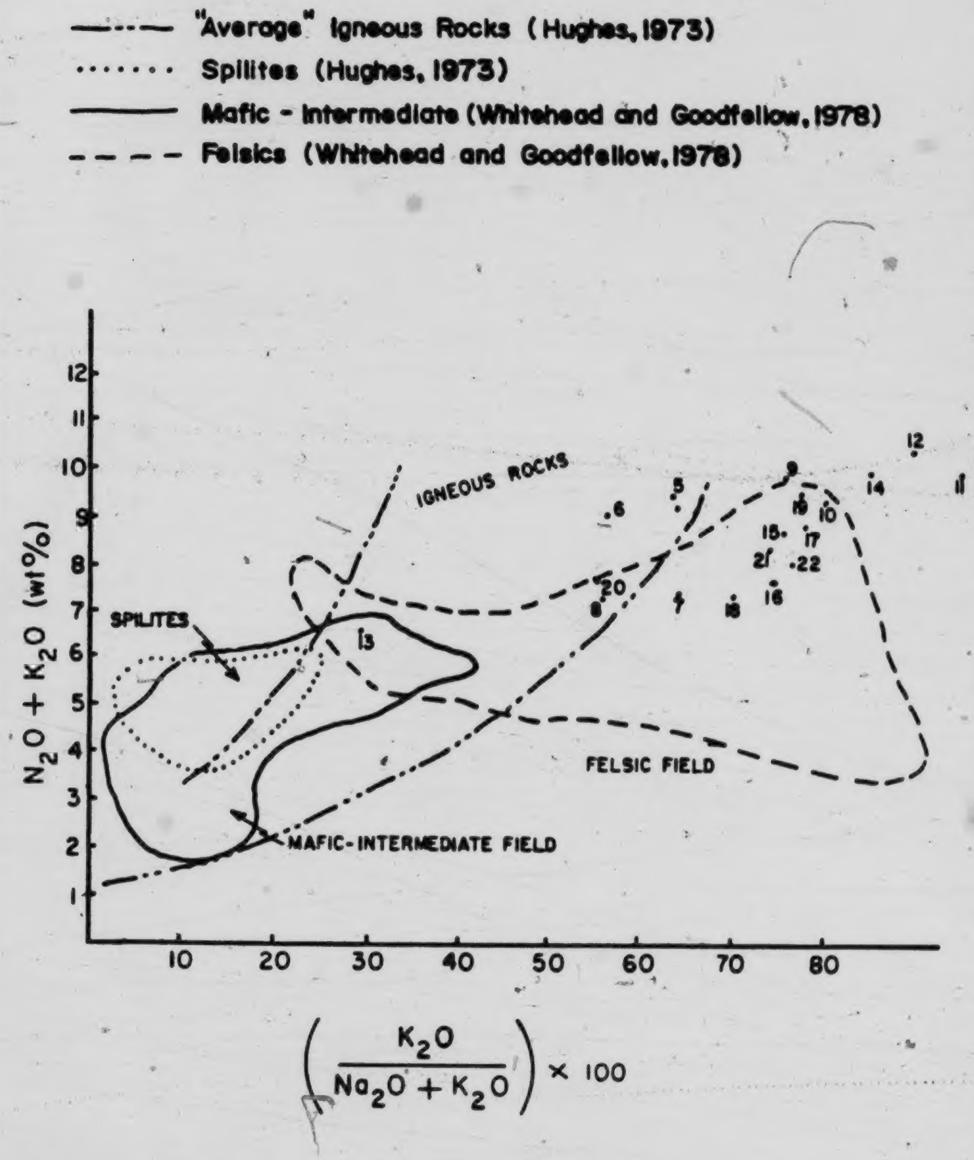

FIGURE 2.5 Blackdome Volcanics:
TiO_2 (weight %) vs. SiO_2 (weight %)
(adapted after MacDonald and Katsura, 1964)

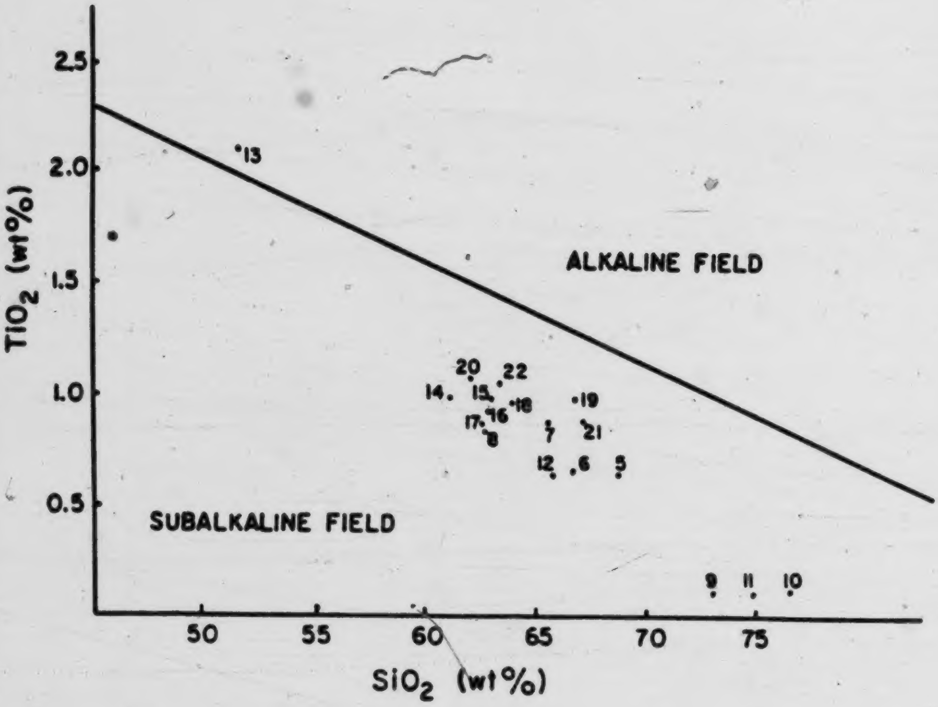

sample remains in the alkaline field and that same sample, number 13, is the only sample classed as a mafic-intermediate volcanic by Whitehead and Goodfellow's classification (Figure 2.4).

The distribution of samples on the AFM diagram (Figure 2.6) shows the Blackdome volcanic suite as belonging to a calc-alkaline magmatic series. The Al_2O_3 versus normative plagioclase composition generally helps verify this (Figure 2.7). The results of these plots are clearly subject to the effects of alkali metasomatism. The AFM diagram of Figure 2.6 (Irvine and Baragar, 1971) does not place any of the rocks within the tholeiitic field, while the Al_2O_3 versus normative plagioclase composition reveals 2 samples (Numbers 16 and 17) within the tholeiitic field. There is no iron enrichment trend apparent from the AFM diagram but there is a strong trend from iron depletion to alkali enrichment. In general, there is a strong affinity towards a dominant calc-alkaline rock suite, whilst a minor false affinity exists toward a tholeiitic source (Figure 2.7). The false tholeiitic source is felt simply to be a result of alkali metasomatism of the volcanic suite in certain sectors.

It is thus also evident that alteration has given an impression that on the basis of the major element classifications the volcanics of Blackdome are more felsic than they appear to be in terms of their mineralogy and modal compositions (Table 2.2).

FIGURE 2.6 Blackdome Volcanics:
AFM Plot
(adapted after Irvine and Baragar, 1971)

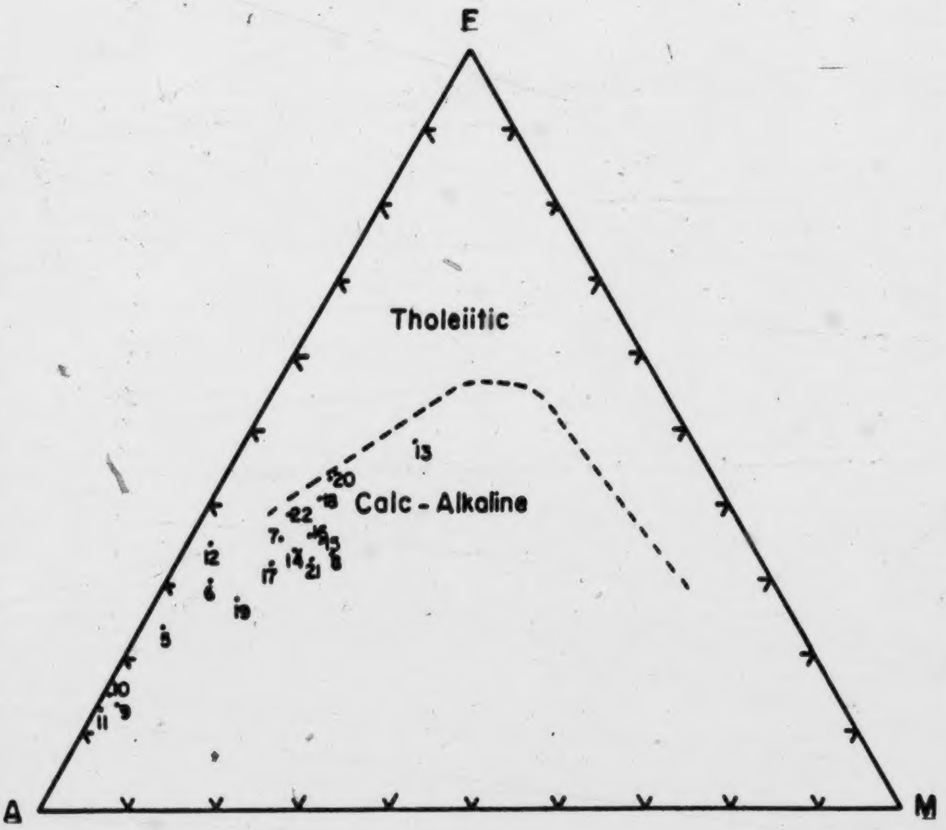

$A = Na_2O + K_2O$
$F = FeO + .9Fe_2O_3$
$M = MgO$

FIGURE 2.7 **Blackdome Volcanics:**
Al_2O_3 (weight %) vs. Normative Plagioclase Composition
(adapted after Irvine and Baragar, 1971)

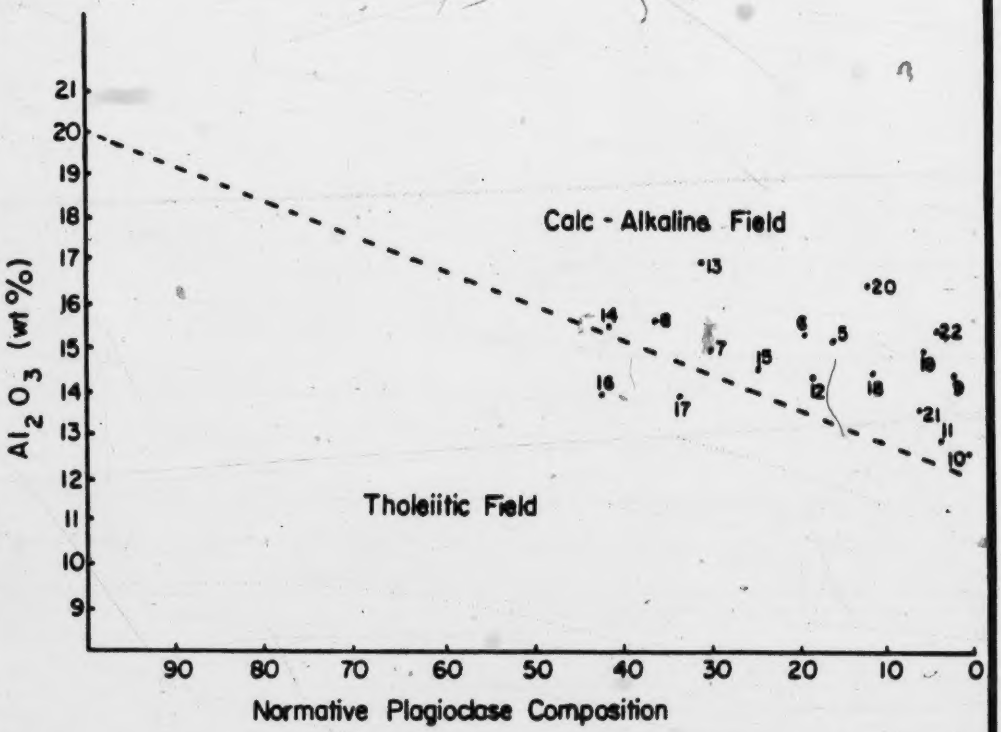

G. TRACE ELEMENT CHEMISTRY

Trace element geochemistry offers a potentially more discriminatory method of rock classification. The interpretation of trace element distribution in minerals has been outlined by three emperical rules devised by Goldschmidt (1937, 1954) which proved to have a very powerful influence on our understanding.

These are:

i) If two ions have the same radius and charge, they will enter into solid solution in a given mineral in amounts proportional to their abundances. A trace element is "camouflaged" by a major element (for example, Rb is camouflaged by K in alkali feldspar).

ii) If two ions have similar radii and the same charge, the smaller ion will be preferentially incorporated by the solid solution. The chemical bond is weaker for the larger ion, which is evident in a lower melting point.

iii) If two ions have similar radii and different charges, the ion with the higher charge will be preferentially incorporated by the solid solution. If the trace element has a higher charge than a major element, it is "captured" by the major element and becomes concentrated in the early crystallizing fractions of the solid solution. If the trace element has a lower charge than the major element, it is "admitted" by the major element and tends to be concentrated in the late-crystallizing solid solutions.

i) Trace Element Occurrence

A scheme to discriminate between alteration assemblages is clearly needed after viewing Table 2.2. There is a large discrepancy between Irvine and Baragar's classification and that of thin-section descriptions. Trace element occurrences are listed in Table 2.3.

The four most prominent trace elements are Ba, Rb, Sr and Zr. It was originally felt that the Ba was due to the presence of barite in the volcanic host-rocks. After close examination of thin sections of the host rocks and carrying out some X-Ray Diffraction experiments, it was determined that the Ba was most likely sited within Ba-feldspar (celsian).

Niobium, rubidium and strontium, with their higher radii and charges, are most easily substituted or camouflaged in feldspars (mostly for K, but some Na). These elements show an increase during the progression of igneous crystallization and are enriched in the residual liquids.

Zirconium occurs primarily in zircon but can substitute into pyroxene and magnetite. Zirconium's high charge and relatively large radius does not allow for substitution into common rock-forming minerals. Zirconium is abundant in late differentiates of igneous suites.

The rare earths Lanthanum and Yittrium show little tendency to substitute in essential minerals during magmatic crystallization, due to their specific charges and large radii.

TABLE 2.2

Irvine and Baragar versus Petrographic Classification

SAMPLE NO.	IRVINE/BARAGAR CLASSIFICATION (as per Figure 4)	PETROGRAPHIC CLASSIFICATION
06 - 7.5	not run	Andesite
06 - 12.5	not run	Andesite
06 - 37.5	Dacite	Andesite
06 - 45.0	Dacite	Dacite
06 - 50.0	Dacite	Andesite
84 - 15.0	Andesite	Andesite
84 - 50.0	Rhyolite	Rhyolite
84 - 70.0	Rhyolite	Rhyolite
84 -100.0	Rhyolite	Rhyolite
84 -120.0	Dacite	Andesite/Dacite
129 - 10.0	Andesite	Basalt/Andesite
129 - 40.0	Andesite	Andesite
129 - 60.0	Dacite	Andesite
129 - 80.0	Andesite	Dacite
129 -110.0	Andesite	Andesite
137 - 20.0	Dacite	Dacite
137 - 30.0	Rhyolite	Andesite
137 - 45.0	Dacite	Andesite
137 - 55.0	Rhyolite	Andesite
137 - 75.0	Rhyolite	Andesite

Note: Sample Numbers are quoted as the DDH Number and Depth in metres.

TABLE 2.3 Trace Element Geochemistry Data

Sample No.	As	Ba	Ce	Co	Cr	Cu	La	Mo	Ni	Nb
			(all values in ppm)							
06-37.5	4	1419	35	4	0	10	26	0	6	17
06-45	8	1406	35	4	0	13	27	0	4	19
06-50	8	1344	36	13	23	8	17	0	14	13
84-15	3	910	25	12	17	22	20	0	14	11
84-50	25	1074	17	0	0	5	10	47	6	19
84-70	8	941	36	0	0	6	32	0	2	18
84-100	9	1185	17	0	0	7	21	0	6	16
84-120	19	1360	59	0	0	22	36	0	4	23
129-10	8	282	33	24	42	34	19	0	42	21
129-40	10	816	33	15	29	26	16	0	19	10
129-60	13	699	42	22	27	25	22	0	18	10
129-80	8	644	16	11	26	14	18	0	18	10
129-110	11	687	35	18	29	29	10	0	21	10
137-20	75	732	20	16	29	28	15	0	23	11
137-30	21	742	13	9	29	29	5	0	24	10
137-45	33	944	19	13	34	32	15	0	25	11
137-55	17	663	19	16	29	25	13	0	21	11
137-75	128	825	11	15	33	33	15	0	24	12

TABLE 2.3 Trace Element Geochemistry Data- continued

Sample No.	Pb	Rb	S	Sr	V	W	Y	Zn	Zr
			(all values in ppm)						
06-37.5	14	157	30	193	29	3	29	76	434
06-45	13	133	324	253	30	2	30	75	456
06-50	15	143	35	282	67	5	23	63	194
84-15	16	111	47	341	67	0	20	54	183
84-50	18	220	49	94	13	9	16	23	225
84-70	18	206	43	64	8	2	29	19	240
84-100	23	295	33	261	8	0	27	44	226
84-120	16	243	9664	181	20	7	36	83	343
129-10	21	77	51	273	153	5	28	108	198
129-40	12	260	43	230	98	4	22	63	155
129-60	13	208	35	136	98	5	17	65	144
129-80	12	181	29	166	94	0	19	63	139
129-110	13	225	80	136	83	4	17	68	154
137-20	14	162	31	127	110	3	19	71	147
137-30	11	236	14	145	98	4	18	70	154
137-45	14	131	0	308	103	5	19	77	161
137-55	14	195	37	113	109	6	18	68	142
137-75	13	199	22	148	108	8	21	74	150

The La and Y in the volcanic host-rocks of Blackdome probably represents replacement of Ca^{2+} in accessory apatite. It is also possible that some substitution of rare earths in the epidotes took place during late-stage events.

Vanadium occurs mostly in magnetite, proxying for Fe^{3+}. It's radius is greater than that of the ferric ion, but its electronegativity is much lower. Vanadium's crystal field of stabilization energy is higher. These two factors are responsible for vanadium being enriched in early-formed magnetite. Vanadium may also occur in pyroxenes, amphiboles, and biotite.

Arsenic and molybdenum can be tetrahedrally coordinated with oxygen in silicate liquids to form three dimensional networks, often called network-forming elements. These elements are usually excluded from tetrahedral coordination in silicate minerals (Ringwood, 1955b) and are thus concentrated in later low-temperature residual liquids, representative of later stage fractionation.

Cobalt is a divalent ion comparable in size to ferrous-iron ion and is therefore camouflaged into ferrous components. The Co:Fe ratio is greatest in early-formed minerals and decreases steadily with increasing fractionation. Cobalt may also be removed in early-formed magnesian minerals. Chromium is present in magmas as the Cr^{3+} ion. The radius of Cr is similar to that of Fe^{3+}, but Cr shows a higher degree of preferential concentration relative to the ferric ion. Chromium is removed in the early stage of crystallization in spinels.

The copper ion is a very difficult element to follow. It has been suggested that copper does not enter readily into the silicate minerals, due to a predictable but unusual lattice distortion, energy destabilization effect. It is this characteristic which makes Cu a variable quantitative element. Nickel has essentially the same radius and charge as magnesium and should be camouflaged in magnesian minerals. However, the Ni:Mg ratio is highest in early-formed crystals and shows a steady decline as fractionation continues. Ni competes successfully with Fe^{2+} and Mg^{2+} for octahedral lattice sites.

The most abundant of all heavy elements, Pb, is found in silicate material of many igneous rocks. Pb exhibits a diadochic substitution for the K+ ion. Due to lead's ionic charge, it should be captured by potassium minerals, such as feldspars, but the larger electronegativity weakens this tendency and Pb is admitted rather than captured by potassium minerals.

Sulfur was detected as a trace element and shows a relatively low concentration. This may be due to the fact that sulfur occurred within the H_2S gas phase and in the case of this explosive suite the gaseous phases were frequently depleted. Sulfur concentration also reflects the sulfide content of the rocks, especially sample 13 which shows visible pyrite.

ii) Trace Elements as Compositional and Tectonic Classifiers

Trace elements have been used more frequently as discriminating classifiers of altered volcanic rocks than have the major elements. The major oxides of SiO_2 and TiO_2 were used with trace element chemistry to produce a realistic composition and tectonic environment for the host rocks of the No. 1 vein.

The two diagrams suggested by Winchester and Floyd in 1977, SiO_2 vs Zr/TiO_2 and Zr/TiO_2 vs Nb/Y are the best discriminants.

The SiO_2 vs Zr/TiO_2 diagram (Figure 2.8) suggests the volcanic host-rock suite to be more intermediate in composition and range from andesitic to dacitic in character. A problem arises in the fact that this diagram still uses SiO2 and most of the host rocks from Blackdome appear to have been affected by some degree of silicification. This diagram is thus still not totally discriminatory and applicable.

From the standpoint of classifying the host-rock suite, the Zr/TiO_2 vs Nb/Y diagram is the most discriminatory diagram. This diagram reveals the closest agreement in classifications with the petrographic classifications. The six samples which plot as being felsic (dacite to rhyolite) are the same samples that were classified as being felsic on the basis of petrography. There is a very slight disagreement with a couple of samples

FIGURE 2.8 Blackdome Volcanics:
SiO_2 (weight %) vs. Zr/TiO_2 (ppm)
(adapted from Winchester et al, 1977)

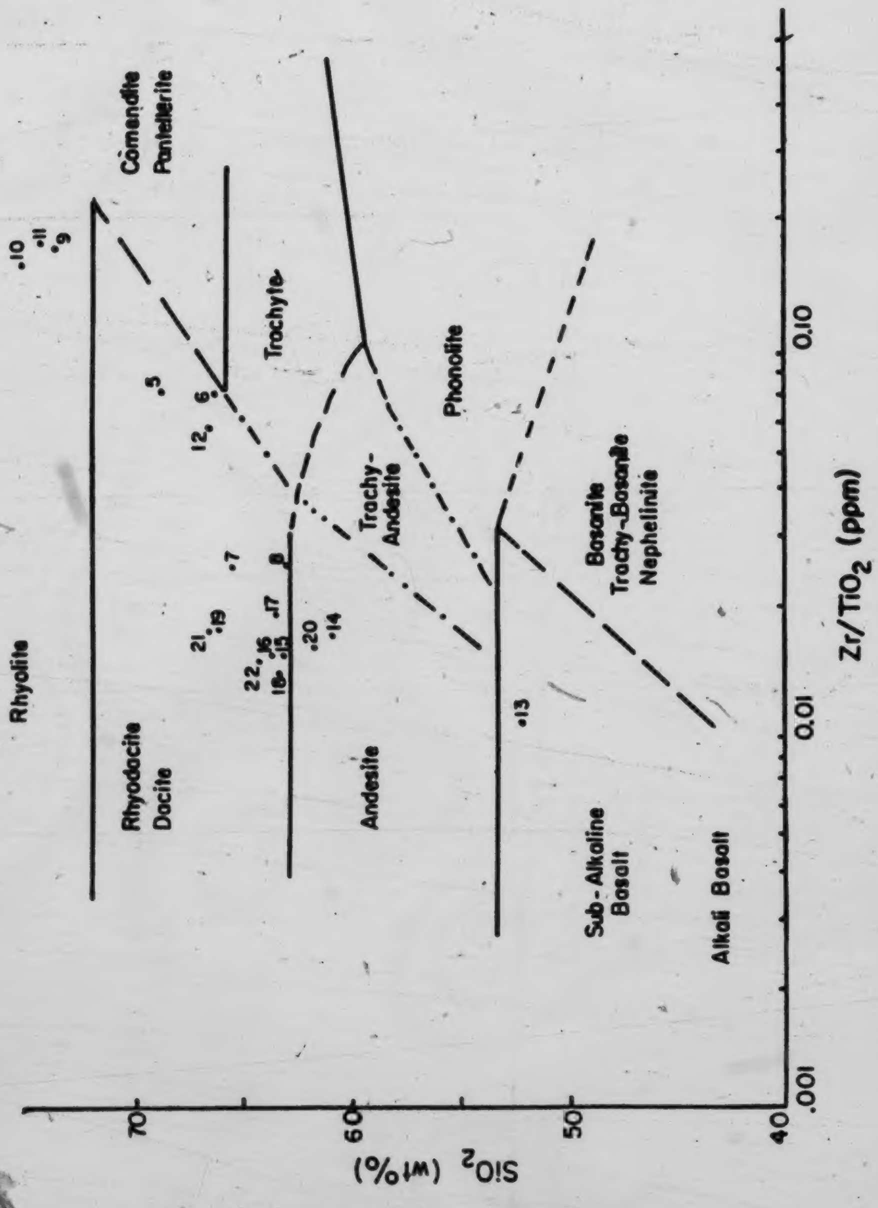

(numbers 16 and 18), but this may be due to the slight variation in the zirconium values (Figure 2.9).

The classification of a tectonic environment allows for some cross-use between major element-oxide data and stable trace element data. The following diagrams help classify the orogenic environment of the Blackdome volcanics:

The Ti-Zr-Y ternary diagram (Figure 2.10) displays a slight calc-alkaline trend in this assemblage. This diagram is clearly more applicable to mafic metavolcanic rocks, as most of the Blackdome suite lies outside the four main classification fields. These samples show very little variation in composition using these relatively immobile elements. The Pearce and Cann (1973) diagram is of some use in classifying more intermediate- to felsic- assemblages. Here the samples plot closer to the calc-alkaline basalt-volcanic- arc field. Ti-Zr-Y are difficult elements to use for classification of evolved compositions due low concentrations in these type of environments.

As has been suggested by Goff (1984), Fe/Mg could be seriously affected by Mg mobility and Fe/Cr was found to be too sensitive to Fe-enrichment. Thus, total Fe as FeO, for an anhydrous composition, was plotted against Zr/TiO2. A calc-alkaline trend shows a FeO depletion through time and therefore a negative slope results (Figure 2.11). This diagram presents the clearest separation between tholeiitic and calc-alkaline suites than any existing plot.

FIGURE 2.9 Blackdome Volcanics:
Zr/TiO_2 (ppm) vs. Nb/Y (ppm)
(adapted from Winchester and Floyd, 1977)

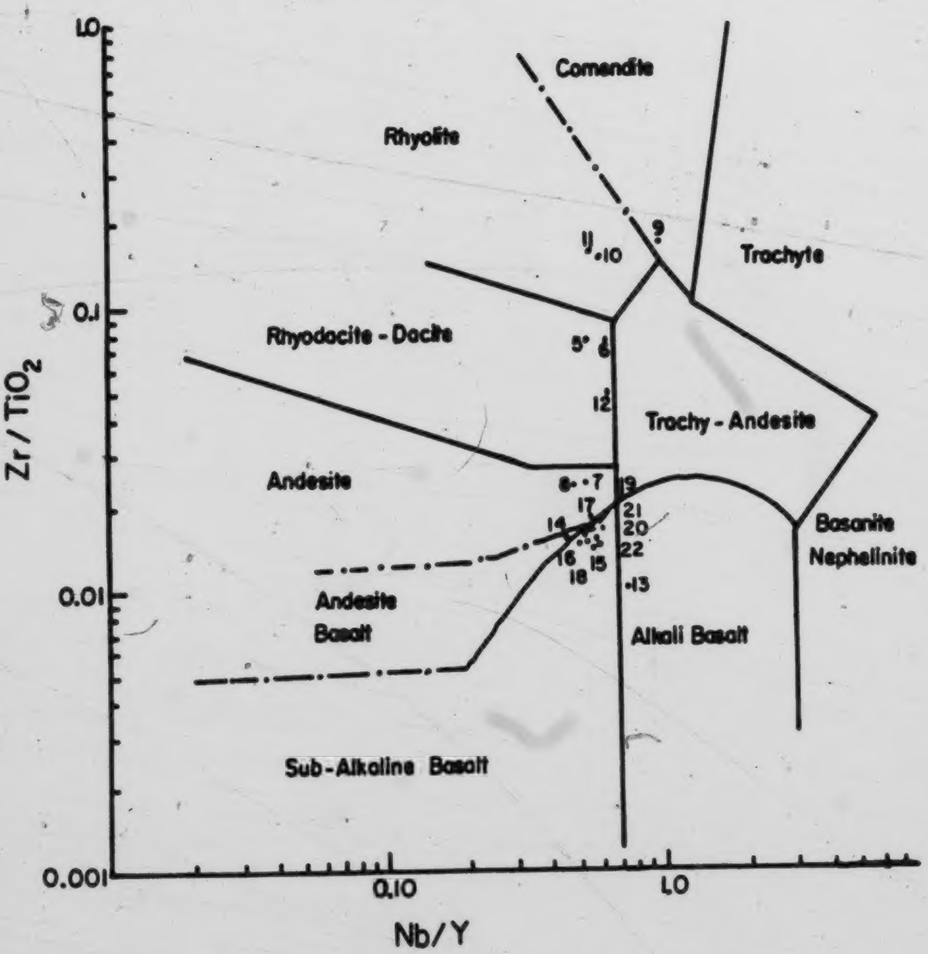

FIGURE 2.10 Blackdome Volcanics:
Ti-Zr-Yx3 Plot
(adapted after Pearce and Cann, 1973)

A: Low K-Tholeiites
B: Ocean Floor Basalts, Low K-Tholeiites, Calc-Alkali Basalts (Volcanic Arc)
C: Calc-Alkali Basalts (Volcanic Arc)
D: Within Plate Basalts (Ocean Island or Continental)

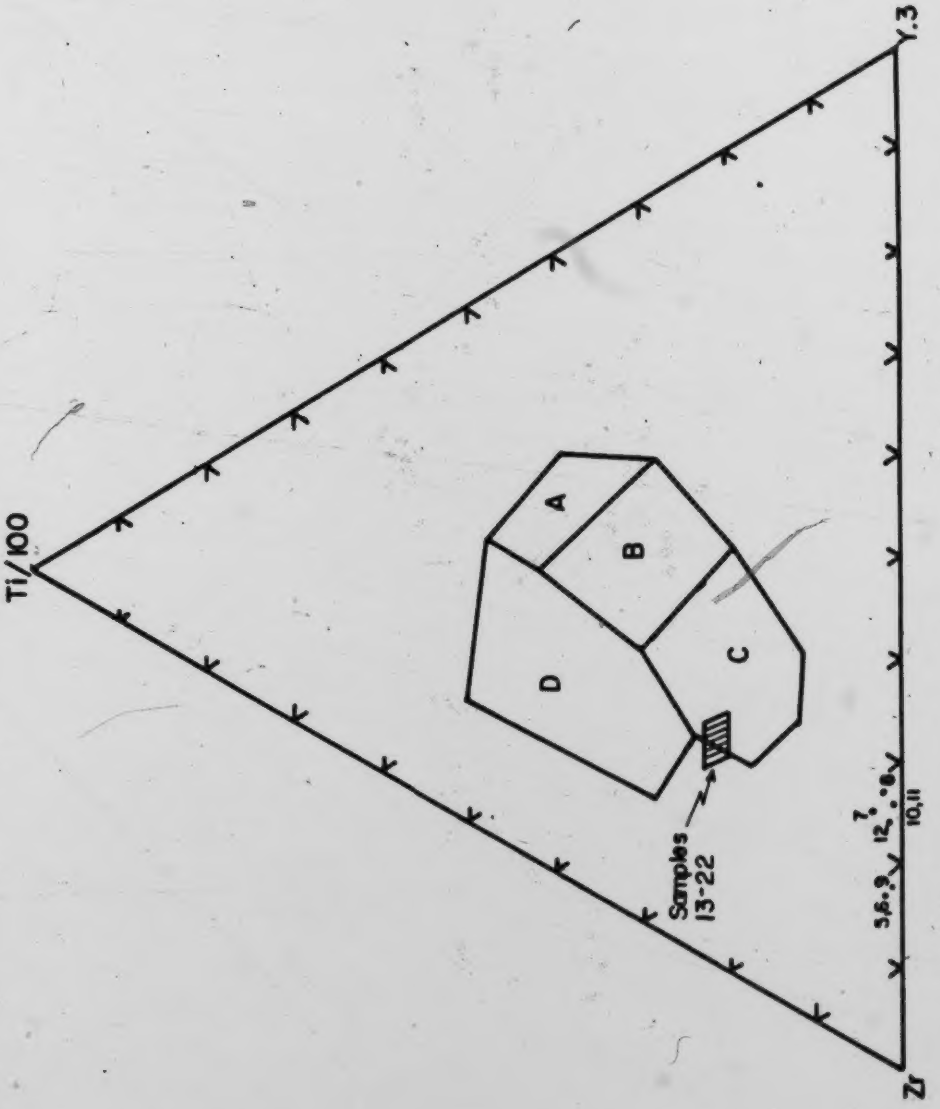

FIGURE 2.11 Blackdome Volcanics:
FeO*(weight %) vs. Zr/TiO$_2$ x10^4
(adapted after Goff, 1984)

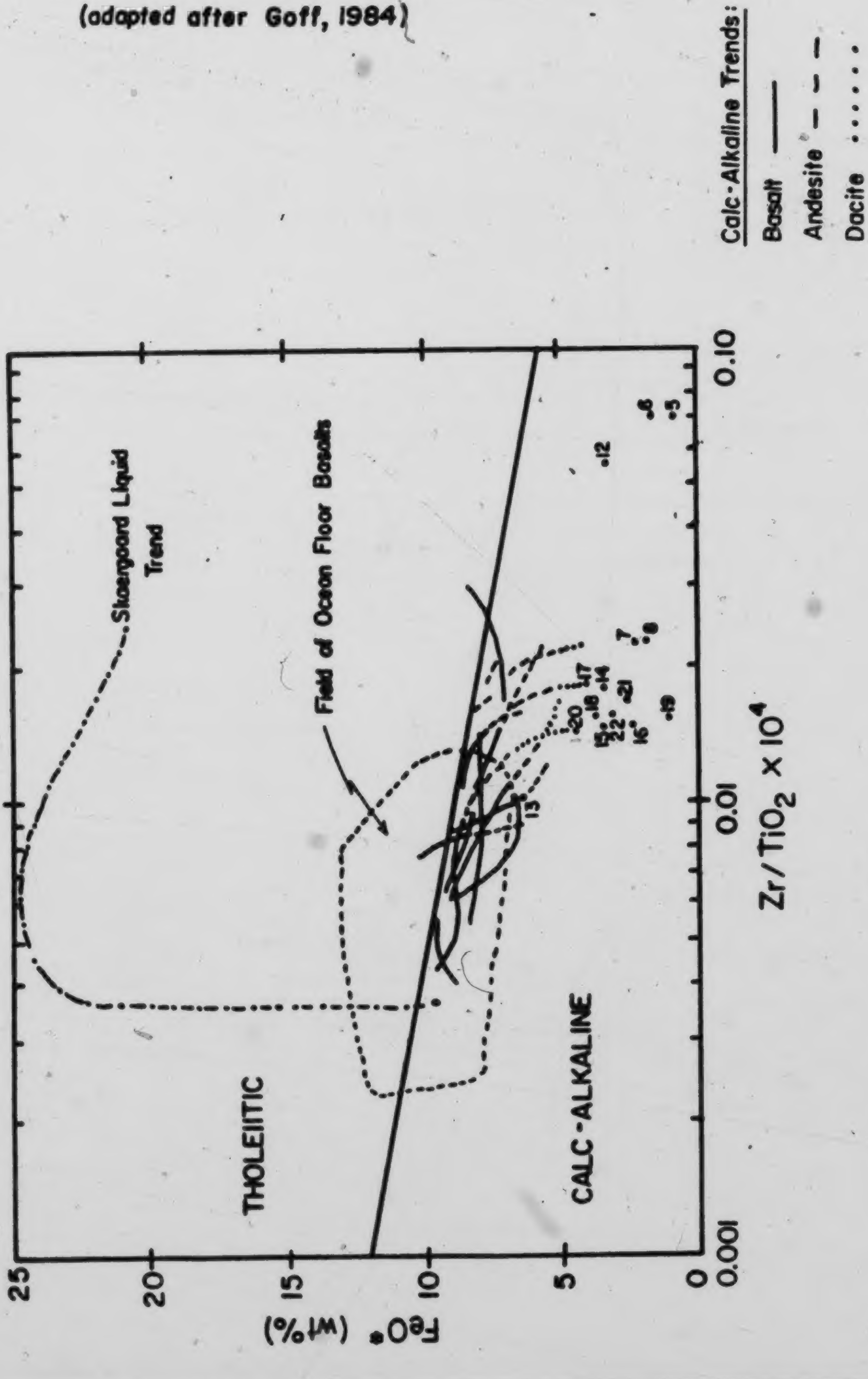

The diagram which plots ratios of Nb/Y vs Zr/P_2O_5 is the best discriminatory plot for rocks that contain higher alkali compositions (Figure 2.12). This diagram, as suggested by Floyd and Winchester (1975) and de Albuquerque (1979), shows no meaningful tectonic discrimination, due to a very high transition zone or overlap. This diagram has been used to classify a number of altered volcanic suites, but there has never been a detailed check as to the consistency in classification of these plots. The Blackdome suite is situated well within the continental tholeiitic field and specifically the oceanic floor and island tholeiite field.

The TiO_2 vs Zr and Y vs Cr diagram (Figure 2.13) of Pearce (1980) shows the clearest classification of within plate and arc mafic to felsic suites yet available. Pearce has adopted, using stable trace elements, proxies for alkalies, iron and magnesium. The dividing lines are associated with suites of Phanerozoic compositions that have been analyzed. This diagram presents a clear calc-alkaline trend. Pearce (1980) suggests that basalts can show a very wide scatter on this diagram. Sample 129-10 represents basaltic to andesitic composition and was the most mafic rock analyzed. This sample lies outside the calc-alkaline trend.

H. CONCLUSIONS

The Blackdome Ag-Au vein in British Columbia is hosted within a suite of calc-alkaline volcanic rocks. The

FIGURE 2.12 Blackdome Volcanics:
Nb/Y vs. $Zr/P_2O_5 \times 10^4$
(adapted after Floyd and Winchester, 1975,
and de Albuquerque, 1979)

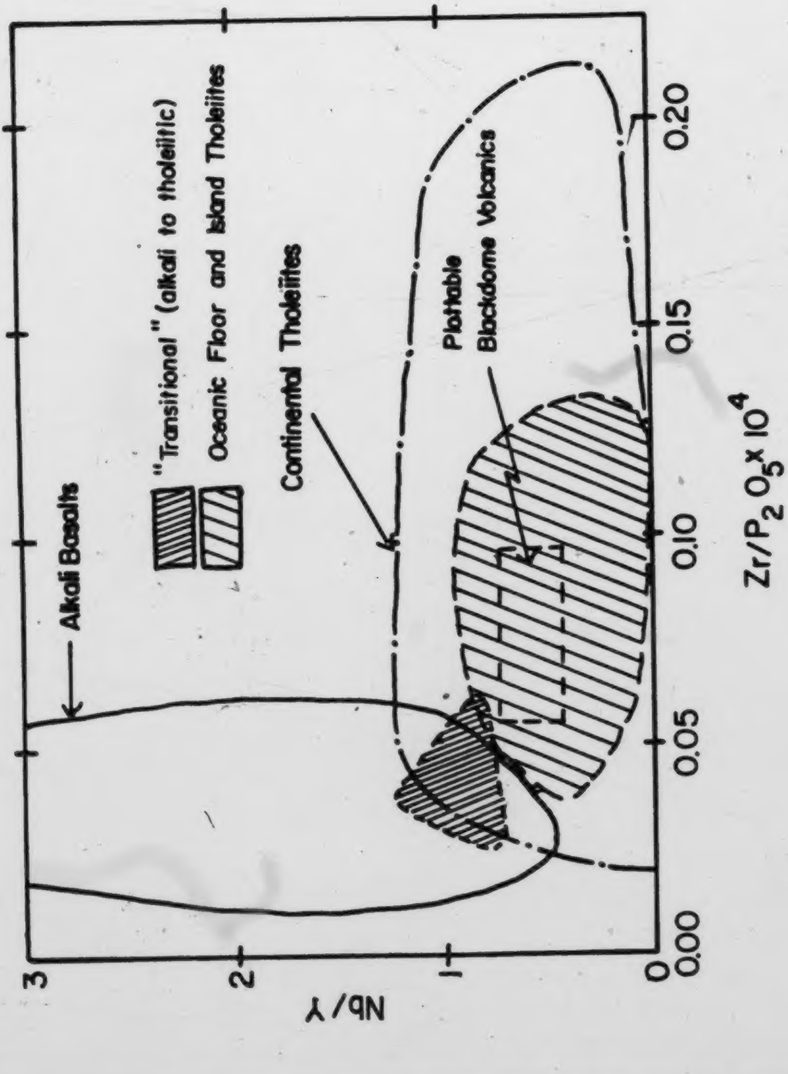

FIGURE 2.13 Blackdome Volcanics:

Zr Y - TiO_2 - Cr

(adapted after Davies et al, 1979)

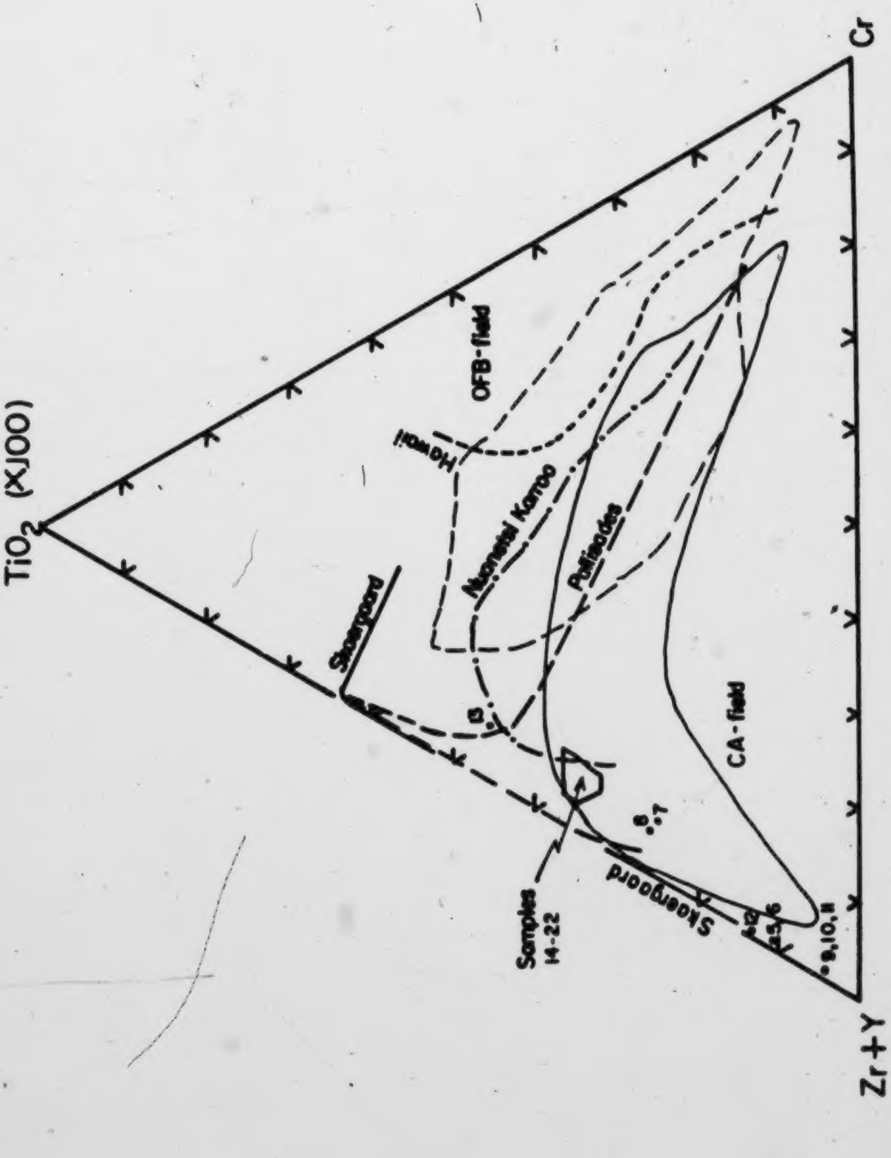

host suite ranges from being slightly mafic to strongly intermediate, with a felsic component within the environs of the vein system. Specifically the host rocks are dominated by andesites (and minor basalt) with a substantial component of dacitic and rhyolitic rocks.

The mineralogy of this suite is dominated by variable anorthite contents of the plagioclase phenocrysts, minor pyroxene, amphibole, potassium feldspar and quartz. The modal percentages are a function of bulk chemical composition and potassium feldspar and quartz become more abundant in the later differentiates.

The textures of the Blackdome volcanic suite suggest that flows were dominant and a significant pyroclastic component was present.

The host volcanic assemblage adjacent to the veins is hydrothermally altered and has replacive sericite, kaolinite/ montmorillonite/illite, chlorite, epidote, carbonate, quartz and potassium feldspar (adularia).

In the environs of the Blackdome Ag-Au vein system, major oxide data were not sufficiently discriminatory, either as compositional or as tectonic classifiers, as major silicification and K-metasomatism are primary alteration effects. The Blackdome volcanics were more easily and accurately classified on the basis of immobile trace elements (Ti-Zr-Y-Nb), as well as using total Fe as FeO due to high mobilities of Mg and Cr with respect to Fe. It was shown that the host rocks of the Blackdome veins are calc-alkaline and originated within a volcanic-arc system. This volcanic-arc constituted part of Stikinia (Monger et. al., 1982), an allochthonous component of the Canadian Cordillera that was accreted on to the North American continent.

III. CLAY MINERAL ANALYSES OF THE BLACKDOME NO. 1 AG-AU VEIN SYSTEM

The Blackdome Ag-Au vein system in south-central British Columbia is considered to be of "epithermal" origin. The alteration patterns seen within the Blackdome drill core correspond to well-documented alteration packages in other "epithermal" systems. It is not the intent of this study to document fully the major zonal distributions of alteration, rather, the objective is to concentrate upon local argillic alteration adjacent to the fault/mineralized zone.

This Ag-Au system has not been tested to any great depth. Twenty drill core samples, from 6 diamond drill holes, were selected to represent the alteration at Blackdome. Thus, the present study constitutes a limited view of the alteration package. It is hoped that the results will shed some light upon the physical and chemical restraints within the mineralized zone and the immediate wall rocks.

A. CLAY MINERAL ANALYSES

i) Smectite

Throughout the fault/ore zone the abundance of smectite is variable and constitutes between 0% (sample 01-10.3) and 67% of the clay fraction.

Primary identification of smectite was based on the 001, 002 and 004 reflections and the corresponding d-spacings of 16.9-17.2A, 8.5A and 4.2A, respectively. Upon Ca-glycolation smectite was characteristically identified by a reflection at 17A. Saturating smectite with K+ and heating to 300°C and 550°C collapses smectite to a 10A reflection as outlined by Foscolos (Ignasiak et al, 1983), Table 3.1:

Table 3.1 Treatments for the Identification of Smectite and the Corresponding d-spacings

Treatment	Ca-54%	Ca-glyc.	K-0%	K-54%	K-300°C	K-550°C
Smectite	15-16A	17A	10A	12-13A	10A	10A

The smectite composition appears to be of dioctahedral character based upon the X-ray diffractograms of Brindley and Brown, page 171(1980) (Figure 3.1). Dioctahedral smectites reveal the appearance of the (060) reflection at a d-spacing of 1.48 A to 1.50 A. The trioctahedral smectites reveal (060) reflections in the order of 1.525 A to 1.56A. It is suggested that the smectites in the Blackdome samples are either montmorillonite or beidellite. Evidence from Thorez (1976), in a table from Harward et al, 1969 (Table 3.2) and upon scanning electron microscope work (see appendix III) suggests the montmorillonitic smectite varies from being very well crystallized to poorly crystallized. The peak to valley ratio (indicated in Figure 3.2a, after Biscaye, 1965) is a first order approximation of crystallinity (excellent crystallinity shows peak:valley ratios of much greater than

FIGURE 3.1: Diffractometer patterns of a Ca-montmorillonite, Saponite and Hectorite. Note the patterns of the Ca-montmorillonite (dioctahedral smectite) vs. the patterns for Saponite and Hectorite (trioctahedral smectites). The dioctahedral smectite reveals a lower d-spacing than the trioctahedral smectites for the (0$\bar{6}$0) reflection (adapted after Brown, 1961).

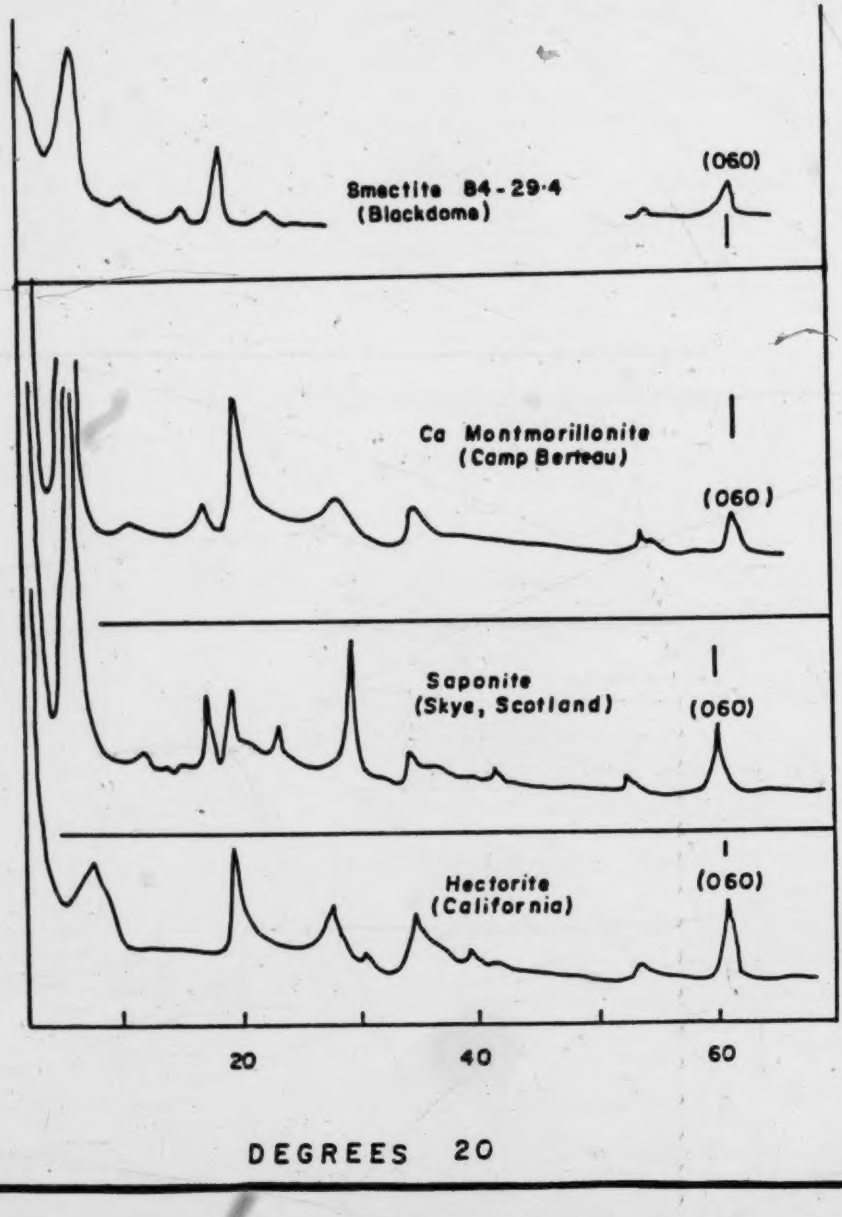

FIGURE 3.2

DISCRETE ILLITE

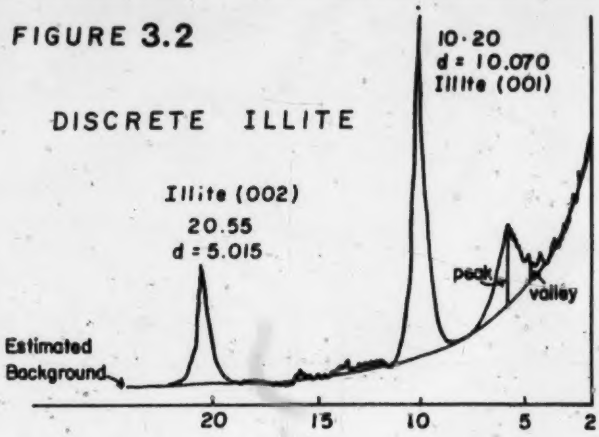

Vertical Scale = 1×10^3

Horizontal Scale = 1cm = 1°2θ

BLKDM 06 - 24.5

(Ca^{++} — glycolated)

FIGURE 2b

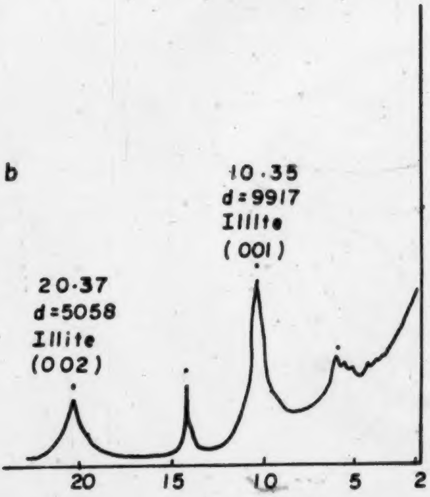

Vertical Scale = 4×10^3

Horizontal Scale = 1cm = 1°2θ

BLKDM 84 - 26.3

(Ca^{++} — glycolated)

MIXED LAYER — ILLITE / SMECTITE

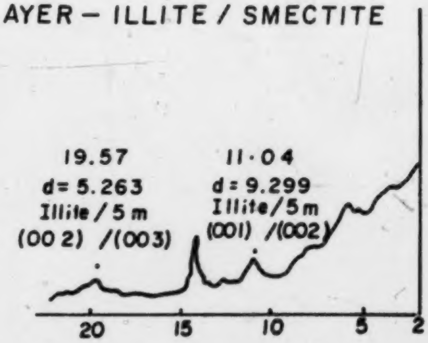

Vertical Scale = 2×10^3

Horizontal Scale = 1cm = 1°2θ

BLKDM 139 - 156.2

(Ca^{++} — glycolated)

NOTE: FIGURE 2b REVEALS THE MOVING 10 Å PEAK

0). The smectites which exhibit poorer crystallinity may be coincident with low smectite abundance.

Table 3.2 Treatment of K+ at 54% Humidity for Distinguishing Montmorillonite From Beidellite

Saturating cation	Moisture conditioning	Montmorillonite d(001)A	Beidellite d(001)A
K	54%RH	12-1	11.6

A scanning electron microscope with a Kevex energy dispersive analytical facility permitted identification of the major ions contained within the smectite structure. These ions are Ca++, K+ and sometimes Fe++ (the latter most likely is adhered to the surface of the smectite surface and explained by increased proportions of limonitic contamination, see the S. E. M. photo-micrographs in the appendix).

ii) Illite

The illite component identified in the fault zone has a characteristic d-spacing of 10.1A. Illite's (001) reflection is maintained at 10.1A, no matter what the treatment (figure 3.2a). The 10A peak is enhanced during heat treatments, due to the smectite component collapsing down to 10A.

Illite comprises the dominant clay mineral of the fault zone. Illite's abundance is variable with any given section, as can be seen from the 0% illite obtained in section 129-128.2 and the 94% illite obtained in section 06-24.5.

The illite, in most cases, was well crystallized, as can be seen from the narrow, relatively symmetrical peaks and the intense reflections. In the cases where the illites appear poorly crystallized, as represented by weaker, asymmetrical peaks and broad reflections, they probably represent degraded illites (the illite structure has undergone partial breakdown).

Most of the illitic material within the ore zone appears to be Fe-rich. The (001/002) reflection ratios are greater than 2 and sometimes approaching 3. This is typical of Fe-rich illite compositions (Thorez, 1976).

The illite appears to be a dioctahedral illite, on the basis of the intense, relatively sharp, basal reflections and the high (001/002) reflection ratios. Identification of illite has been confirmed by use of the scanning electron microscope (see Appendix III).

iii) Chlorite

Chlorite, in the fault zone, has the characteristic 14A peak and upon heating to 550°C, the peak approaches 13.7A. One of the most prominent features is the lack of any intensification of the 7A peak upon heating. This is due to the breakdown of the brucite layer. The clay-chlorites in the alteration/fault zone are almost non-existent except for a couple of samples (both in DDH 139). Here the chlorite comprises less than 3% of the combined clay fraction.

The fact that the host rocks contain chlorite and the fault/ore zone almost lacks chlorite is probably best explained by the absence of wall-rock clasts within the ore zone across the sampled portions of the system. Chlorite only appears in the zone where the host fragments are most abundant.

The chlorite is fairly well-crystallized as it exhibits an integral series of basal reflections from the (001) reflection at 14A down to the (005) reflection of 2.8A. This chlorite is considered a normal or true chlorite on the basis of the increase in intensity of the (001) reflection upon heating to 550°C and the essential disappearance of the 7A peak. This more intense (001) reflection, upon heating, indicates that the chlorite is not Fe-rich (Thorez, 1976) and thus the chlorite is presumed to be clinochlore. The clinochlore classification from Martin (1955) and modified by Thorez (1975) is only a first approximation (Table 3.3).

Table 3.3 Proper Identification of Clinochlore

	No Treatment		550° C/30 min.	
Reflection	d(A)	I	d(A)	I
001	14.5	W	14	vs
002	7.2	S	7	almost gone
003	4.75	W	4.64	NA
004	3.55	M	3.53	NA

Clinochlore, in the Blackdome vein system, occurs as a trace constituent. The lack of clinochlore is probably attributable to the breakdown of the brucite layer, hence decomposition of the chlorites, which might be expected to exist.

iv) Kandite Group

In the oriented sample preparations, a kandite group mineral was identified by its (001) sequence of harmonic reflections. These reflections occur at 7A(001), 3.58A (002) and 2.37A (003). These three prominent reflections remain constant upon glycolation. The characteristic feature of this kandite is the disappearance of the 7A peak upon heating to 550^{o}C. It is concluded that this mineral is kaolinite (sensu stricto). The basis of this identification is the work of Thorez (1976), (Table 3.4).

Table 3.4 Oriented Aggregates - Reflection Characteristics for Kandite Group

Kaolinite (sensu stricto)	Kaolinite (disordered)	Metahalloysite	Halloysite Hydrated or De-hydrated
4.43A,4.35A and 4.15A disappears. Intensity of 7.1 and 3.56A are increased	4.43-4.12A low intensity 7.1 and 3.56A increase intensity	4.4-4A band with I=7 and 3.56A	No 10A peak reveals tailing towards 7A.

The kaolinite identified throughout the vein/ alteration/ore zone is clearly dioctahedral, since trioctahedral kandites have higher (001) reflections than 7.1A (approaches 7.2-7.3A). This dioctahedral kandite is fairly well-crystallized, as can be seen from the relatively sharp and symmetric (001) and (002) reflections. The fact that both of these reflections are comparable in intensity also indicates good crystallinity. The scanning electron microscope was used to confirm the identification of kaolinite (see Appendix III).

v) Mixed Layer - Illite/Smectite

The classification of the illite/smectite mixed-layer composition is based upon the identification of moveable peaks, primarily the illite (001) reflection, between 9.7A and 10.19A (see Figure 3.2b). This peak rarely satisfies the discrete illite classification of 10.19A. The work of Hower (1981) and Srodon (1984) was used to identify these moveable 10A peaks (figures 3.3 and 3.4). These diagrams illustrate a range of illite or smectite contained within the mixed layer material. When two separate peaks can be used for identification, a range of values is obtained. When only one peak can be used, only a first order approximation may be derived. The abundance of illite/smectite in each sample is given in Table 3.6 listing the appearance and abundance of all clay fractions identified.

FIGURE 3.3 Position of the diffraction peaks for randomly interstratified illite/glycol smectite and ordered illite / glycol smectite in the calculation for abundance of illite. (adapted after Hower, 1981)

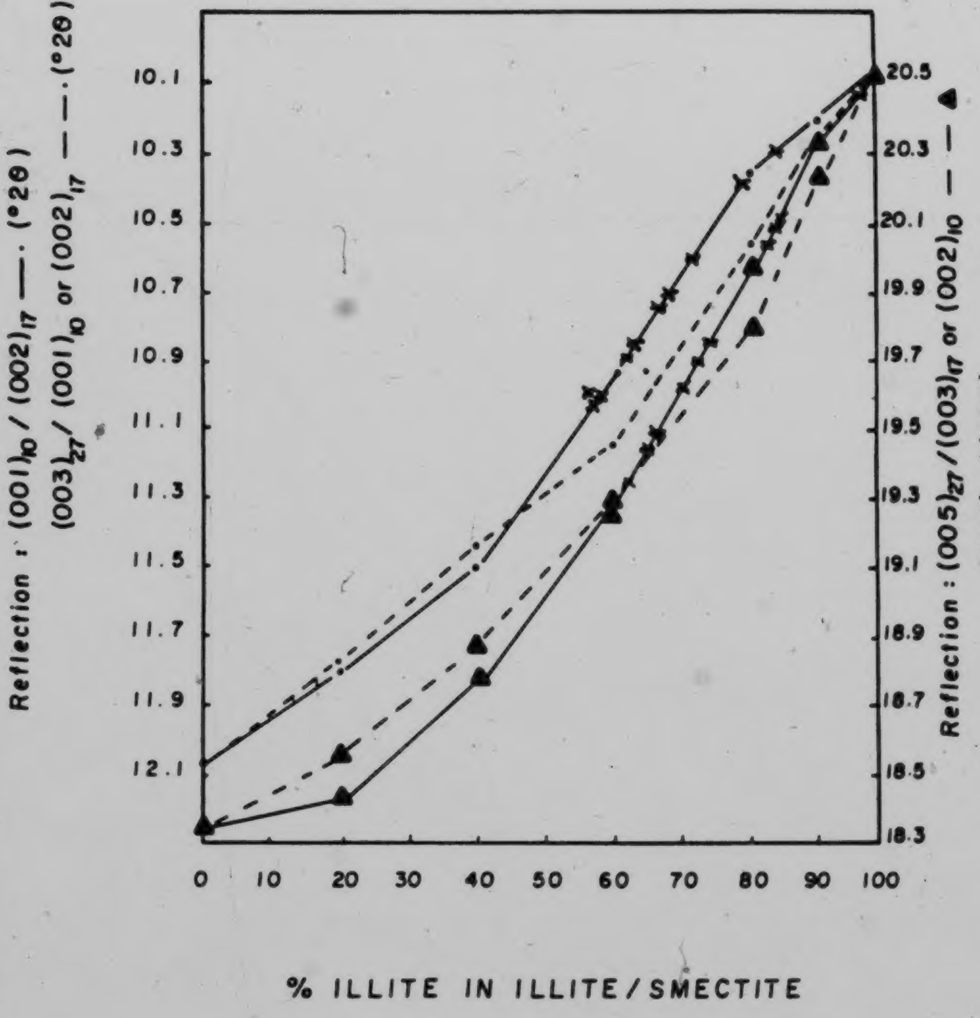

x - Blackdome sample points

FIGURE 3A: Plot for determining smectite : illite ratio using 002 and 003 reflections in ordered illite / smectites. (adapted after Srodon, 1984)

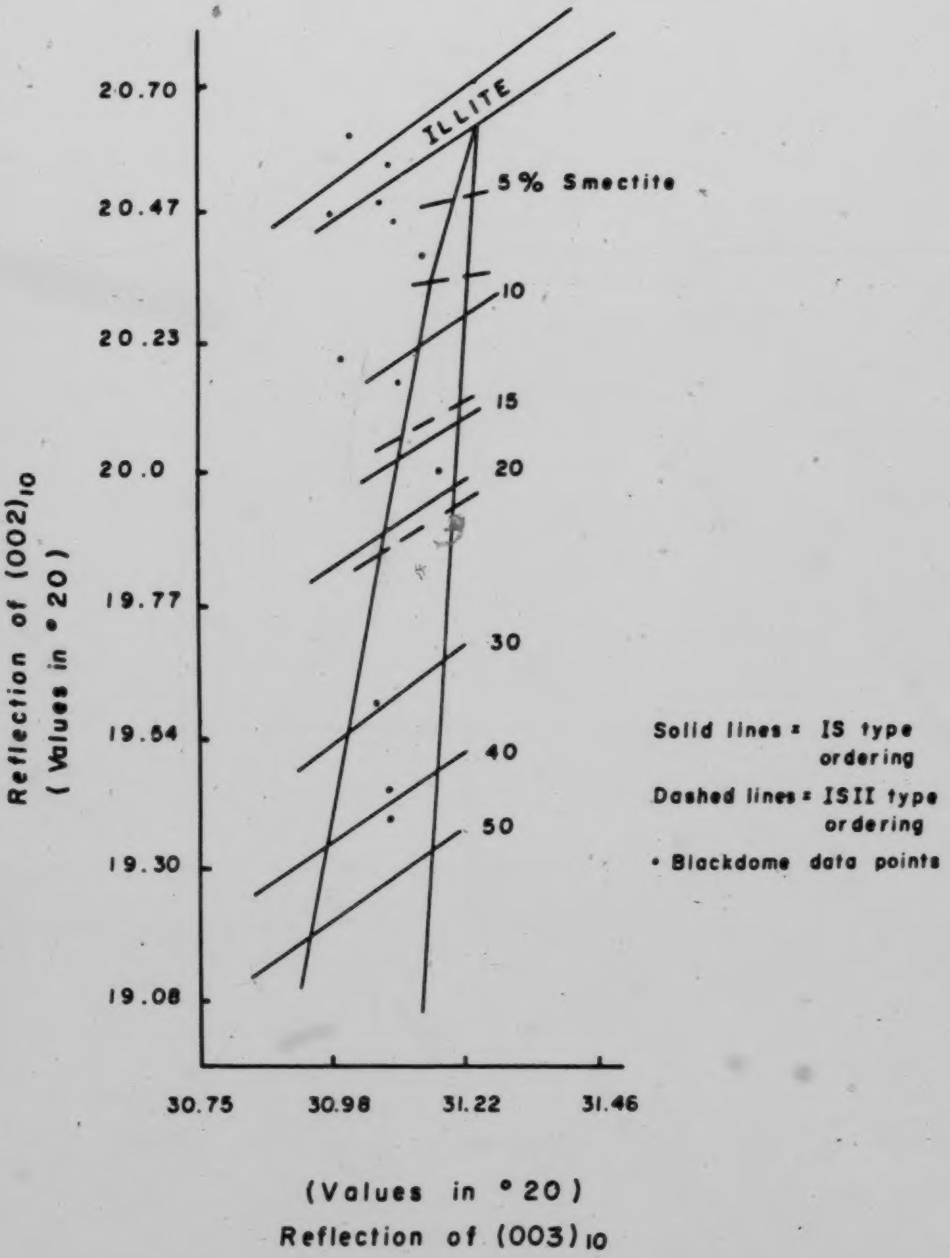

The illite/smectite mixed-layer composition identified within the Blackdome No. 1 vein system shows variable indices for nature of crystallinity. The interlayered material is poorly crystallized illite/smectite, as can be seen from the poor $(001)_{10}/(002)_{17}$ reflections. The poor reflections may also be a proportional representation of the abundance of mixed layered material in the samples.

The most common classification problem arises from the fact that the smectite diffraction peaks occurring at positions higher than 30°2θ cannot be used. This is due to the intense masking by feldspar and quartz reflections within this region. The type of ordering which occurs within the mixed layer illite/smectite is very difficult to determine when the higher angle reflections cannot be recorded. A first order approximation scheme for the estimation of the type of ordering is taken from Srodon, (1984) (figure 3.4). This diagram uses the BB1 reflection $[(002)_{10}/(003)_{10}]$ of the illite/smectite material to identify the ordering of the mixed layer material. The closer the BB1 reflection approaches the actual 10.19A peak for discrete illite, the composition of the illite/smectite moves from an IS (illite- smectite) type ordering to an ISII (illite- smectite-illite-illite) type ordering. If this is in fact the case, then the ordering of the illite/smectite mixed layer around the 10A peak is most likely approaching the ISII type ordering, due to its close proximity to the

10A peak. This, ISII type ordering, is in fact representative of most of the mixed layer material from the Blackdome suite.

A simplified scheme for the classification of the ordering of a mixed layer clay material is taken from Hower, (1981). This scheme allows most diffractograms of illite/smectite to be categorized in one of three categories outlined in Table 3.5.

Table 3.5 Compositional Variation of Interstratification of Illite/Smectites

	I/S Composition	**Number of Illite layers between each smectite**	**I/S Type**
Low T	0--60% illite	>0	random I/S
	~65-70--~85% illite	>1	"allevardite ordered" I/S
High T	~85--100% illite	>3	"kalkberg ordered" I/S

The classification scheme of Table 3.5 shows the majority of the mixed layer clay material at Blackdome to be characterized by "allevardite" type ordering. This would appear to satisfy the temperature regime at Blackdome, in that the illite/smectites are low- to medium- temperature types (<300° C). Illite/smectites approaching "kalkberg" type ordering would appear to be almost pure illites, which in fact can be the case. Pure illites may contain up to 10% smectite layers and still be classified as a pure end-member. There is some evidence at Blackdome (samples 139-156.2 and 139-155.2) of the "random" type ordering, representative of low temperature regimes. This could be explained by the initial transformation of smectite to illite/smectite at depressed temperatures (possibly less than 100° C). The data from Hower (MAC short course, Vol. 7, 1981, pgs 45-46) which allow determination of the abundance of illite in mixed layer IS are presented in figure 3.3. The smectite component in mixed layer I/S is revealed in figure 3.4.

Table 3.6 lists the final deduced compositions of all the clay samples analyzed. This table indicates the modal abundances of each clay fraction normalized to 100%. Only four of the samples analyzed were actually made up of a 100% clay fraction (these samples are indicated by an asterisk). The remaining samples contain a fairly high abundance of fault gouge material. This fault gouge material comprises vein quartz, K-feldspar (adularia+ orthoclase) and Na-feldspar (predominantly in the oligoclase/andesine compositional range). The Na-feldspar is indicative of host-rock fragments being caught up in the gouging event.

Opaque phases were recorded during the X-Ray diffraction analyses, but exact identification was left for reflected light microscope and microprobe analyses.

The practical application of identifying reflection peaks from two unbiased samples is shown in figures 3.5a and 3.5b.

TABLE 3.6. Clay Mineralogy Analyses of the Blackdome No. 1 Vein Zone

Sample Nos.	Kaolinite (%)	Illite (%)	Chlorite (%)	Smectite (%)	Il/Sm (%)	Total (%)
139-160	2	90	3	5	0	100
139-158.9	56	—	—	31	13(60)	100
139-156.2	57	—	—	13	30(58-68)	100
139-155.2	54	10	5	15	16(58-65)	100
139-152.7	17	—	—	63	20	100
139-151.4	34	28	—	38(10)	—	100
129-128.2	85	—	—	15	—	100
84-32.4	6	92	—	2(?)	—	100
84-31.5	59	13	—	22	6(?)	100
84-30.5	15	77(90-95)	—	8	—	100
84-29.4	3	80(87-93)	—	17(5)	—	100
84-28.2	32	27	—	34	7	100
84-26.3	15	81(85-90)	—	4	—	100
23-23.1	46	—	—	41	13(63-74)	100
23-20.1	56	—	—	36(10)	8(?)	100
06-24.5	—	94(90-100	—	6	—	100
06-17.5	49	—	—	—	51(74-80)	100
01-14.7	33	—	—	67	—	100
01-10.3	90	10(?)	—	—	—	100
1916-12120	67	—	—	—	33(63-69)	100

Note: All bracketed values indicate percent illite in the sample.

FIGURE 3.5a

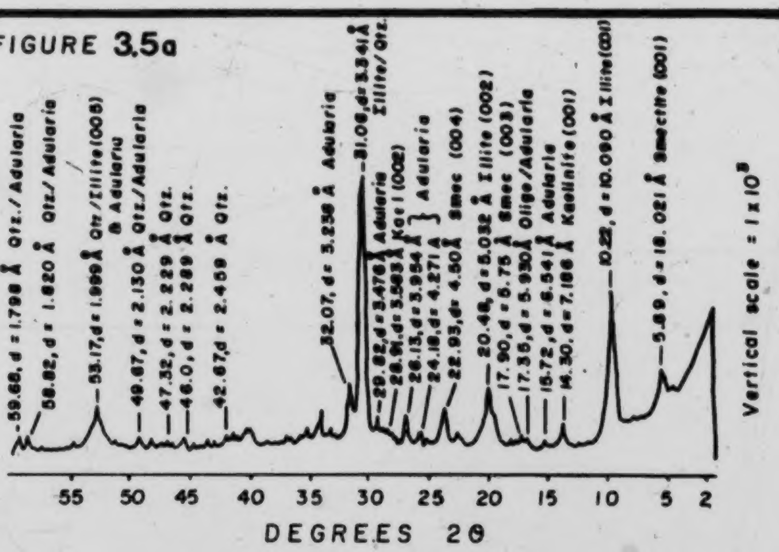

Sample is BLKDM 84-32-4 Ca^{++} glycolated

Note: Figure 5a shows the identification procedure of peaks by use of the J.C.P.D.S. cards. The remaining unidentified peaks in Figure 5a are all Adularia.

FIGURE 3.5b

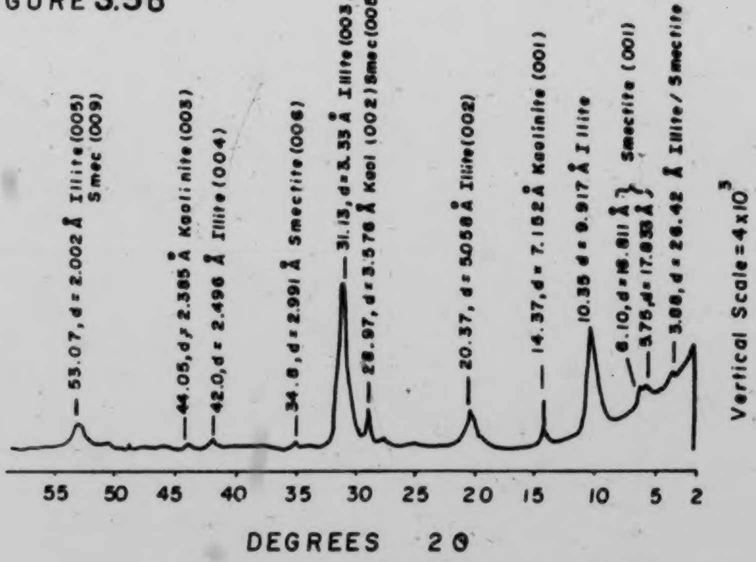

Sample is BLKDM 84-26-3 Ca^{++} glycolated

IDENTIFICATION PROCEDURE OF REFLECTION PEAKS

B. Non-Clay Fraction

i) Quartz

Accurate identification of quartz was based upon the appearance of very intense peaks at 4.26A and 3.343A. Higher angle reflections also permitted absolute identification of quartz (2.458, 2.282, 2.237, 2.128, 1.980 and 1.817A).

ii) Potassium Feldspar (Adularia)

The identification of the potassium feldspar component was derived from the appearance of numerous reflection peaks between 24°2Θ and 34°2Θ. The discrimination between K+- and Na+- feldspars is based upon the intensity and reflection angles of certain peaks.

It was determined that most of the potassium feldspar in the Blackdome suite was adularia. The basis for this conclusion is the presence of reflections found at 3.31, 3.29 and 3.24A. In contrast, orthoclase has a 3.31 and 3.18A peak in this area. The 3.31A peak for adularia and the 3.18A peak for orthoclase are the most intense peaks for these two minerals. There is some indication that orthoclase is also present with the adularia at Blackdome.

iii) Plagioclase Feldspar

The plagioclase feldspar in the Blackdome samples is derived from the host material which was caught up in the vein material as fault gouge. The plagioclase feldspar identification is based primarily on the 3.43 and 3.15A peaks. The potassium feldspars are not characterized by either of these peaks. The peak at 4.03A is a good discriminatory peak for plagioclase if there is no orthoclase. Throughout most of the Blackdome suite, orthoclase is absent.

The Blackdome plagioclase feldspar was identified as being in the range of oligoclase to andesine.

C. Discussion

The study of the clay minerals in the Blackdome Ag-Au vein was somewhat restricted, due to the limited depths of exploration to date. The deepest portion of the studied mineralized zone was 135 meters, whilst the shallowest was 15 meters. The horizon referred to at Blackdome as the No. 1 vein zone, shows a total depth variation of 120 meters along its strike. The physical control of depth appears to play only a minor role in the clay mineralogy of the Blackdome system.

It was felt that the composition of the clays would be most instrumental in revealing the possible chemistry of the fluid system.

The clay mineral analyses are best represented by figures 3.6-3.10. These figures reveal modal percentages of each clay fraction across the ore zone. Eight sections were chosen for analyses. Seven of these sections were selected primarily upon their representation of ore grade material

FIGURE 3.6 Diamond Drill Hole 139 —
Clay Mineralogy vs. Depth

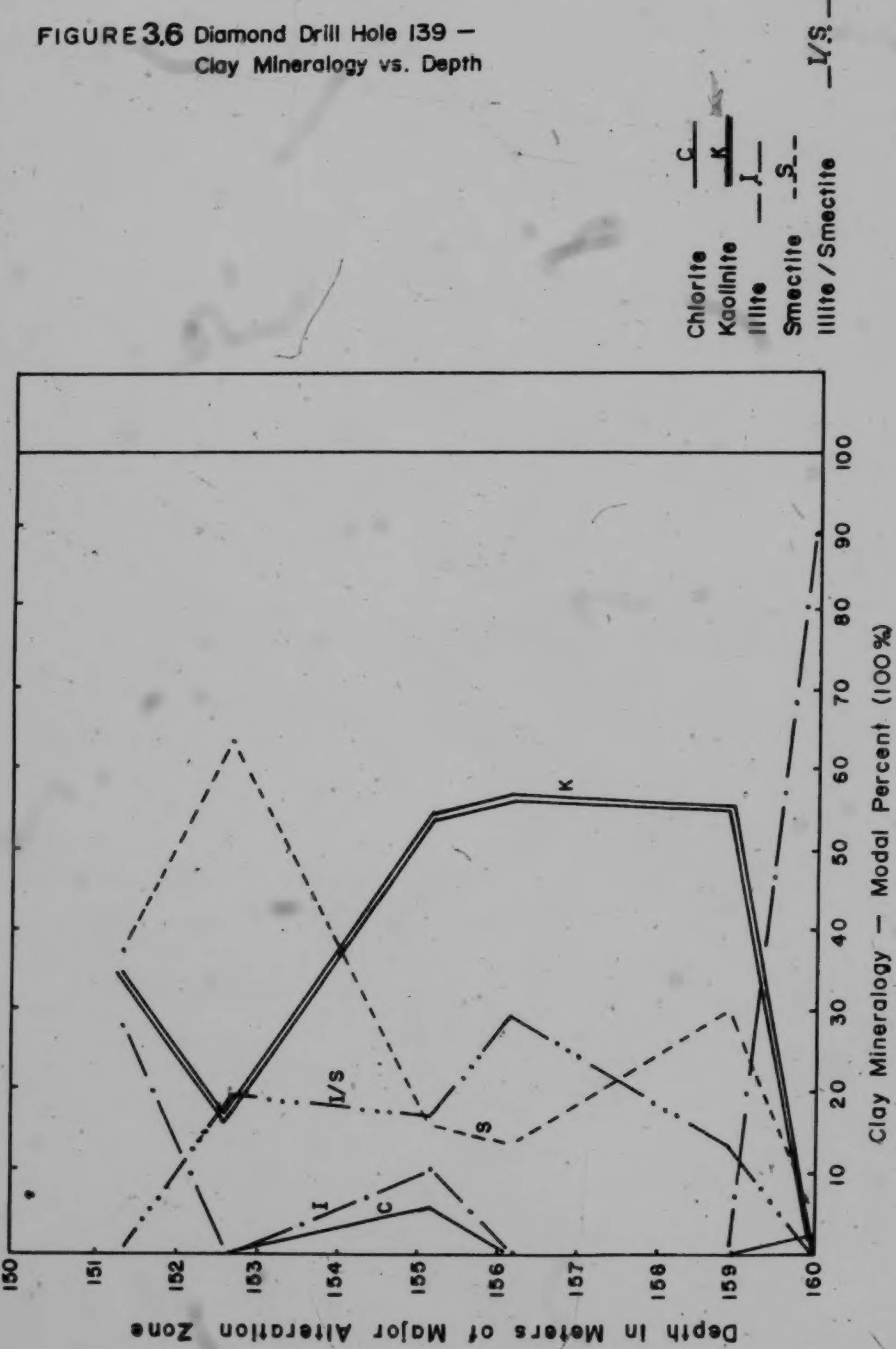

FIGURE 3.7 Diamond Drill Hole 84 — Clay Mineralogy vs. Depth

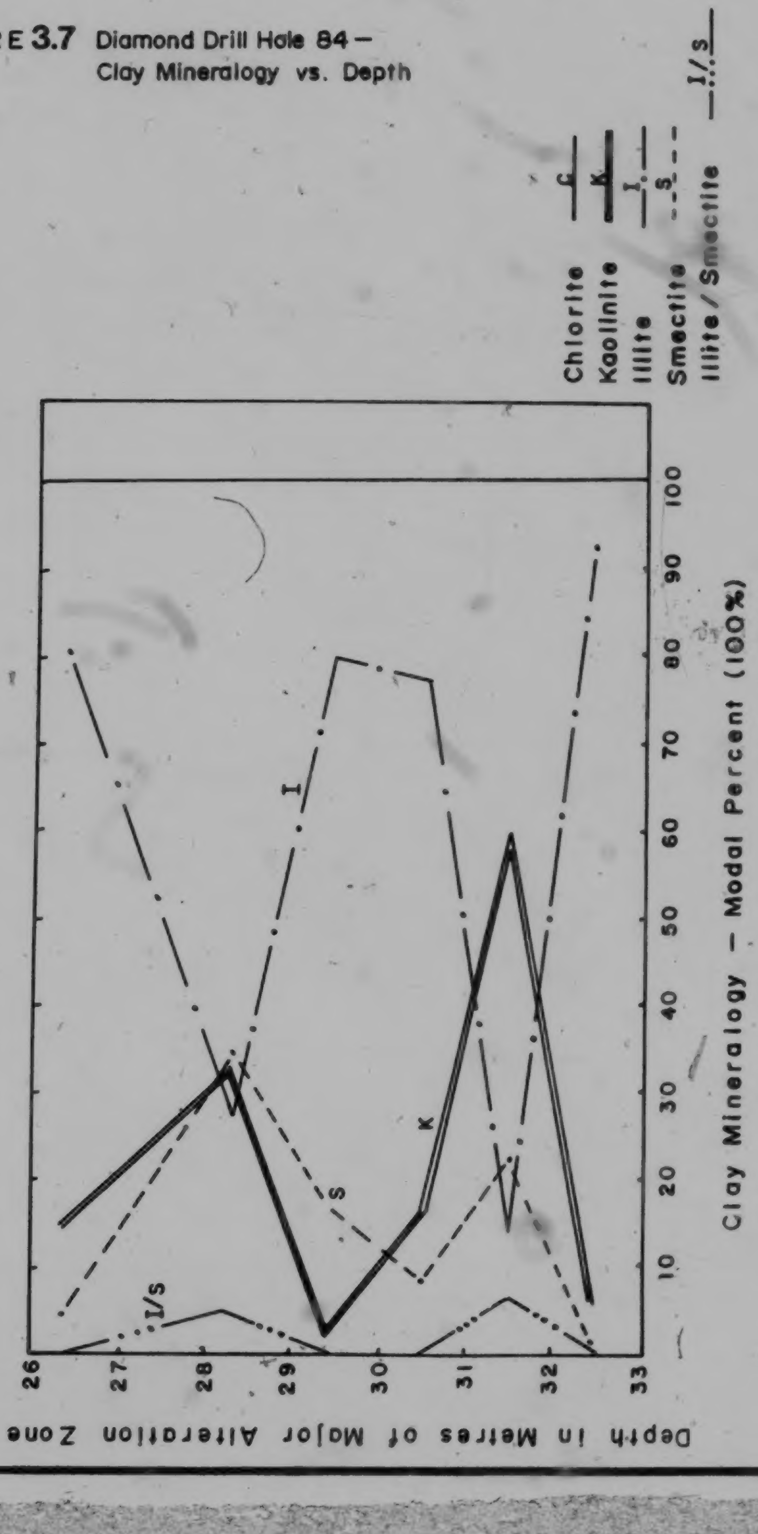

FIGURE 3.8

DIAMOND DRILL HOLE 23
CLAY MINERALOGY VERSUS DEPTH

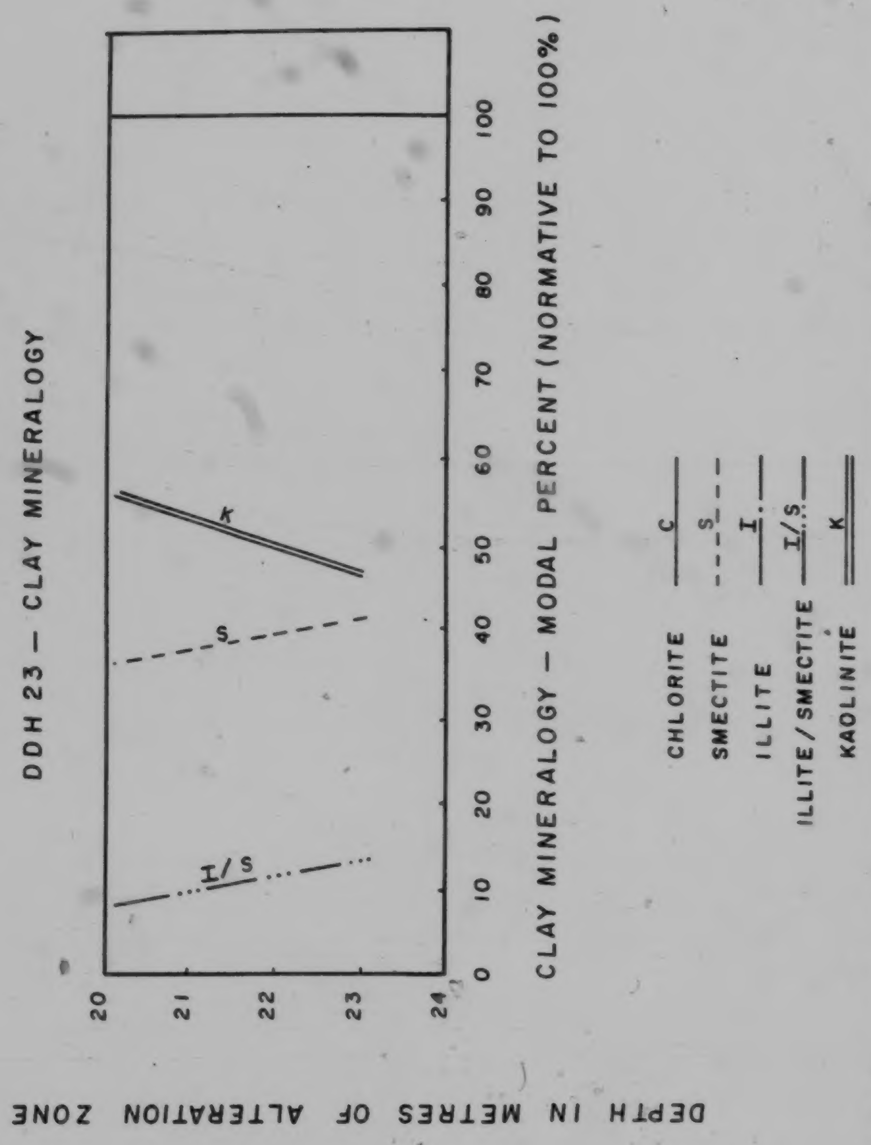

FIGURE 3.9

DIAMOND DRILL HOLE 06
CLAY MINERALOGY VERSUS DEPTH

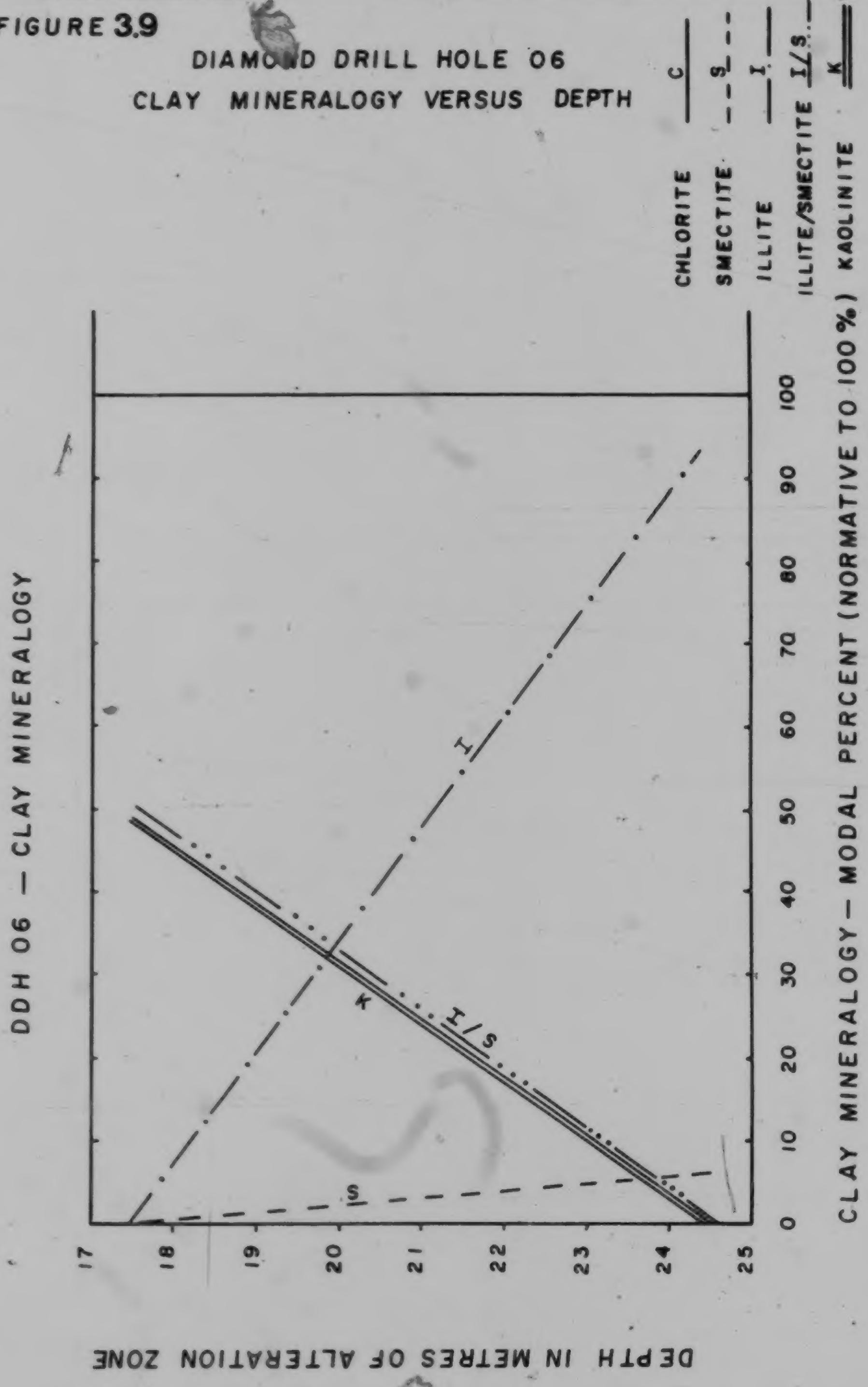

FIGURE 3.10

DIAMOND DRILL HOLE 01

CLAY MINERALOGY VERSUS DEPTH

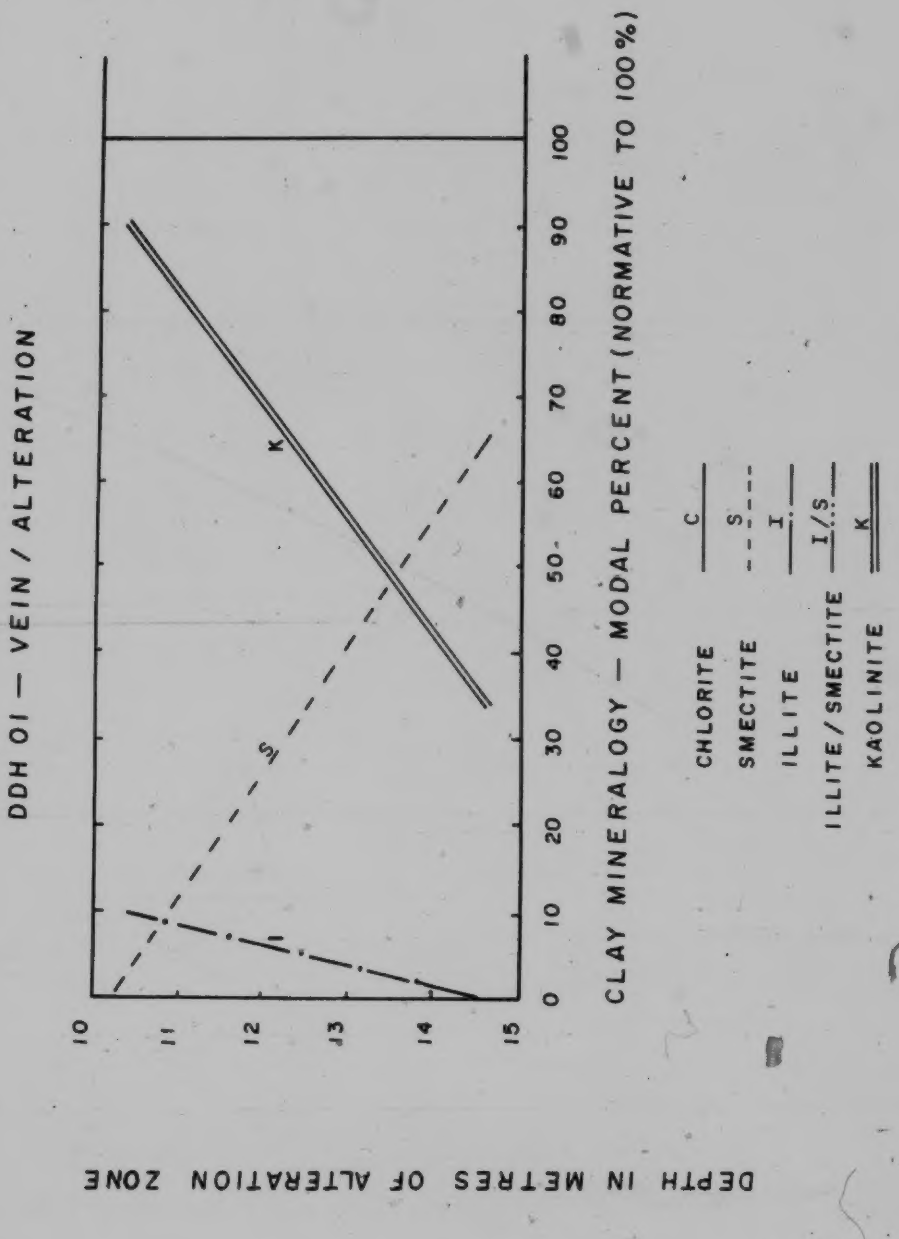

whilst the eighth (ddh 139) was selected for its extensive alteration package. Two of the drill holes (08 and 136) show very little alteration, (mostly silicification due to brecciation) and were therefore omitted from clay mineral analyses.

The clay minerals have formed at the expense and alteration of volcanic glass, plagioclase and to some extent ferromagnesian minerals and were precipitated into pores and cracks or fluid passageways.

Figures 3.6-3.10 reveal five major characteristics:

i) kaolinite and illite/smectite formed primarily from the transformation of smectite. DDH 84 indicates kaolinite did not form at the expense of smectite. An overprint of supergene alteration has probably increased the kaolinite content. To classify supergene kaolinite is not within the scope of the present study.

ii) illite shows an inverse relationship to kaolinite and illite/smectite. The formation of more illitic material occurs at the expense of the kaolinite and the randomly interlayered illite/smectite with increasing K^+ fixation in the interlayers (Steiner, 1968; Eberl and Hower, 1977; Srodon, 1980 and 1984).

iii) illite also shows an inverse relationship to smectite. Documentation, as above, suggests primary formation of illite occurs as a transformation/alteration product of the smectite component through an intermediate mixed-layer fraction.

iv) in dealing with a simple two component system, illite/smectite and smectite relationships are not discrete. Illite/smectite is an intermediate composition between smectite and illite, and can therefore be situated near either end-member making direct relationships indiscrete.

v) the chlorite component is insignificant within the ore zone and is thought to merely represent xenoliths of altered host material caught up in the system (fault gouge and cataclasts).

It has been shown (Steiner, 1968) (Figure 3.11) that the most common sequence of clay genesis is one of Ca-montmorillonite --- mixed-layer illite-montmorillonite (rich in interstratified montmorillonite) --- mixed-layer illite-montmorillonite (deficient in interstratified montmorillonite) --- and finally illite. Primary genesis of the kaolinite is through the alteration of feldspars by sulphuric acid-bearing solutions. These solutions form by the oxidation of hydrogen sulphide and/or pyrite by oxygen dissolved during the downward percolation of meteoric waters. It is suggested that the primary genesis of kaolinite at Blackdome was of two origins: i) supergene alteration occurring in temperatures not exceeding 60°C, and ii) hydrothermal formation occurring in temperatures above 100°C but not exceeding 230°C.

FIGURE 3.11 : The observed genetic sequence of hydrothermal alteration of silicic glass to illite.
(adapted from Steiner, 1967. Clay minerals in hydrothermally altered rocks at Wairakei, New Zealand.)

Silicic Volcanic Glass

⇓

Ca – Montmorillonite

⇓

Mixed-Layer illite-montmorillonite
rich in interstratified montmorillonite
10.40 Å to 12.45 Å

⇓

Mixed-Layer illite-montmorillonite
deficient in interstratified montmorillonite
10.16 Å to 10.28 Å

⇓

ILLITE
9.93 Å to 10.04 Å

The montmorillonite has been shown (by scanning electron microscope) to be a Ca-montmorillonite with, in some cases, significant amounts of K^+. This smectite was derived directly from the volcanic glass of the wall rocks. The primary formation of the Ca^{++} and K^+ montmorillonites took place at temperatures below 160°C. If there are in fact Fe-smectites, then the formation temperatures may have been as high as 200°C.

The mixed-layer clay fraction, illite/smectite, is dominated by ISII ordering due to the abundance of illite in the mixed-layer material. The ordering in some samples approaches IS, which reflects how far along the transformation process the system has developed. Suggestions have been made by Shimoda and Sudo (1960) and Sudo et al (1962) that the formation of the illite/smectite clay fraction occurs through the transformation of illite by way of retrograde metamorphism. This process might in the Blackdome case be a simple function of a cooling fluid system in its waning stages. The alteration of volcanic glass is a much more viable alternative. Eberl and Hower (1977) also reveal the hydrothermal transformation of potassium smectite into mixed-layer clay and then to illite (Figure 3.12). The starting composition has to be K-rich. The temperatures are elevated compared to most "epithermal" systems. Their genetic sequence is: glass(K-rich) --(1)-- 100% expandable K-smectite --(2)-- I/S random + kaolinite + SiO_2 --(3)-- I/S ordered +/- pyrophyllite + SiO_2. The vital

FIGURE **3.12** : The observed genetic sequence of hydrothermal alteration from a $K^{\pm}$ rich starting composition to a mixed-layer clay. *(modified after Eberl and Hower, 1977. The hydrothermal transformation of Sodium and Potassium smectite into mixed-layer clay).*

$K^{\pm}$ rich starting composition
(temperatures between 260° C and 400°C)

⇓

100% expendable potassium smectite

⇓

illite / smectite ramdom + kaolinite
+ $SiO2$

⇓

illite / smectite ordered ± pyrophyllite
+ $SiO2$

transformations in this sequence are 2 and 3 in the conversion into illite layers. Conversion occurs primarily through the substitution of Al^{3+} for Si^{4+} and the net negative charge on the 2:1 layers is balanced by an increase in interlayer potassium. Substitution of Al^{3+} for Si^{4+} continues until the attraction between the 2:1 layers and interlayer potassium is greater than the attraction between potassium and its shell of hydrating water. The potassium dehydrates, water is expelled from the interlayers and potassium becomes fixed, converting the expandable smectite structure into that of an illite.

Reaction of K-smectite layer being converted to an illite layer is as follows:

$$\overset{\text{(K-smectite)}}{Al_2Si_{3.66}Al_{0.34}O_{10}(OH_2)K_{0.34}} + \overset{\text{(water)}}{0.57H_2O} =$$

$$\overset{\text{(illite)}}{0.43Al_2Si_{3.2}Al_{0.8}O_{10}(OH)_2K_{0.8}} + \overset{\text{(kaolinite)}}{0.57Al_2Si_2O_5(OH)_4} + \overset{\text{(quartz)}}{1.14SiO_2}$$

It should be noted here that kaolinite is one of the resulting products of the reaction of K-smectite with water. This occurs through the coupled ionic substitution where Al^{3+} substitutes for Si^{4+} and K^+ is needed to balance the net negative charge. The net result of the coupled substitution is to release Al^{3+} and Si^{4+} to form kaolinite and SiO_2.

The predominant temperature range for the formation of the illite/smectite mixed-layer clay appears to be ~160°C to 230°C.

The illite component in the Blackdome system is composed of 10A material. It is believed that some of the illitic material was generated by the breakdown of larger mica-like fractions (some biotite, muscovite and sericite). The primary origin of most of the illitic clay material was through the breakdown and transformation of other precurser clay materials, such as mixed-layer clays. As stated earlier, Steiner suggests the progressive transformation of volcanic glass to illite represents the primary genetic sequence for clays in a hydrothermal system. This has been proven by Eberl and Hower (1977) as well, using a starting composition of K-rich material. The Blackdome "plumbing" system was clearly potassium-rich.

The formation of illite is based upon the availability of K^+ to the system. The proper temperatures have to be reached to permit transformation of illite/smectite to illite. The temperature range for the expected transformation of illite/smectite to illite is approximately 230°C. Kristmannsdottr (1978) suggests that temperature may be the major controlling factor in the alteration process where the original rocks are similar, the geothermal fluid is of the same origin, permeability is high and the effects of the overburden pressure is insignificant. These are all criteria that are satisfied at Blackdome. The association of illite and adularia in the Blackdome system suggests that they both derive their potassium from ascending geothermal fluids.

Chlorite in the vein zone or fluid passageways at Blackdome is very limited. Chlorite is more dominant in the permeable host rocks. It is felt that the appearance of chlorite in the Blackdome "plumbing" system is due to the alteration of host-rock xenoliths in the fault zone. The lack of chlorite in the overall system at Blackdome would seem to suggest the chlorite had not formed from a montmorillonite precurser but from the alteration of original ferromagnesian minerals in the host material. The temperature range for chloritic clays can occur over a wide range.

There are some discrepancies noted in the clay analyses shown in figures 3.6-3.10 (ore zone analyses). One of the major discrepancies occurs with respect to the kaolinite. Kaolinite is most probably of dual origin in the Blackdome system; the first being supergene, and the second being hydrothermal. It is not within the scope of this thesis to discriminate between the two sources, hence some problems arise during the interpretation. There is a minor discrepancy noted within the ore zone with reference to mixed-layer clays. DDH 01 at 10.3 metres reveals only illite (10%) and kaolinite (90%). At 14.7 metres DDH 01 has smectite (68%) and kaolinite (32%). There is not an intermediate illite/smectite component noted. Irregularities like this may be the result of varying permeabilities and hence, uneven concentration of K^+ ions in the solution. The result is a variance in the [illegible] of montmorillonite layers. The illite/smectite component that might be expected in DDh 01 is absent due to poor permeabilities and therefore no potassium fixation. It should be noted that the illitic component measured in this section could be a fine-grained mica fraction. The 10A material may not be a genetic clay, which would then indicate there has been little or no potassium fixation at this point in the Blackdome system.

D. Conclusions

The study of the clays in this Ag-Au bearing vein system has been somewhat cursory and confined to shallow depths. Yet, it has given a valuable insight into some of the physical/chemical characteristics of the No. 1 vein system.

The clay mineral analyses carried out on the ore zone material reveals five major clay phases. These clay phases are kaolinite, Ca^{++} - K^{+} montmorillonite, mixed-layer illite/smectite (with varying illitic layers), illite (all 10A phases) and chlorite.

The clay analyses have revealed the important roles the K^{+} ion, and to a lesser extent the Ca^{++} ion, have played in the alteration within and around the veins.

Clay genesis in the Blackdome "plumbing"system was dominated by the chemistry of the alteration of the silicic and/or potassium-rich groundmass of the host-rocks. The original alteration of a silicic/potassium-rich groundmass allowed the formation of Ca^{++} and/or K^{+} smectite.

Subsequent temperature increases and available Ca^{++} and K^{+} in the system facilitated the development of illite/smectite and kaolinite (possibly coevally) and finally illite. The abundance of each clay mineral depended heavily upon permeabilities in the ore zone. Since pressure was only a negligible parameter at Blackdome, it is believed that the primary physical constraints on clay genesis were temperature and time. The paragenetic sequence determined for Blackdome is summarized in Figure 3.13.

FIGURE 3.13 Paragenetic sequence of the Clay Phases and other Major Gangue Phases.

NOTE: The minerals listed below are considered to make up the first stage of mineralization at Blackdome. The diagram reveals two phases of kaolinite. The kaolinite formed below 60°C is supergene kaolinite and is therefore not considered first stage.

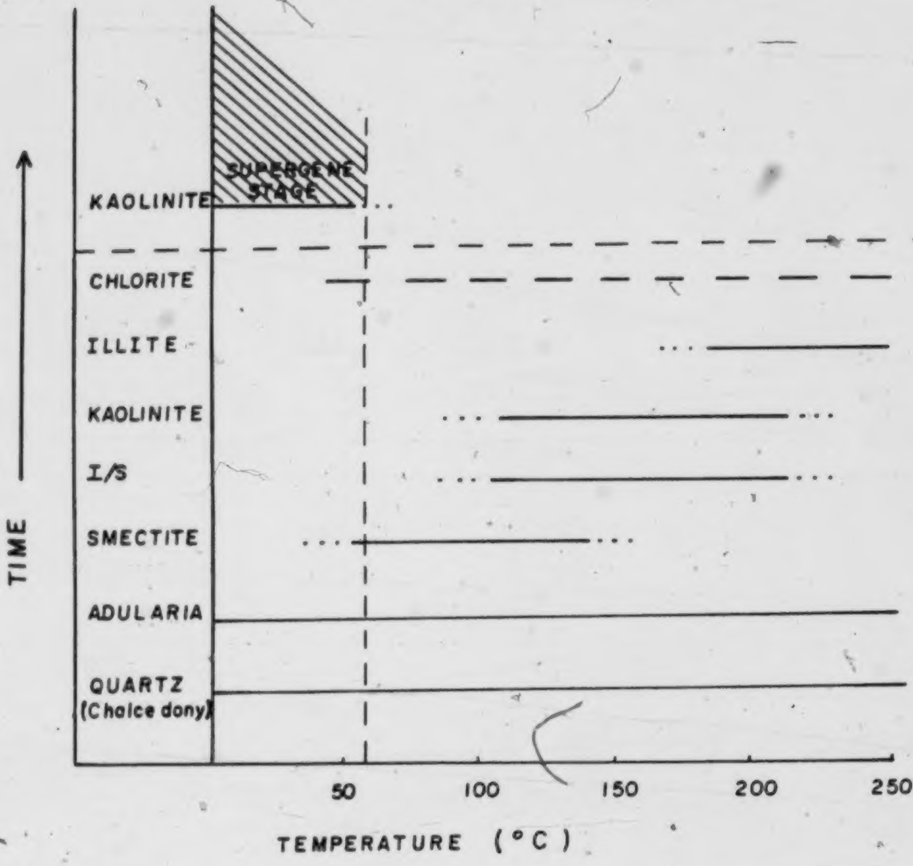

Diagram is constructed primarily on data from Steiner (1968); Steiner(1953); Steiner and Rafter, (1966); Velde, (1966) and MAC Short Course (Clays and the Resource Geologist, Vol 7, 1981).

IV. FLUID INCLUSION STUDY

Numerous fluid inclusion data have been published on epithermal systems (Buchanan, 1982). Buchanan suggests that homogenization temperatures in the range of 150-300° C are typical for fluid inclusions in such systems. The hydrothermal fluids exhibit salinities of less than 3 weight percent equivalent NaCl. In many deposits, effervescence (boiling) has been noted, i.e. the systems have clearly been hot-springs, geysers or fumaroles, vented to surface. A typical zonational model is illustrated in Figure 4.1 as published by Sutherland Brown (1986). It illustrates the opinions of former authors as to the zonational position of the Blackdome system.

The present investigation constitutes a detailed study of one Blackdome gold-silver vein system. It should be noted that all data herein refer entirely to the No. 1 vein system. Every effort has been made to determine the composition, temperature and pressure of inclusions in all gangue phases. Quartz is the most prominent and transparent gangue phase hosting fluid inclusions used in this study. Adularia is a significant component but very difficult to do any microthermometric studies upon.

A) METHODS OF INVESTIGATION

Small chips of quartz, belonging to a range of paragenetic stages, were prepared for investigation. One side of the quartz chip was polished and the sample mounted

FIGURE 4.1 B.C. EPITHERMAL GOLD SILVER DEPOSIT MODEL (SECOND APPROXIMATION)

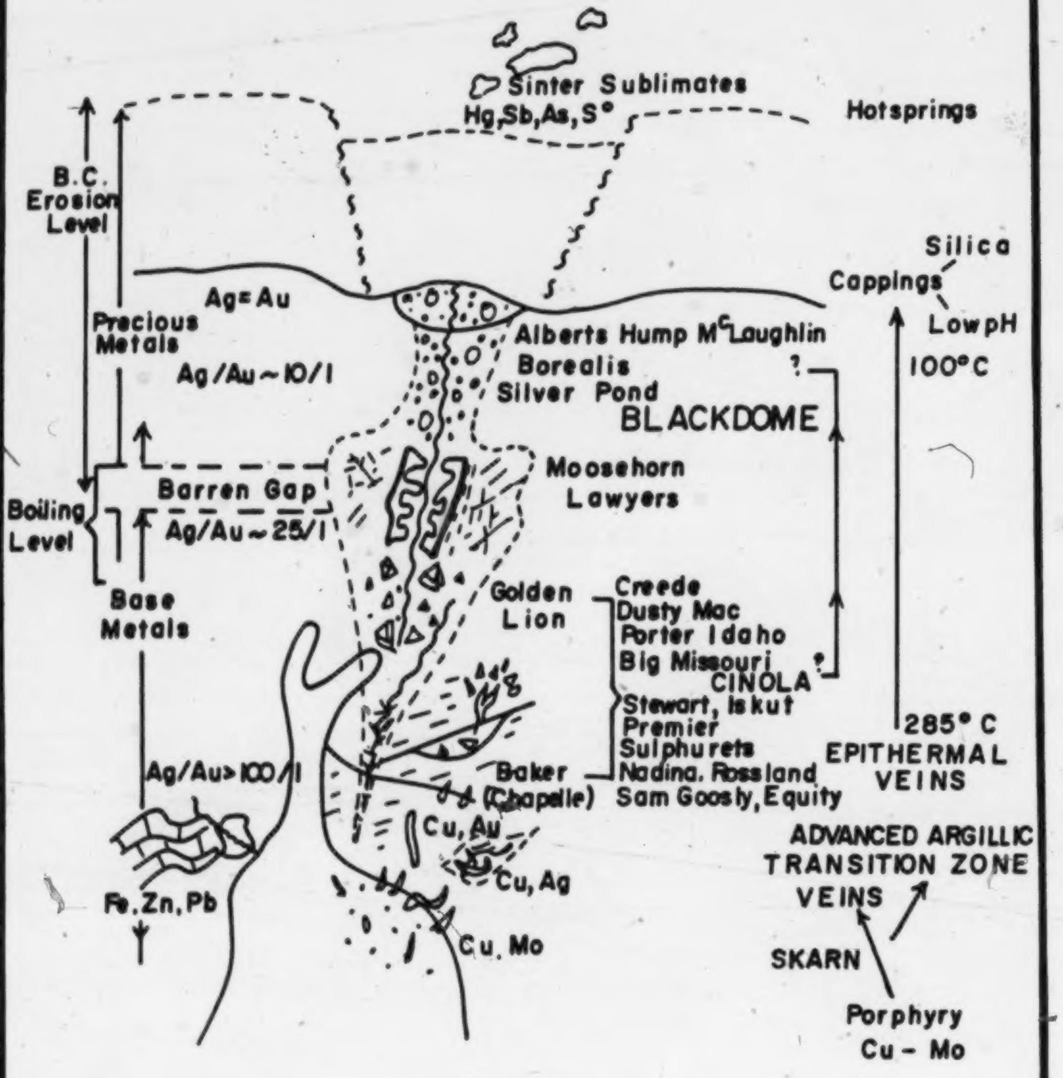
Sinter Sublimates
Hg,Sb,As,S°
Hotsprings
B.C. Erosion Level
Silica
Cappings
Low pH
Ag=Au
Precious Metals
Alberts Hump McLaughlin
Borealis
Silver Pond
Ag/Au~10/1
?
100°C
BLACKDOME
Moosehorn
Lawyers
Barren Gap
Boiling Level
Ag/Au~25/1
Base Metals
Golden Lion
Creede
Dusty Mac
Porter Idaho
Big Missouri
?
CINOLA
Stewart, Iskut
Premier
Sulphurets
Nadina, Rossland
Sam Goosly, Equity
285° C
EPITHERMAL VEINS
Ag/Au>100/1
Baker
(Chapelle)
Cu, Au
Cu, Ag
Cu, Mo
Fe, Zn, Pb
ADVANCED ARGILLIC
TRANSITION ZONE VEINS
SKARN
Porphyry Cu - Mo

(adapted after Panteleyev, 1983 and Schroeter, 1983) on a glass slide with LOC- WAX 40 (high molecular weight glycopthalate thermoplastic) and left for a couple of hours to dry. All samples were then ground to varying thicknesses (preferably around 0.3 millimetres) depending upon the transparency of the minerals. The quartz chips were then polished. These polished plates were then studied under a petrographic microscope and inclusions suitable for microthermetric work selected. The microthermometric experiments were carried out using a Chaixmeca model VT2120 heating and freezing stage. The instrument was calibrated using freezing point temperatures of distilled water and of liquid CO_2. The correction found to be applicable to the freezing data of the Blackdome materials was -0.9°C. The heating experiments were calibrated by using a series of standards supplied by the Centre de Recherches Petrographiques et Geochimiques, Nancy, France. This series of Merck Co. solid melting-point standards has a range in M.P. from +70°C to +398°C. A series of three runs on the same inclusions gave a measured temperature variance of +/- 0.9 to +/- 3.2°C from +70°C to 398°C, respectively. It was assumed for ease of corrections that at temperatures approaching 300°C, the maximum correction was +/- 3°C.

B. CLASSIFICATION OF INCLUSIONS

The classification of fluid inclusions in this study is the same as that given by Roedder (1981) and is based upon the origin of the inclusions. Following

Roedder's classification scheme, the inclusions in the quartz chips were classified as primary, secondary or pseudo-secondary (see photomicrographs in the Appendix IV).

All three types of inclusions were identified in the quartz. The primary inclusions were identified on the basis of their random orientation, isolated occurrences, and larger dimensions. The secondary inclusions were identified on the basis of their oriented patterns along healed fractures. One of the essential characters of secondary inclusions in this study was their presence in fractures which continued through grain boundaries. Secondary inclusions were generally smaller than the primary inclusions. The pseudo-secondary inclusions were identified on the basis of their oriented pattern along healed fractures, but these fractures terminated over short distances or they did not approach grain boundaries. The pseudo-secondary inclusions were the most difficult to perform microthermometric experiments upon, due to their small size.

C. TYPES OF INCLUSIONS

The fluid inclusions analyzed in the quartz chips were of variable shapes and sizes. The size range of the inclusions, along the longest axis, varied from less than 1 micron to more than 180 microns. The average size of the fluid inclusions was less than 1 micron in most chips but some of the quartz chips revealed minimum sizes of 1-3 microns. The inclusions were commonly fairly equant, ameboid in shape but irregular, subsequent and negative crystals were observed.

The inclusions studied belonged to three or four different paragenetic stages, namely: (i) The quartz representative of Stage 1 (early barren quartz) occurred as veinlets of crystalline quartz, cross-cutting strongly silicified and metasomatized wall rocks. This finer crystalline quartz also lines the outer vein zone adjacent to the wall rocks (not noted in all sections).
(ii) Stage 2 (assuming this to be the mineralization stage quartz) contains euhedral, cockscomb quartz and, in some zones, equal amounts of quartz and adularia. Adularia appears to be the major introduced gangue phase in Stage 2. The inclusions seen in minerals of this stage are usually larger than the Stage 3 inclusions. (iii) The Stage 3 fraction (late stage, smaller euhedral, cockscomb and mosaic quartz) is the open-space filling constituent in this vein system. If a Stage 4 exists, it is the latest open-space fillings of carbonate, zeolites and late stage cross-cutting quartz seams. All four stages are not ubiquitous in all parts of the vein.

Although four paragenetic stages have been identified, the actual fluid inclusions in minerals of these distinct stages do not show much variation from specimen to specimen.

i) Type 1 Inclusions

This type of inclusion is dominant. It is a two-phase, liquid-vapour inclusion with an estimated 10-40 volume percent of vapour. They homogenize in the liquid phase.

ii) Type 2 Inclusions

These are two-phase, vapour-liquid inclusions which have an estimated 10 per cent or less of the vapour-phase. These inclusions constitute only a minor portion of the total inclusions. These may represent entrapped vapour within a boiling or effervescing system.

iii) Type 3 Inclusions

These inclusions are liquid-dominated, containing variable amounts of the vapour phase, much like Type 1. This type of inclusion is characterized by the presence of daughter crystals which are birefringent and commonly show an acicular habit. These daughter crystals have yet to be positively identified.

The coexistence of both fluid- and vapour-rich inclusions with variable filling ratios within the same sample is indicative of effervescence or boiling in the hydrothermal system.

D. SALINITIES OF THE HYDROTHERMAL FLUIDS

The salinities of the fluid inclusions were determined by the freezing-point depression technique. Inclusion sizes range from less than 1 micron to more than 180 microns. Inclusions used in the freezing experiments were generally greater than 15 microns. Freezing experiments were carried out primarily on Type 1 inclusions but some Type 3 inclusions were also examined.

In general, the inclusions were frozen to -60 to -70°C to ensure that the system was totally frozen. Most inclusions showed that the formation of the vapour bubble at -35 to -42°C. There were two cases where the inclusions had to be frozen below -70°C. [illegible] first melting point (Te) temperature was observed to begin, within most inclusions, between +0.65°C and -0.24°C. The temperatures were corrected by subtracting 0.9°C. The corrected temperature range of -0.25° to -1.14°C was found to be close to the first melting temperature (0°C) of pure water. The presence of other salts, KCl and $CaCl_2$, depresses the first melting temperature (Crawford, 1981). It is thus thought that the Blackdome fluids closely approached simple $NaCl-H_2O$ brines.

In a simple $NaCl-H_2O$ system the melting temperature is controlled by the salinity. After carrying out freezing experiments salinities can be calculated by the following equation:

Weight % NaCl equivalent = $(1.76958 \times X) - 4.2384 \times 10^{-2} X^2 + 5.2778 \times 10^{-4} X^3$, where X=the melting temperatures (Potter et al, 1978).

The salinities determined by this method range between 0.20 and 2.05 wt% NaCl equivalent and are presented in Table 4.1 and plotted in figure 4.2. The experimental results indicate that a very narrow range of salinities

TABLE 4.1 TEMPERATURE AND SALINITY DATA FOR HYDROTHERMAL FLUIDS IN THE BLACKDOME GOLD-SILVER VEINS, B.C., CANADA

Sample No.	Mineral	Stage	Type	Th(°C)	Tf(°C)	Salinity (wt% NaCl equiv)
139-153	Quartz	2,3	P	235	-0.65	1.173
139-158	Quartz	3?	P	213	-0.90	1.559
	Quartz	2,3	P	209	-0.75	1.304
	Quartz	2	S		-0.65	1.173
137-51.6	Quartz	2	P	279	-0.15	0.265
	Quartz	2	P	268	-0.40	0.701
	Quartz	2	S	276	-0.45	0.788
	Quartz	2	S	281	-0.40	0.701
137-55	Quartz	2	P	273	-0.60	1.046
148-164.7	Quartz	1,2	P	299	-0.70	1.218
	Quartz	1,2	P	285	-0.60	1.046
	Quartz	2	S	230	-0.60	1.046
	Quartz	2	S	236	-0.80	1.388
148-165	Quartz	2	P	279	-0.43	0.756
136-43.5	Quartz	1,2	P	286.5	-0.95	1.643
135-60	Quartz	2	P	258	-0.12	0.213
	Quartz	2	P	250	---	---
	Quartz	2	P	253	---	---
84-29.5	Quartz	2	P	264	-0.75	1.304
84-30.5	Quartz	1,2	P	290	-0.90	1.559
	Quartz	2	P	289	-0.78	1.403
	Quartz	2	P	295	-0.83	1.439
	Quartz	2	P	287	---	---
84-30.1	Quartz	2,3	P	215	---	---
	Quartz	2,3	P	219	---	---
	Quartz	2	P	225	---	---
84-33.5	Quartz	1,2	P	294	---	---
	Quartz	1,2	P	301	---	---
	Quartz	2	S	267	---	---
	Quartz	2	S	286	---	---

Sample No.	Mineral	Stage	Type	Th(°C)	Tf(°C)	Salinity (wt% NaCl equiv)
84-34.2	Quartz	2	P	280	---	---
	Quartz	1,2	P	294	---	---
	Quartz	2	P	256	-0.60	1.046
30-11.4	Quartz	1,2	P	313	-0.50	0.902
	Quartz	1,2	P	298	-0.45	0.787
	Quartz	1	S(?)	306	---	---
30-11.8	Quartz	1,2	P	307	-0.51	0.913
	Quartz	2	P	292	-0.45	0.787
	Quartz	2	P	287	-0.47	0.841
30-13.9	Quartz	2	P	263	-0.90	1.559
	Quartz	2	P	268	-0.60	1.046
	Quartz	1,2	P	280	-0.65	1.173
	Quartz	2	P	263	-0.70	1.218
	Quartz		P	289	---	---
23-22	Quartz	2	P	293	-0.65	1.173
08-30.5	Quartz	2	P	278	-0.94	1.633
	Quartz	2	P	265	---	---
08-32.2	Quartz	2	P	285	-0.80	1.388
	Quartz	1,2	P	289	-0.75	1.304
	Quartz	2	S	284	-0.75	1.304
	Quartz	2	S	276	-0.70	1.218
06-17.3	Quartz	1,2	P	283	-0.94	1.633
	Quartz	2	P	267	-1.04	1.887
06-15.0	Quartz	2	P	274	---	---
	Quartz	2	P	278	---	---
	Quartz	2	P	280	---	---
01-10.3	Quartz	2,3	P	249	-0.75	1.304
	Quartz	2	P	258	-0.75	1.304
01-12.5	Quartz	2	P	263	-0.60	1.046
	Quartz	2	P	258	-0.65	1.173
	Quartz	1,2	P	255	-0.75	1.304
01-15.3	Quartz	2	P	280	-1.14	2.073

Note: P = Primary inclusion; S = Secondary inclusion; Stage of quartz is referred to in text.

FIGURE 4.2:

WEIGHT PERCENT NaCl equivalent

VS. FREQUENCY

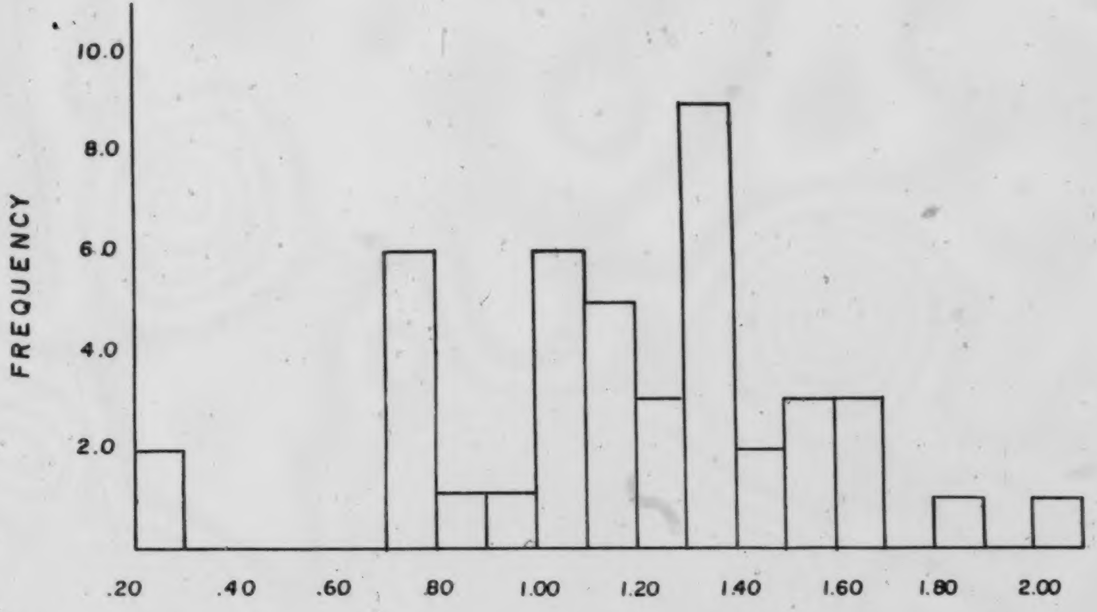

wt % NaCl equivalent

$$\text{Wt \% NaCl} = (1.76958 \times X) - 4.2384 \times 10^{-2} X^{2} + 5.2778 \times 10^{-4} X^{3}$$

X = MELTING (Freezing) TEMPERATURES

existed in the Blackdome hydrothermal fluids. Determining the sequence of entrapment of the inclusions was not possible and therefore temporal variations in salinity of the hydrothermal fluids was not estimated.

E. TEMPERATURES OF THE HYDROTHERMAL FLUIDS

Homogenization temperatures of both primary and secondary inclusions were measured. It is believed that some of the measurements may have involved pseudo-secondary inclusions, but this was not substantiated. It was not always possible to perform the heating experiments upon the same inclusions as those which were frozen.

No problems were encountered with decrepitation of inclusions before the homogenization temperatures were reached. The only difficulty arose when the vapour bubble disappeared into dark corners of the inclusions, just before the homogenization temperature was reached. In these cases, it was necessary to estimate the final homogenization temperatures. The estimate of the homogenization temperature in any single experiment would not differ by more than 5-10°C from the temperature of disappearance. Taylor (1983) has reported similar problems.

The results of the heating experiments are listed in Table 4.1 and plotted as a histogram in Figure 4.3. The results of Table 4.1 are corrected for pressure effects. The pressure effects were calculated using Figure 4.4 and are assumed to be the maximum or actual trapping

FIGURE 4.3 :

HOMOGENIZATION TEMPERATURES VS. FREQUENCY

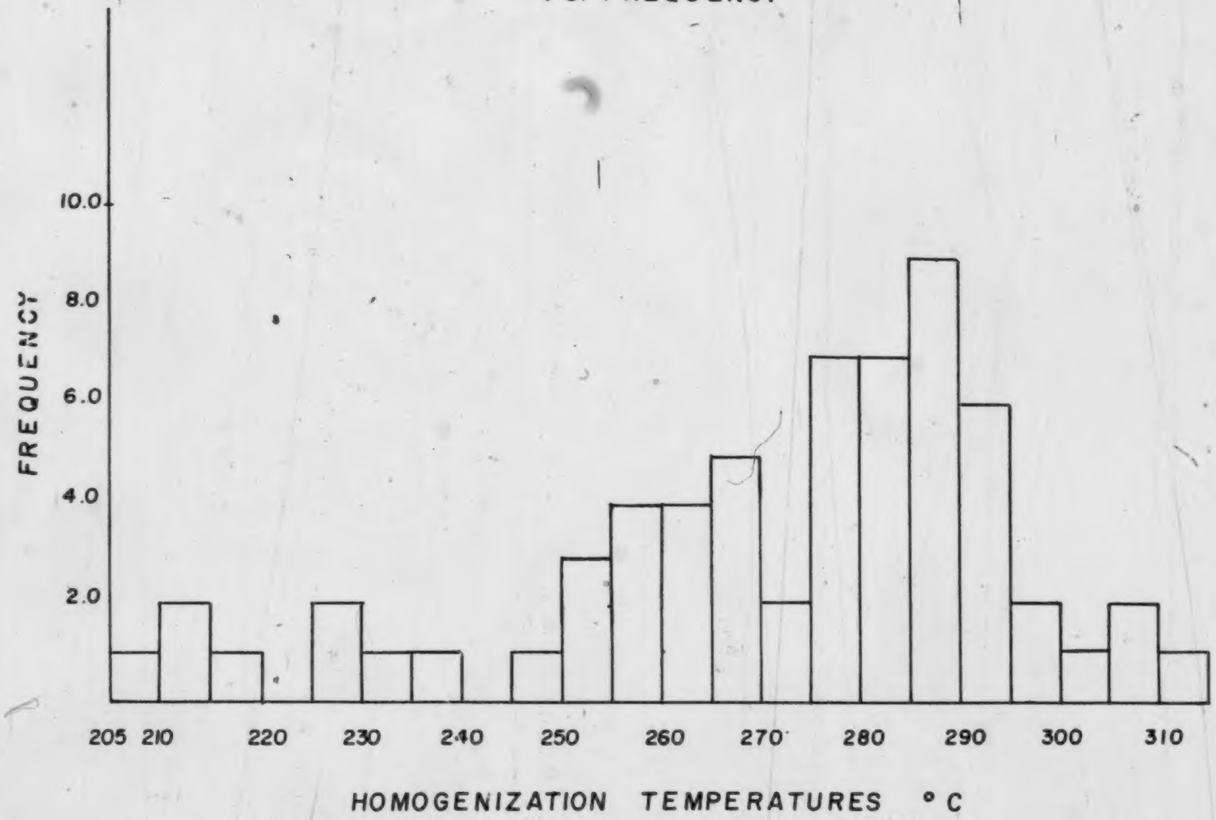

FIGURE **4.4** : Pressure determinations from fluid inclusion studies. Diagram after Urosova (1975), Potter & Brown (1979), Sourirajan & Kennedy (1962), Bumhametal (1969), Keenan etal (1969), and Haas (1976) : from Roedder & Bodnar (1980) Geologic pressure determinations from fluid inclusion studies.

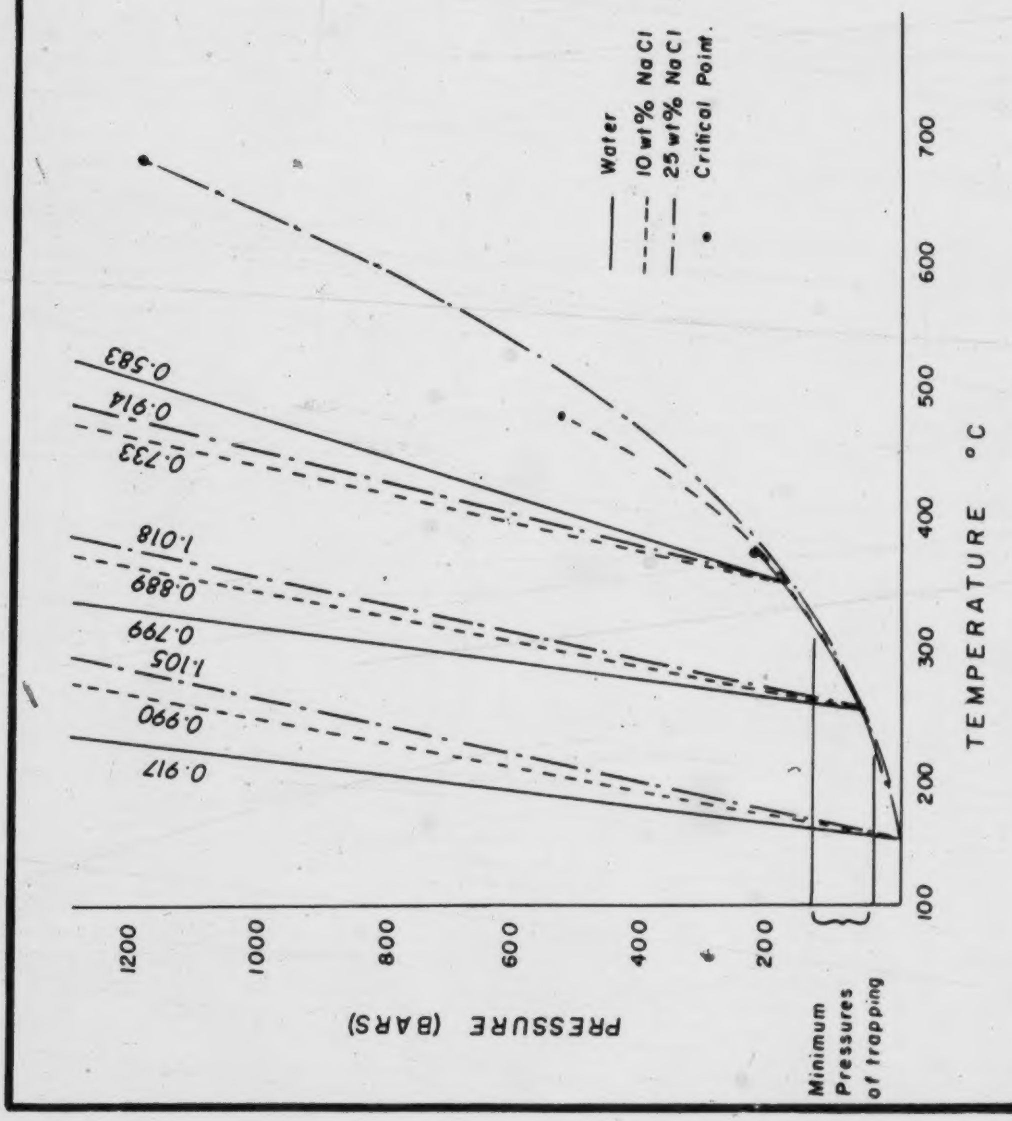

temperatures, on the basis of evidence of boiling or effervescence in some samples.

The heating experiment data suggest only one main thermal stage. This stage varies between 260°C and 295°C. Higher temperatures of 308°C and 313°C have been obtained within the Blackdome system. However, it is felt that there are insufficient data to reveal distinct temperature regimes. Some lower temperatures of 209°C, 215°C and 226°C were obtained, but again the sample population is too small to substantiate a distinct lower temperature regime.

The temperature of homogenization signifies a minimum temperature of trapping. Pressure corrections frequently have to be made and subsequently added to the homogenization temperature in order to obtain the true trapping temperature. However, at Blackdome varying filling ratios were observed (i.e. the coexistence of vapour-rich and liquid-rich inclusions within the same sample). Due to the fact that these inclusions homogenized at very similar temperatures, it is clear that the hydrothermal fluids were boiling or effervescing within this system. This therefore negates the need for pressure corrections and shows the homogenization temperatures observed during the heating experiments to be, in fact, the true trapping temperatures.

Knowing the salinity of the fluids and the temperature of homogenization one can estimate pressures (hydrostatic) as indicated by Haas (1971). Low salinity fluids can be approximated by the H_2O-NaCl system. Haas determined from numerous experimentation data that depth to an isotherm is a percentage of the depth to an isotherm in a H_2O system. Densities from the fluids at Blackdome have been estimated at 0.72 to 0.81 g/cm^3 with the corresponding depths to be approximately 0.5 km to 1.1 km.

F. CONCLUSIONS

The homogenization temperatures appear to be relatively constant through the various vein-filling stages. The lack of discrete temperature regimes also suggests that the hydrothermal fluids remained at quasi-constant temperatures during the period of mineralization. The predominant temperature range for mineralization was clearly 260°C to 295°C.

The salinities of the hydrothermal solutions also remained stable over time and depth and ranged between 0.26 and 2.05 weight percent equivalent NaCl. Such salinities are well within the range for meteoric waters which are considered to have been the major source for the mineralizing fluids in the system.

Varying filling ratios and daughter crystals present in the fluid inclusions suggest that the hydrothermal fluids were at or near the point of boiling. The pressures achieved in this system, once boiling is assumed, are maximum pressures of trapping. These maximum trapping pressures would range between 45 and 110 bars (4500-11000 kilopascals, hydrostatic pressure). The maximum depth at which the crystals grew was 0.5 - 1.1 km.

V. SULFUR-OXYGEN AND HYDROGEN-ISOTOPIC COMPOSITION OF THE ORE FLUIDS AT BLACKDOME

The present investigation constitutes a cursory enquiry into the isotopic composition of the hydrothermal fluids responsible for deposition of metals in the Blackdome vein system. Dr. A. Changkakoti and Mr. P. Maheux, University of Alberta, kindly analyzed oxygen and hydrogen isotopes in quartz and their fluid inclusion waters on my behalf. The laboratory facilities were provided by Dr. J. Gray and Dr. K. Meuhlenbachs and funded by NSERC. Samples of present-day mine waters were also analyzed for reference purposes. Dr. R. Krouse, University of Calgary, kindly analyzed gaseous extracts for sulfur isotopes from selected samples of metasomatized- and silicified- wallrocks and vein fragments.

A. Experimental Techniques

The standard BrF_5 technique (Clayton and Mayeda, 1963) was employed for oxygen extraction from the quartz samples. D/H ratios were measured on fluid inclusion waters extracted from quartz by thermal decrepitation, and the released waters were reacted with uranium metal at 750°C to produce hydrogen gas. Mine water samples were also treated in the same manner. The mass spectrometric results are presented in the standard S-notation, with V-SMOW and Canon Diablo Troilite being the reference standards for oxygen and sulfur respectively. Analytical reproducibilities are +/-

0.1 per mil for oxygen, and +/- 3.0 per mil for hydrogen from fluid inclusion waters.

Sulfide samples were separated, crushed and hand-picked to ensure sample purity. The crushed and cleaned samples were reacted under vacuum with a 50:50 Cu_2O-CuO mixture at approximately 1000°C for one-half hour. SO_2 derived from this reaction was frozen off, purified and analyzed by mass spectrometry to determine the sulfur isotope ($^{34}S/^{32}S$) ratio of each separate. Lack of suitable samples precluded the use of sphalerite and galena as sulfide pairs for geothermometry. Analytical reproducibility for the $S^{34}S$ determinations was +/- 0.1 per mil.

B. RESULTS

The oxygen-, hydrogen- and sulfur- isotope results are presented in Table 5.1. The SD values of the fluid inclusion waters vary from -125 to -134 per mil, whilst the SD values of the mine waters vary from -128 to -141 per mil. The constancy in $S^{18}O$ clearly reflects a uniform reservoir oxygen isotopic composition and also a relatively constant temperature of the hydrothermal fluid during deposition of the paragenetic range of minerals sampled.

The theoretical isotopic composition of the hydrothermal fluids was determined from the $S^{18}O$ values of the quartz using the assumed temperature of crystallization (i.e. the mean homogenization temperatures determined from fluid inclusions in the quartz). The following equation,

TABLE 5.1 STABLE ISOTOPE DATA FOR HOST ROCKS, QUARTZ AND HYDROTHERMAL FLUIDS IN THE BLACKDOME AG-AU DEPOSIT, BRITISH COLUMBIA, CANADA

Sample No.	Depth meters	Lithological Description	$S^{18}O$	SD	$S^{18}O(H_2O)^1$	$S^{34}S$
			(values in %		, SMOW)	(%)
DDH 01	16.3	massive, crystalline quartz	0.2	-126	-8.8	---
DDH 23	21.9	massive, crystalline and euhedral quartz	0.9	-130	-7.5	---
DDH 08	31.8	euhedral quartz	1.1	-125	-7.5	---
DDH 129	125.3	massive, crystalline	1.2	-128	-7.4	---
DDH 148	164.7	large euhedral qtz	0.9	-130	-7.5	---
Drift 1960' Elevation	12120N	massive, crystalline quartz	1.8	-134	-6.8	---
2		mine water	---	-132	---	---
4		mine water	---	-138	---	---
5		mine water	---	-140	---	---
7		mine water	---	-141	---	---
10		mine water	---	-128	---	---
DDH 137	60	andesite, stockwork	---	---	---	+3.1
DDH 84	35	andesite, stockwork	---	---	---	+0.1
DDH 06	30	rhyolite, siliceous	---	---	---	+0.4
DDH 129	122.5	andesite, stockwork	---	---	---	0.0
DDH 84	120	andesite, siliceous	---	---	---	-1.8
Drift 1960' Elevation	12050N	felsic agglomerate, siliceous	---	---	---	+4.0

Note: [1] The $S^{18}O$ values of the hydrothermal fluids calculated from the $S^{18}O$ values of quartz, and homogenization temperatures of fluid inclusions.

(after O'Neil et al., 1973), was used for the calculation of theoretical isotopic composition of the hydrothermal fluids:

$$1000 \ln x \, (Q-W) = 3.57 * (10^6/T^2) - 2.73$$

where x is the fractionation factor, Q is quartz, W is water, and T is the temperature in ^{o}K. The theoretical isotopic compositions of the hydrothermal fluids were found via this method to vary from -8.8 to -6.8 per mil $S^{18}O$ SMOW.

The sulfur isotopic composition expressed as $S^{34}S$ is defined as a per mil deviation of the $^{34}S/^{32}S$ ratio of the compound relative to that of the troilite phase of the Canon Diablo meteorite ($^{34}S/^{32}S$ = 0.0450045; Ault and Jansen, 1963). The sulfur isotopic compositions of the pyrites analyzed vary from -1.8 to +4.0 per mil. The narrow range for the $S^{34}S$ values indicates a common origin.

C. Origin of the Hydrothermal Fluids

The origins of epithermal gold deposits are becoming well documented in areas of the southwestern United States, Mexico and other parts of the world. In the majority of these deposits, circulating meteoric water has clearly been the dominant source for the mineralizing fluids, with apparently little or no fluid contribution from any magmatic source (Taylor, 1973; 1974; 1979; O'Neil and Silberman, 1974; Kamili and Ohmoto, 1977). Thus the magmatic role appears to be confined to that of a "heat engine" driving a convectional geothermal system.

The SD values of the ore fluids are normally found to be similar to the SD values of local meteoric waters, whereas the oxygen isotopes of the ore-fluids are commonly found to have been exchanged to various degrees with the volcanic country-rocks of the vein-systems.

The present investigation of the isotopic composition of the hydrothermal fluids in equilibrium with the vein minerals at Blackdome revealed a very narrow range of $S^{18}O$ values. As mentioned earlier, the uniformity noted in both isotopic composition and temperature from fluid inclusions indicates the involvement of only one type of fluid during that paragenetic phase of deposition of the vein system.

The SD of the fluid inclusion waters and mine waters, and the calculated $S^{18}O$'s of the ore-fluids are plotted in Figure 5.1. The SD values of the fluid inclusion waters were found to be slightly enriched in D, in comparison with SD values for the present-day meteoric water of the region. This suggests that the isotopic composition of Tertiary meteoric water did not deviate much from the present-day meteoric water of the region. However, as with other epithermal deposits, a positive shift in $S^{18}O$ was observed in case of the Blackdome ore-fluids, which is obviously due to isotopic exchange of the thermal waters with their country rocks.

In the case of the $S^{34}S$ values, data were obtained only from pyrite samples. This precluded any opportunity to

FIGURE 5.1 . δD vs $\delta^{18}O$ plot of ore fluids from the Blackdome Ag-Au deposit (adapted after O'Neil and Silberman, 1974)

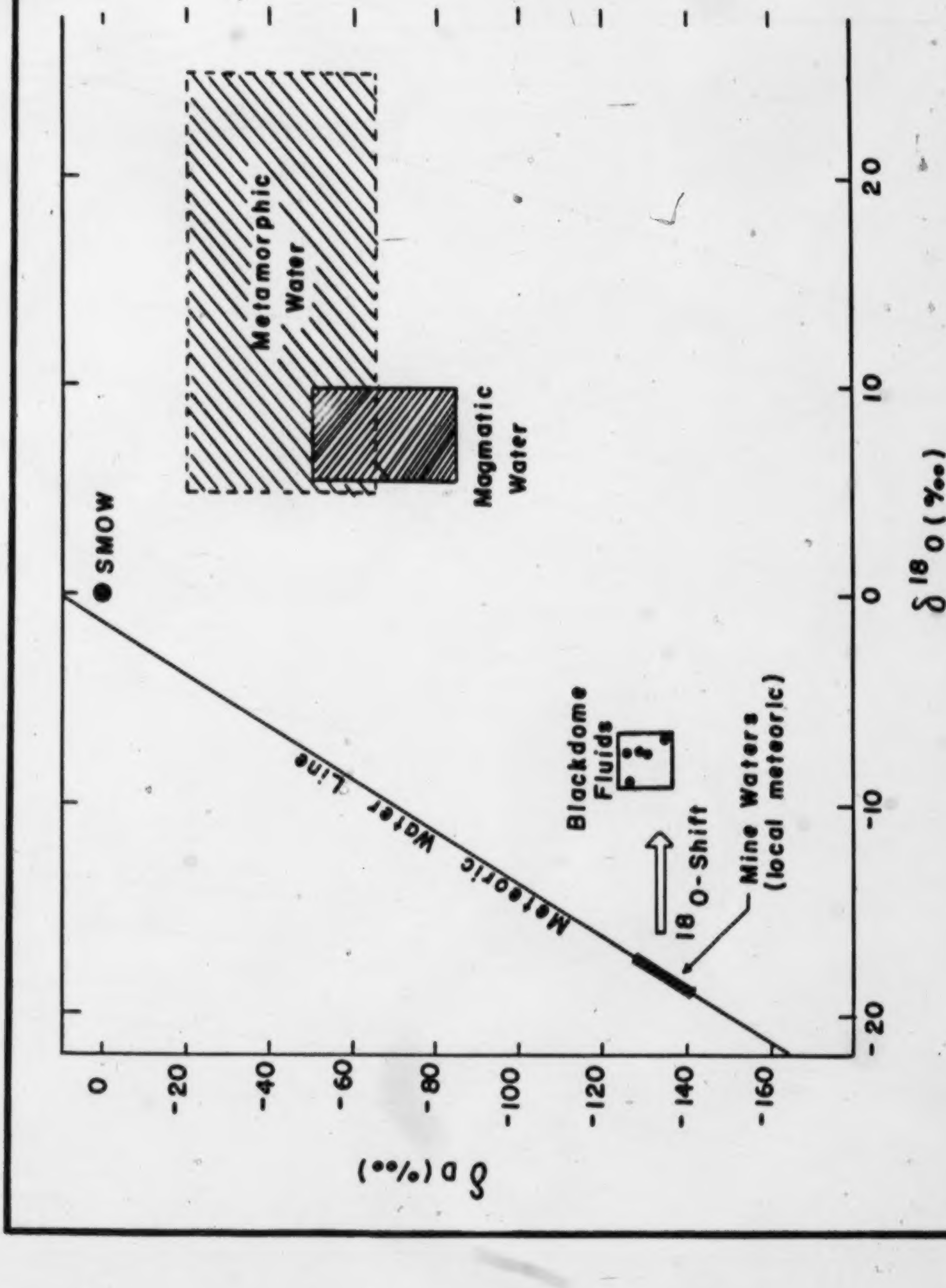

use sulfide pairs for geothermometry and thus the information obtained from the sulfur isotope study was essentially one dimensional. The sulfur isotopic composition of the pyrite ranges from -1.8 to +4.1 per mil. This suggests that sulfur was derived from an igneous source (Figure 5.2). Many epithermal deposits are associated with calc-alkaline intrusives and lack sulfate minerals, like Blackdome, and have $S^{34}S$ values of their sulfide minerals in a narrow range near 0% . The sulfur in these ore-forming fluids also appears to have been derived from igneous sources and the sulfides precipitated under pH-fO_2 conditions where H_2S was the dominant sulfide species (Ohmoto and Rye, 1979).

D. Conclusions

The Blackdome epithermal deposits represent an excellent example of the type of mineralization generated in a volcanic-arc environment subjected to the incursion of meteoric waters down fracture systems. High grade Ag-Au-(Sb-Cu-Fe-Zn-Pb-S-Se-As)- silica deposits formed when acidified, Tertiary meteoric groundwaters penetrated into the volcanic edifice. The geothermal fluids apparently exhibited an isotopic signature slightly removed from the parent meteoric waters. A significant degree of hydrative metasomatism caused a positive, exchange shift in the $S^{18}O$ value, away from the meteoric water line. Also, a minor positive shift in the SD value of the fluid might have been

FIGURE 5.2. Range of $\delta^{34}S$ values of sulphides and sulfates from various hydrothermal ore deposits (adapted after Rye and Ohmoto, 1974)

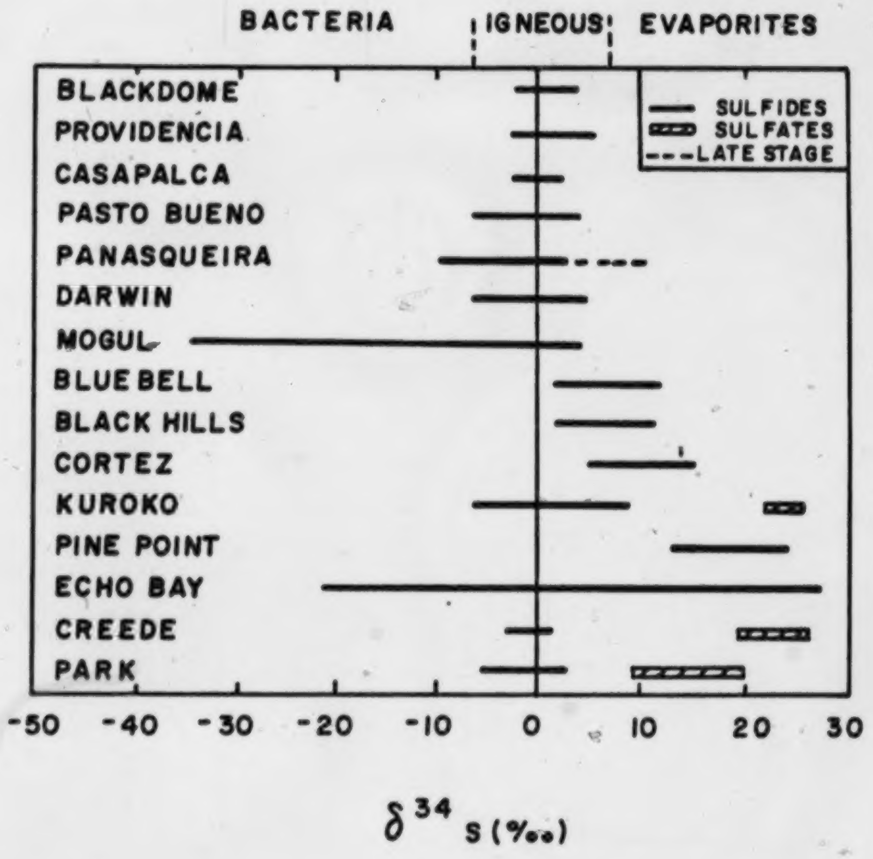

effected either by vapour - loss of water from a boiling fluid system and/or by selective hydrogen metasomatism of the wall rocks.

The $S^{34}S$ values indicate an igneous source for the sulfur and that the sulfides precipitated within the vein system under pH-fO_2 conditions dominated by the H_2S sulfide species.

VI. VEIN PETROGENESIS, MINERALOGY AND PARAGENESIS

The Blackdome No. 1 vein system hosts a portion of a larger Tertiary 'epithermal' Ag-Au deposit. This No. 1 vein system is part of an intense fracture system within Tertiary intermediate volcanics. The petrogenesis of the No. 1 vein system provides a primary insight into the genesis of this Ag-Au system. Mineral morphologies and occurrences will allow for postulation of the relative timing and importance of the hydrothermal pulses responsible for ore deposition.

A. BACKGROUND AND METHODS

The Blackdome Ag-Au vein system has discrete and distinct mineralogies in each depositional stage. Quartz is always the dominant mineral, comprising 70-100 modal percent of the pre-ore stage, 60-90 percent of the ore stage and 65-95 percent of the post-ore stage assemblage.

A study, involving three polished sections and fifty polished-thin sections, was completed in order to identify the opaque minerals. From this study, a paragenetic sequence of the stages and the vein system was deduced. Opaque-mineral identification was accomplished by observation of the reflected light characteristics of each mineral. Each mineral has its own characteristic color, bireflectance, anisotropy or isotropy and reflectance at 547 nm. A Nomarsky Phase Interference Contrast device was used in the determination of relative polishing hardness of adjacent minerals. Transparent (gangue) minerals were identified in thin-section by characteristic staining techniques and X-ray diffractometry.

Many of the precious-metal minerals were identifiable using the reflected-light microscope technique but sulfosalt minerals were difficult to accurately identify. Difficulty arises in the identification of sulfosalt minerals as all sulfosalts have similar optical properties. A cursory investigation into the proper identification of these sulfosalts was undertaken using an energy dispersive analysis system on an EEDS-II electron microprobe. The in-house software program, EDATA 2 (Smith and Gold, 198), was used to calculate the composition of each mineral from its x-ray spectrum. This cursory study did not allow for a detailed investigation of each mineral and thus only a few minerals were totally analyzed. The elemental analyses of each of these selected minerals are shown in Table 6.1.

B. VEIN PETROGENESIS AND MINERALOGY

The No. 1 vein system at Blackdome appears to have been formed by the infilling of dilatent tensional fractures by quartz, adularia, carbonate, sulfides and numerous other hydrothermal minerals. The infilling of these tensional fractures took place in three separate stages, namely: the pre-ore stage, the ore stage, and the post-ore stage.

The pre-ore stage signature is typified by stage 1 quartz, as outlined by the fluid inclusion study, and

TABLE 6.1 Electron Microprobe Analyses of Some Ore Minerals at Blackdome Mine, British Columbia, Canada

Sample No.		12080(a) *3 inclusions	12080(b)	32.5(a)	32.5(b)	15.2
Wt%	Ag	35 - 72	69.75	85.88	9.07	41.87
	Se	2.7 - 3.80	7.98	---	---	---
	Cu	0 - 3.13	---	0.57	---	---
	Fe	3.36-19.60	---	0.49	---	---
	Sb	5.81-10.27	---	0.47	---	---
	S	9.7 -20.35	8.01	9.17	---	---
	Ni	---	---	0.48	---	---
	Au	2.5 - 9.3	14.27	2.94	90.92	58.13
Recalculated Total		99.96-100.06	100.01	100	99.99	100
Original Sum		98.6-102.3	92.68	122.64	101.6	108.60
Mineral Name		Tetrahedrite Polybasite-Stephanite	Acanthite-Aguilarite	Acanthite	Gold	Electrum

* This mineral is as of yet unidentified. The original sums lying outside the 100.0 +/- 1.50 range are probably due to poorly polished sample surfaces.

comprises quartz and sulfide minerals deposited on the vein walls.

The ore stage was dominated by the deposition of quartz, adularia, and numerous other minor silicate phases, along with sulfide and precious-metal minerals. During the post-ore stage, quartz, carbonate, zeolites and other hydrothermal minerals dominated as fracture- infillings, overgrowths and minor open-space fillings. The polished thin-sections allowed for a detailed study of the vein mineralogy and provided a valuable basis for the depositional sequence and mineralogy for each stage. The No. 1 vein system is typical of "epithermal" systems in general, in that there appears to be little deviation in mineral content with varying depth in the system. It is evident that the depositional environment was rather stable over a significant vertical distance, i.e. in the order of a few hundred metres. Vein mineralogy may be broken down into four major categories - gangue minerals; Au-bearing opaque minerals, including native Au; Ag-bearing opaque minerals, including native Ag; and non-precious-metal opaque minerals.

i) Gangue Minerals

In the following sections on vein mineralogy the term 'major' is used to describe a mineral comprising over five modal percent of the vein material within a given paragenetic stage. The term 'minor' refers to a mineral comprising less than five modal percent of the vein material in a given paragenetic stage.

a) Quartz

Quartz is the most abundant and dominant gangue mineral in all stages of the Blackdome vein system. In the pre-ore stage, quartz appears as massive crystalline quartz, lining veinlets and vein walls. It also occurs as euhedral, cockscomb quartz with clear to milky crystals up to a maximum of ten centimetres in length. Crustifications, due to impurities, sulfides, are noted along the vein walls. Quartz deposited during the ore stage is predominantly a mosaic of massive milky and gray material commonly intergrown with adularia and minor carbonate and sulfides but may also be of euhedral form. The post-ore stage quartz appears as overgrowths and as vein infillings. This quartz appears as euhedral to anhedral grains and is predominantly transparent. Fluid inclusions, ranging in size from a few microns up to 200 microns, are abundant in the quartz.

b) Adularia

Adularia is a major gangue phase of the ore and post-ore stages. In the ore stage, adularia is almost as common as quartz in some sections. Adularia occurs as anhedral mosaics intergrown with quartz, as replacement textures in altered host and primarily as micro-veinlets within brecciated fragments in the fault zone. In the post-ore stage, adularia is still a 'major' component, although much less abundant than in the ore stage, and occurs as fracture infills. Adularia vs orthoclase was identified primarily by X-ray diffractometer patterns but also due to its existence as a K-feldspar in low- to moderate- temperatures of vein petrogenesis.

c) Carbonate

The carbonate mineral was identified as calcite, based not only upon its very strong birefringence and negative uniaxial sign in thin-section, but also on its strong effervescence when attacked by dilute HCl. The calcite is a 'minor' component in the ore stage, but may constitute up to five percent. Calcite occurs primarily as anhedral mosaics intergrown with the quartz and adularia. In the post-ore stage, calcite occurs as a major component and appears as anhedral mosaics intergrown with quartz and adularia.

d) Clay Minerals

The clay minerals observed within the ore zone vary from being a 'major' to a 'minor' component of the vein-fill material and are a function of the stage, chemistry and temperature. Pre-ore stage clay material consists of Ca^{++}-K^{+} montmorillonite, mixed-layer illite/smectite and minor kaolinite. The ore stage is dominated by K^{+} metasomatism, hence by abundant illite, lesser amounts of mixed-layer illite/smectite and minor kaolinite. The post-ore stage clay minerals are dominated by illite.

Chlorite can occur in any paragenetic stage, but is of trace amounts as a vein-fill material. Kaolinite was dominant during supergene alteration.

ii) Ore Minerals

a) Au-bearing opaque minerals

1) Native Gold - Au

Native gold occurs as a 'minor' constituent of the ore mineralogy and appears as minute, isolated grains of different sizes in tiny veinlets of pyrite and primarily within the acanthite-aguilarite grains. These tiny grains vary from a few microns up to a maximum of one millimetre in diameter. This native gold also occurs as free gold in vugs and appears to be closely associated with illite and illite-smectite mixed-layer clays. The native gold has a greenish tint and has a reflectivity of greater than 70% in air.

2) Electrum Au-Ag (25% or greater Ag)

The mineral electrum, like gold, is a 'minor' constituent of the vein mineralogy but is much more common at Blackdome than is native gold. It exhibits a brighter 'golden' yellow colour than does native gold but can appear creamy white. Electrum within the Blackdome Ag-Au deposit varies in size from 10-15 microns up to 2-3 millimetres. In hand specimen, the majority of visible gold that is seen appears to be electrum. The scanning electron microscope photomicrographs show a Au grain vs an electrum grain

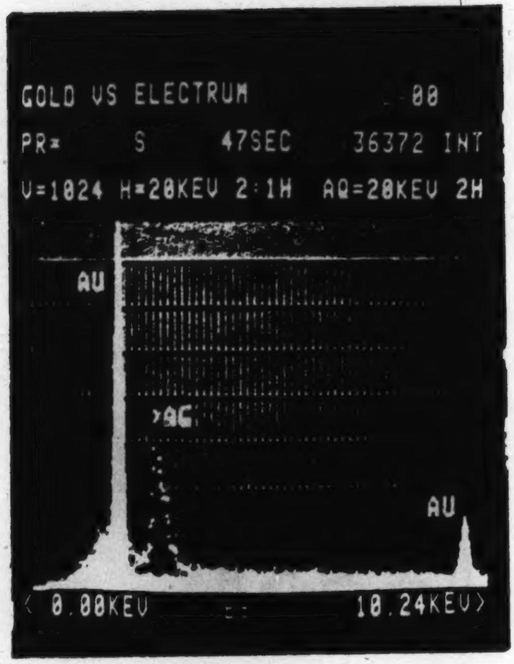
GOLD VS ELECTRUM
-00
PR= S 47SEC 36372 INT
V=1024 H=20KEV 2:1H AQ=20KEV 2H
AU
AG
AU
< 0.00KEV
10.24KEV>

6.1

6.2

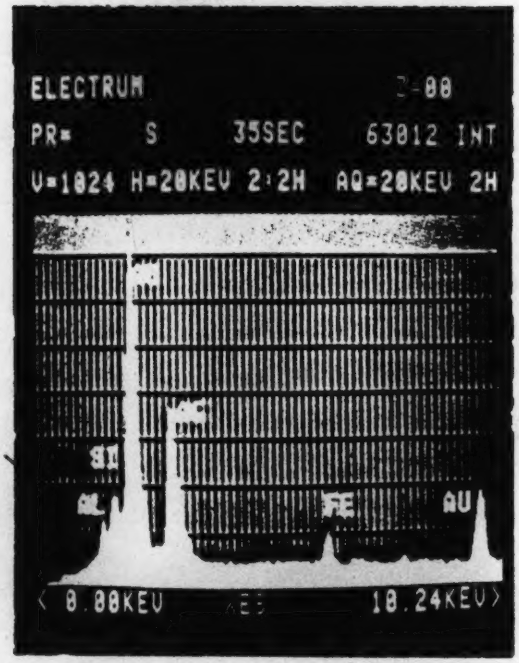
ELECTRUM
3-00
PR= S 35SEC 63012 INT
V=1024 H=20KEV 2:2H AQ=20KEV 2H
AG
SI
AL
FE
AU
< 0.00KEV
10.24KEV>

(Figure 6.1) and an electrum grain from the No.1 Vein (Figure 6.2). Electrum occurs within quartz, between quartz and adularia grains, within tiny veinlets cutting pyrite and chalcopyrite, as well as within the acanthite-aguilarite grains and masses. It is common to see electrum replacing Ag-sulfosalts and Ag-minerals. Electrum exhibits essentially the same reflected light characteristics as the gold, but usually shows higher reflectivities, (>80%), due to its Ag content.

b) Ag-bearing opaque minerals

1) Acanthite - Ag_2S

The mineral acanthite is a 'minor' component of the total vein mineralogy but may be the most abundant silver mineral, along with minerals of the acanthite-aguilarite series. Acanthite commonly occurs as abundant, gray fine-grained disseminations in the veins and veinlets of quartz-adularia-carbonate and clay minerals. It also occurs as inclusions in pyrite, associated with chalcopyrite, galena and sphalerite. The acanthite can contain up to 4.7 percent Se (Petruk et al, 1974) before it is referred to as acanthite-aguilarite. The acanthite in the Blackdome No. 1 vein system reveals a reflectivity in air of approximately 30% and shows a greenish tint. Polished-thin sections revealed reflected light characteristics of the argentite-acanthite series but positive identification was based upon the cursory electron microprobe study. Silver sulfide was identified as acanthite based on Petruk et al classification and is shown in Table 6.1.

2) Acanthite-Aguilarite - Ag_2S- Ag_2Se

The solid solution end members acanthite (Ag_2S) and naummanite (Ag_2Se) can be compositionally variable in either sulfur or selenium to produce the acanthite-aguilarite species. Petruk et al's classification of acanthite says that it contains up to 4.7% Se and the acanthite-aguilarite composition can contain up to 13% Se. As can be seen from the cursory electron microprobe study, at Blackdome, the Se content does not appear to rise above 8 percent. This silver mineral containing between 4.7 percent and 13 percent selenium is therefore referred to as acanthite-aguilarite. The acanthite-aguilarite composition has the same morphological appearance as acanthite, which is a gray, fine-grained disseminated, slightly-metallic material. This mineral species is only a 'minor' constituent, but is the second most abundant vein silver mineral. Elemental analyses of a typical acanthite-aguilarite composition are given in Table 6.1.

3) Native Silver - Ag

Native silver was not absolutely identified within any of the polished thin-sections or polished mounts. It has been interpreted as being present, by previous authors, and is most likely present in the No. 1 vein system, but was not observed during this study. Native silver is a common mineral in supergene alteration zones and may therefore be present higher-up in the vein system. The microprobe analyses, from a few of the mineralized zones, indicates that some of the acanthite and acanthite-aguilarite grains contain very high silver (up to 88%). Due to this very high silver content, low S content (up to 4.5%) and Se (up to 5.5%), these microprobe analyses strongly suggest that native Ag may be a mineral phase intergrown with the acanthite-aguilarite composition.

4) Silver-Sulfosalts

The elemental analyses from the microprobe indicates that there does not appear to be enough elemental As or Sb to constitute the identification of Ag-sulfosalt within the major silver stage. Previous writers, including myself, have indicated that Ag-sulfosalts are present in the Blackdome No. 1 vein system. It has been determined that the greenish-gray material, included within the inclusions of chalcopyrite and galena in pyrite, is a sulfosalt mineral such as tennanite- tetrahedrite, polybasite or stephanite. The microprobe study, although cursory, indicates abundant Fe and minor Cu in this mineral, enough to imply tetrahedrite, but it also contains anomalous Ag, enough to imply polybasite or stephanite. Note the compositional ranges for this phase within the inclusions of Table 6.1. It is here that an assumption must be made. It would be understandable to have tetrahedrite formed initially due to the abundant base-metal content in these inclusions but upon enrichment of silver in the system, the mineral is compositionally becoming Ag-rich. Elemental analyses indicate there is a lack of As in the mineral but the Sb component is sufficient enough to imply a composition between tetrahedrite, polybasite and/or stephanite. Further microprobe work is needed to study the inclusions within the pyrite.

c) Non Au- or Ag-bearing Minerals

1) Pyrite - FeS_2

The most abundant opaque sulfide mineral in the Blackdome No. 1 vein system is pyrite. In sections, pyrite may constitute up to 20% of the vein mode, but generally pyrite is no more abundant in the quartz-rich gangue than two percent. It occurs primarily as minute disseminated cubes up to one millimetre across, intergrown with pre-ore stage quartz. It commonly occurs as disseminated grains, veinlets or is contained in masses associated with ore-stage quartz. In post-ore stage material, pyrite is generally disseminated and often shows alteration to goethite and limonite. Pyrite is generally subhedral to euhedral in this stage and is usually less than 0.5 millimetre in diameter.

2) Chalcopyrite - $CuFeS_2$

The second most abundant sulfide is chalcopyrite and although it is only a 'minor' mineral in the vein, it constitutes the major base-metal component. Chalcopyrite commonly occurs as anhedral grains and aggregates. It stands out as apparently being an exsolution phase in inclusions within pyrite and is probably most abundant in this form. The chalcopyrite is commonly associated with the silver sulfide minerals in the pyrite.

3) Galena - PbS

Galena constitutes a base-metal sulfide mineral of trace amounts in the vein. It commonly occurs with chalcopyrite, sphalerite and silver sulfides as exsolution (?) phases within inclusions of pyrite. They are generally up to 50 microns across and are always anhedral in form. There are very few galena grains of euhedral nature within the vein-fill materials.

4) Sphalerite - ZnS

Sphalerite occurs in lower concentrations than does galena. No individual grains of sphalerite were observed in the vein-fill material, but significant amounts were found as inclusions, exsolution phases, within pyrite and associated with chalcopyrite, galena and silver sulfides.

5) Marcasite - FeS_2

This low-temperature form of Fe-sulfide occurs only as trace amounts throughout the No. 1 vein system. It occurs as long, acicular, radiating lamellae resulting from inversion of pyrite. A pyrite core was common. Marcasite is not only an excellent indicator of lower temperatures but also indicates the onset of more acidic conditions.

There are also trace amounts of pyrrhotite and arsenopyrite found within the No. 1 vein system. Bornite, digenite and covellite also occur at Blackdome, but occur in very minor amounts. Pyrolusite occurs as fine-grained anhedral crystals, associated with Fe-hydroxides and clay minerals within the vein zone.

C. NATURE OF THE ORE FLUIDS AS EVIDENCED BY GANGUE AND ORE MINERALOGY AT BLACKDOME

The main gangue phases in the ore at Blackdome are adularia, calcite and clay minerals. This suggests a two-phase region in the fluid system where the fluid began to effervesce, giving off steam of CO_2, H_2S, H_2 and other dissolved gases. The gases given off at this point allowed the pH to increase and the deposition of a characteristic assemblage of adularia and calcite, particularly in upflow zones (Browne and Ellis, 1970). The most prominent requirement for the formation of a Au-Ag (base-metal poor) deposit is a fluid relatively high in H_2S and CO_2, but of low salinity. The physical attributes, of being a Ag-Au (base-metal poor) deposit and ore fluids of low salinity, are clearly satisfied at Blackdome. The necessity of needing a fluid high in H_2S and CO_2 was not confirmed during the fluid inclusion study, but appears to have been the case as evidenced by adularia and calcite deposition. The deposition of the Ag-Au mineralization at Blackdome appears to be analogous to that at Broadlands. Gold and silver were carried in solution perhaps as a bisulfide complex. A critical point was reached, introduction of a cooler meteoric water, where boiling occurs and an initial pH increase due to CO_2-loss begins to undersaturate the fluid. A sustained loss of the more soluble H_2S volatile with the formation of only limited steam lead to supersaturation and ore deposition (Henley and Brown, 1985).

D. DISCUSSION

A schematic diagram showing the paragenetic sequence of gangue and ore mineralogy is given in Figure 6.3. The major mineral phases are indicated by solid lines, whilst dotted lines indicate the deposition of minor minerals. This diagram is an idealized schematic representing only the relative timing and importance of each mineral.

The three idealized stages of vein formation, indicated by mineralogy and morphology, are as follows:

1) Pre-ore stage- involved the initial fracturing, cataclasis and brecciation of the intermediate host-rocks. This stage involved the deposition of predominant quartz and adularia with minor calcite and pyrite. The earliest quartz phase is characterized by fine-grained material on the vein walls but gives way to cockscomb quartz crystals, up to 7 centimetres in length, also present along the vein walls. The growth of the quartz crystals suggests that deposition of the pre-ore material was slow, that the fault system was inactive for an extended period of time and that the crystals grew relatively undisturbed. Another primary

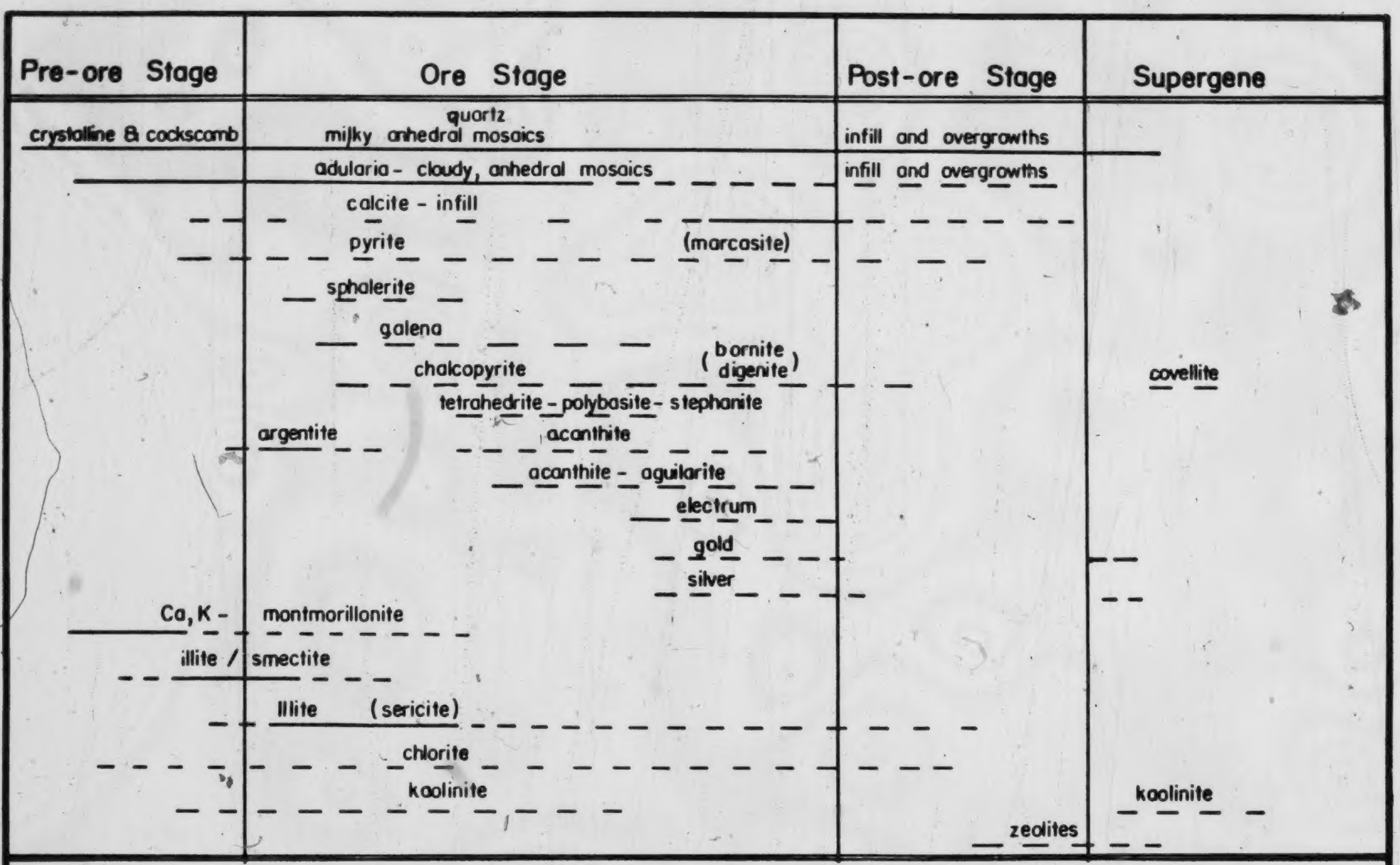

FIGURE 6.3 Paragenetic Sequence of the Blackdome No. I Vein System

feature of the pre-ore stage is the potassium metasomatism (adularia replacement) of the host fragments in the vein zone, as well as the mosaic texture of adularia intermixed with the fine crystalline quartz. The montmorillonite and mixed-layer illite/smectite are dominant alteration assemblages during the pre- ore stage. Pre-ore stage material comprises up to 20% of the total vein material.

2) Ore stage- was characterized by a brecciation event that cut the host fragments within the vein zone but also cut the breccis of the pre-ore stage. It was also a continuation of infilling the vein zone with the deposition of milky and grey quartz, cloudy adularia, calcite and pyrite, along with freibergite (the Ag-rich tetrahedrite), argentite-acanthite, acanthite-aguilarite, electrum, gold, chalcopyrite, and minor galena,sphalerite, bornite, digenite and covellite. Clay minerals were abundant during this stage with mixed-layer illite/smectite, illite and kaolinite being the most prominent with minor amounts of montmorillonite and chlorite.

Two prominent ore stages occur at Blackdome, with neither stage exhibiting a representative morphology for the abundant gangue phases of quartz, adularia or calcite. As was indicated by Buchanan, (1980 and 1981), and Petruk and Owens, (1974), the original stage was characterized by slightly higher temperatures, hence deposition of sphalerite, galena, chalcopyrite, and argentite occurred. This mineral assemblage, in reference to relative time, is accompanied by the illite/smectite and illite. This appears to be the point at which the fluids were probably the hottest. At this point, the hydrothermal solutions began to cool down and rise in pH. This brought on the deposition of the major phases of the ore stage with the Ag-sulfosalts, acanthite, acanthite-aguilarite, electrum, gold, silver, and minor base-metals occurring. Ore stage material can comprise up to 70-75% of vein mineralogy.

3) Post-ore stage-was dominated by the deposition of quartz with minor calcite and adularia. Quartz appears as infillings in open spaces and as minor overgrowths. Calcite and adularia appear primarily as infill materials. Zeolites (mordenite?) and marcasite are the introduced mineral phases in the post-ore zone. Most of the quartz in the post-ore stage is transparent and varies between euhedral and anhedral. The post-ore stage deposited only 5-10 percent of the total vein material.

It is obvious that it is impossible to deduce the time which elapsed between the end of one depositional stage and the start of another. It does seem that all depositional stages were probably initiated by seismicity (fault movement) and there is a definite indication through brecciation and zones of intense alteration that the pre-ore and ore stages represent one long depositional sequence. The post-ore stage represents a visible change in mineralogy and thus was likely deposited at a later time after some hiatus.

VII. BLACKDOME MINE: A MODEL FOR THE FORMATION OF THE EPITHERMAL AG-AU DEPOSIT

A. Geologic Setting

The Blackdome property is underlain by a localized suite of early- to mid-Tertiary volcanic rocks and associated volcaniclastic sediments, cut by narrow intermediate- to mafic- dykes.

The volcanic horizons strike NNE, with shallow 10-20° dips to the southeast. Tension fractures are the loci of the epithermal, precious-metal bearing veins. The fractures were, apparently, the result of volcanic doming. Minor normal faulting has effected dislocation of some units and has preserved some erosional remnants of younger rocks.

Major- and trace-element analyses suggest a calc-alkaline affinity for the volcanic rocks and also that they originated within a volcanic arc system. This volcanic arc constituted part of Stikinia (as defined by Monger et al, 1982), an allochthonous component of the Canadian Cordillera that was accreted on to the North American continent.

B. Hydrothermal Alteration

The vein systems are hosted by andesites and rhyolitic rocks which exhibit pervasive K-metasomatism and propylitic alteration, with the development of a replacive association of epidote (var.pistacite)-chlorite-carbonate-adularia. The propylitic alteration appears to be a broader-scale feature and is not limited to those areas invaded by metalliferous veins. The rocks of the rhyolitic unit also frequently exhibit strong, localized argillic alteration represented by montmorillonite and illite (any 10A material, including sericite). The argillic alteration is not confined to the spatial extent of the ore zones.

The ore veins are characterized by a distinct alteration halo, which can extend 1-15 m beyond the veins. The alteration zone is characterized by noticeable bleaching of the propylitized host volcanics and by the development of a replacive assemblage of quartz-adularia-sericite (all 10 A material), including illite/smectite-montmorillonite-kaolinite-minor carbonate- and minor chlorite.

C. Oxygen and Hydrogen Isotopic Composition of Ore Fluids

The S18O values of the hydrothermal fluids were calculated to be in the range of -6.8 to -8.8^{o}/oo.

The SD values of fluid inclusion waters vary from -125 to -134^{o}/oo, whilst for present day meteoric water the SD values range between -128 to -141^{o}/oo.

A considerable quantity of fluid inclusion and stable isotope data is available for the epithermal gold deposits of the southwestern U.S.A., Mexico and other parts of the world. In the majority of these deposits, circulating meteoric water has clearly been the dominant source of the mineralizing fluids, with little or no fluid contribution from any magmatic source (H.P. Taylor, 1973;1974; 1979; O'Neill and Siberman, 1974; Casadevall and Ohmoto, 1977; Kamilli and Ohmoto, 1977; and Henley, 1985). The SD values of the ore fluids are normally found to be similar to the SD values of local meteoric waters, but the oxygen isotopes of the ore fluids are commonly seen to have been exchanged by various degrees of reaction with the volcanic country rocks of the vein systems (Field and Fifarek, 1985).

The same is shown to be true at Blackdome as the SD values of the fluid inclusion waters demonstrate a slight enrichment in D by comparison with SD values for the present day meteoric waters of the region. This suggests that the isotopic composition of Tertiary meteoric water did not deviate much from that of the present-day meteoric water. As in other epithermal deposits, however, a strong shift in $S^{18}O$ is observed in the Blackdome ore fluids, which is obviously due to isotopic exchange between the thermal waters and the volcanic country rocks.

D. Salinities, Temperatures and Pressures of Ore Fluids

The Blackdome hydrothermal fluids were of low salinity, varying between 0.26 and 2.07 wt% NaCl equivalent and exhibited only a very limited variation in their dissolved ion contents. The densities of the ore fluids were in the range of 0.720-0.810 g/cm^3.

The homogenization temperatures suggest that the quartz components of the paragenetic sequence record only one peak thermal stage, which varies between 260°C and 295°C. The data are insufficient to postulate a lower and higher temperature regime, although temperatures ranging down to 209°C and as high as 313°C were obtained.

The coexistence of liquid- and vapour-rich inclusions suggests boiling. Boiling obviates the need for pressure corrections to the homogenization temperatures which would then represent the true trapping temperatures and pressures of the inclusions. The pressures from coexisting liquid- and vapour-rich inclusions were between 45 and 110 bars (4500-11000 kilopascals), which corresponds to an approximate maximum depth of ore deposition between 0.5 and 1.1 km below the surface of the volcanic field. This conclusion is based on the concept of the veins constituting an episodic, open, vented, hot spring/geyser system whose fluid pressures would have been dominantly hydrostatic rather than lithostatic.

E. Ore Mineralogy

Three idealized stages of vein formation have been outlined by mineralogy and morphology. The pre-ore stage involved initial fracturing, cataclasis and brecciation of the intermediate volcanic host rocks. Deposition of pre-ore material was slow in that the fault system was inactive for an extended period of time and the crystals grew relatively undisturbed into dilatent fractures. Potassium metasomatism is also a primary feature of the pre-ore stage. Mineralogy associated with the pre-ore stage comprises quartz and adularia along with minor calcite, pyrite, clay minerals and possibly acanthite.

The ore stage was characterized by the continuation of open-space filling of the vein zone by quartz, adularia, increased calcite and pyrite, along with the Ag-sulfosalts, argentite-acanthite, acanthite-aguilarite, electrum, gold and minor base-metals. The clay minerals illite/smectite, illite and kaolinite were prominent during the ore stage as was the brecciation of host fragments, within the vein, and pre-ore breccias.

The post-ore stage was dominated by the open-space filling of quartz with minor calcite and adularia. Minor copper, gold and silver mineralization occurred during the post-ore event along with the deposition of pyrite/marcasite. The post-ore clay minerals, illite and chlorite are a very minor component.

It appears that all depositional stages were probably initiated by a period of volcanism but the pre-ore and ore stages most likely represent one long depositional sequence. The post-ore stage was likely deposited at a later time, after some hiatus.

F. Nature of the Ore Fluids as Evidenced by Gangue and Ore Mineralogy

Adularia, calcite and the clay minerals were the prominent gangue phases during ore deposition at Blackdome.

These gangue phases suggest that the hydrothermal fluids reacted with a cooler meteoric water, that effervescence occurred and steam of CO_2, H_2S, H_2 and other dissolved gases was given off. At this point the pH would increase and the deposition of adularia and calcite, particularly in the up-flow zones, would occur. The Ag-Au (base-metal poor) deposit is characterized by a fluid relatively high in H_2S and CO_2, but of low salinity. These criteria are satisfied at Blackdome and it thus appears the deposition of the Ag-Au mineralization is analogous to that at Broadlands, New Zealand. Gold and silver were carried in solution, perhaps as a bisulfide complex, cooler meteoric water was introduced into the system and boiling occurred. The loss of CO_2 increased the pH and the fluid became undersaturated. A continuous loss of H_2S, with only a limited steam loss, lead to supersaturation and to ore deposition.

G. Conclusions

i) Blackdome as an Adularia-Sericite Type Deposit

A class of epithermal deposits known as the adularia-sericite type deposits was distinguished by Hayba et al, 1985, and is characterized by the following features.

1) Deposits of this type were generated in hydrothermal systems analogous to the present-day Taupo volcanic zone of New Zealand and the Yellowstone caldera of the U.S.A.

2) A deeply circulating, partly boiling brine 'plume'

deposited the metalliferous ores at or near the interface of a cooler meteoric water recharge zone. These fluids are buffered to a near-neutral pH and their redox and sulphidation states are buffered by Fe phases in the wallrocks and veins.

3) The condensation of acid volatiles in the upper portion of the geothermal system provides the acidity needed to effect sericitic alteration.

4) The deposits are generally hosted by a suite of rhyolitic to andesitic volcanics and associated volcaniclastic-sedimentary rocks.

5) Ore mineralogy is characterized by acanthite, native gold, native silver, electrum, some base-metal sulfides and selenides. High Ag/Au ratios are common. Chlorite and Mn-bearing gangue minerals are common in these deposits.

6) These deposits have characteristic sericitic to argillic wallrock alteration, along with abundant development of adularia. Potassium metasomatism is a primary alteration feature and reflects the abundance of the illite over smectites and mixed-layer clays.

7) Most ore deposition occurs at temperatures between 250^{o} to 300^{o}C, but late-stage gangue exhibits lower temperatures of formation around 140^{o} to 200^{o}C. Fluid salinities are generally low (< 3 wt% NaCl equivalent), though some deposits have salinities of up to 12 wt% NaCl equivalent.

8) Most of these hydrothermal systems register paleodepths of 300-600 m but some were operative at 1-1.4 km.

9) Meteoric water appears to dominate the hydrothermal systems, though the magmatic contribution cannot be disregarded.

The same authors classify a second major (but rarer) class of epithermal deposit - the acid-sulphate type. This type of deposit is associated with rhyodacitic, rhyolitic, and trachyandesitic centres and is distinguished primarily on the basis of the alteration suite of advanced argillic +/- sericitic facies, commonly associated with alunite. The argillic alteration zone is characterized by kaolinite, adularia is absent and chlorite is rare in this type of deposit. Enargite-pyrite-gold-electrum and base-metals are characteristically associated with these acid-sulphate type deposits. Some of this class contain bismuthinite, but none carry selenides.

It is clear, therefore, that the Blackdome deposits belong to the adularia-sericite class of Hayba et al, 1985, in that virtually all of the characteristics of the Blackdome system fit exactly those criteria listed above. The strikingly polymetallic nature of the ores - with sulfosalts, selenides, base-metal sulfides and minor arsenides - is noteworthy.

It is concluded that the adularia-sericite-type polymetallic deposits of the Blackdome epithermal field were generated when Tertiary meteoric groundwaters penetrated tensional fracture systems in a cooling, calc-alkalic, emergent island-arc environment. This resultant geothermal field was most likely underlain by a recirculating plume of brine which encountered meteoric waters at paleodepths of 0.5-1.1 km. The precipitation of a wide range of elements leached by the hydrothermal fluids occurred deep within the cooling volcanic edifice. This precipitation was accompanied by extreme local phyllosilicate plus K-metasomatism and silicification of the walls of the geothermal reservoir. This hydrative metasomatism caused a positive exchange shift in the $S^{18}O$ value of the fluids, away from the parent meteoric water line. Occasional venting of the system (resulting in boiling) or selective hydrogen metasomatism of the wallrocks could have effected a minor positive shift in SD value of the fluid. The metalliferous phases were most likely precipitated during episodic boiling of the fluids.

REFERENCES

ABBEY, S. (1977) Studies in "standard samples" for use in the general analysis of silicate rocks and minerals; Part 5: 1977 edition of "useable values". Geol. Surv. Can. paper 77-34, pp 31

BARAGAR, W. R. A. (1968) Major element geochemistry of the Noranda volcanic belt, Quebec-Ontario. Canadian Journal of Earth Sciences, 5, pp 773-790

BARNES, H. L. (1979) Geochemistry of Hydrothermal Ore Deposits; John Wiley and Sons, pp 798

BERGER, B.R., and EIMON, P.I. (1982) Comparative Models of Epithermal Silver-Gold Deposits. Soc.Min.Eng., AIME, Preprint 82-13, 25p.

BERRY, L.G. (Ed)(1974) Selected Powder Diffraction Data for Minerals, Publ. by Joint Committee on Powder Diffraction Standards, 1601 Park Lane, Swarthmore, Pennsylvania

BEST, M. G. (1982) Igneous and Metamorphic Petrology; W. H. Freeman and Company, pp 630

BRINDLEY, G.W. and BROWN, G. (Eds)(1980) Crystal Structures of Clay Minerals and Their X-Ray Identification, Mineralogical Society, London

BROWN, G. (1961) X-Ray Identification and Crystal Structure of Clay Minerals; Mineralog. Soc. London, pp 544

BROWNE, P.R.L. (1978) Hydrothermal Alteration in Active Geothermal Fields. In: Ann. Rev. Earth Planet Sci. 6:229-250

BUCHANAN, L.J.,1980; Ore Controls of Vertically Stacked Deposits, Guanajuato, Mexico, Soc. Min. Eng. of AIME, preprint 80-82, pp 16.

BUCHANAN, L.J. (1981) Precious Metal Deposits Associated with Volcanic Environments in the Southwest : Ariz. Geol. Surv. Digest, Vol XIV, pp.237-262.

CANN, J. R. (1970) Rb, Sr, Y, Zr, Nb in some ocean floor basaltic rocks; Earth Planet. Sci. Lett. 10, pp 7-11

CARMICHAEL, I. S. E., TURNER, F. J., VERHOOGEN, J. (1974); Igneous Petrology, McGraw-Hill

CASADEVALL, T., and OHMOTO, H. (1977) Sunnyside Mine, Eureka mining district, San Juan County, Colorado: geochemistry of gold and base-metal ore deposition in a volcanic environment. Economic Geology, 72, pp. 1285-1320.

CHURCH, R.N. (1980) Exploration for gold in the Blackdome Mountain area, B.C. Pap. B.C. Ministry Energy Mines Petroleum Resour. 1980-81, p 52-4.

CLAYTON, R.N. and MAYEDA, T.K. (1963) The use ofBromine Pentafluoride in the Extraction of Oxygen from Oxides and Silicates for Isotopic Analysis. Geochim. Cosmochim. Acta, 27, pp 43-52.

CRAIG, J.R. and VAUGHN, D.J., 1981; Ore Microscopy and Ore Petrography, John Wiley and Sons, pp 406.

CRAWFORD, M.L., (1981) Phase Equilibria in Aqueous Fluid Inclusions. Mineral Association Canada Short Course Handbook 6, pp. 75-100

DAWSON, J. M. (1983) Report on Blackdome Au-Ag prospect in British Columbia. Unpublished internal paper for Blackdome Exploration

DEER, W. A., HOWIE, R. A., ZUSSMAN, J. (1966) An introduction to the Rock Forming Minerals; John Wiley and Sons, 11th ed, pp 528

EBERL, E. and HOWER, J. (1977) The Hydrothermal Transformation of Sodium and Potassium Smectiteinto Mixed Layer Clay. In: Clays and Clay Minerals, Vol. 25, pp 215-227

ELLIS, A.J. (1979) Explored Geothermal Systems, in Barnes, H.L., ed., Geochemistry of Hydrothermal Ore Deposits: John Wiley and Sons, Inc. (publ.), pp. 632-683.

ENGELL, A. E. J., ENGEL., C. G., HAVENS, R. G. (1965); Chemical Characteristics of oceanic basalts and the upper mantle; Geol. Soc. Amer. Bull. 76, pp 719-734

FIELD, C.W., and FIFAREK, R. H. (1985) Light Stable-Isotope Systematics in the Epithermal Environment. In Geology and Geochemistry of Epithermal Systems; Berger, B.R. and Bethke, P.M., eds. Reviews in Economic Geology, 2, pp. 99-128.

FLOYD, P. A., WINCHESTER, J. A. (1975) Magma Type and Tectonic Setting discrimination using immobile elements; Earth Planet. Sci. Lett., 27, pp 211-218

FLUET, D.W., 1986; Genesis of the Deer Trail Zn-Pb-Ag Vein Deposit, Washington, U.S.A., unpub. thesis, Univ. Alb., Edmonton, Alb., Canada.

GOFF, S. P. (1984) The Magmatic and Metamorphic History of the East Arm, Great Slave Lake, N.W.T.; Unpubl. Ph.D. thesis.University of Alberta

GROSS, W.H., 1975; New Ore Discovery and Source of Silver-Gold Veins, Guanajuato, Mexico; Econ Geol, v. 70, pp 1175-1189.

HAAS, J.L. Jr. (1971) The effect of salinity on the maximum thermal gradient of a hydrothermal system at hydrostatic pressure. Econ. Geol., v. 66, pp 940-46.

HART, S. R., BROOKS, C., KROGH, T. E., DAVIS, G. L., NAVA, D.(1970) Ancient and modern volcanic rocks: a trace element model; Earth Planet. Sci. Lett., 10, pp 17-28

HAYBA, D.O. et al, 1985; Geologic, Mineralogy, and GeochemicalCharacteristics of Volcanic- Hosted Epithermal Precious-MetalDeposits, in: Geology and Geochemistry of Epithermal Systems, Reviews in Economic Geology, v. 2, pp 129-167.

HEALD, P., FOLEY, N.K., and HAYBA, D.O. (1987) Comparative Anatomy of Volcanic-Hosted Epithermal Deposits: Acid-Sulfate and Adularia-Sericite Types. Econ. Geol., Vol. 82, p 1-26.

HENLEY, R. W. (1985) The Geothermal Framework of Epithermal Deposits. Reference 2, pp. 1-24.

HENLEY, R.W. and BROWN, K.L., 1985; A practical guide to the thermodynamics of geothermal fluids and hydrothermal ore deposits, in: Geology and Geochemistry of Epithermal Systems, Reviews in Economic Geology, v. 2, pp 25-44.

HOWER, J. (1981) X-Ray Diffraction Identification Of Mixed Layer Clay Minerals. In: Mineralogical Association of Canada, Short Course in Clays and the Resource Geologist; F.J. Longstaffe (Ed), Vol. 7

HUGHES, C. J. (1973) Spilites, keratophyres and the igneous spectrum; Geological Magazine, 109, pp 513-527

IGNASIAK, T.M.; KOTLYAR, L.; LONGSTAFFE, F.J.; STRATVSZ, O.P.; and MONTGOMERY, D.F. (1983) Separation and Characterization clays from Athabasca Asphaltene,Fuel, Vol. 62

IRVINE, T. N., BARAGAR, W. R. A. (1971) A guide to the chemical classification of the common volcanic rocks; Canadian Journal of Earth Sciences, 8, pp 523-548

KAMILLI, R.J. and OHMOTO, H. (1977) Paragenesis, Zoning, Fluid Inclusion and Isotopic Studies of the Finlandia Vein, Colqui District, Central Peru. Econ. Geol. 72, pp 950-982.

KAY, A., and STRONG, D.F. (1983) Geologic and Fluid Controls on As- Sb- Au Mineralization in the Moretons Harbour Area, Newfoundland. Econ. Geol., Vol 78, pp.1590-1604.

KERR, P. F. (1979) Optical Mineralogy; McGraw-Hill, pp 492
KESLER, T.L. (1970) Hydrothermal Kaolinization in Michocoan, Mexico. In: Clays and Clay Minerals, Vol. 18, pp 121-124, Permagon Press

KOISUMI, M. (1975) Synthesis of Clays and Related Minerals and Their Geochemical Dignificance. In: Proc. Int'l Clay Conference, Applied Publ. Ltd., pp 247-256

KRISTMANNSDOTTR, H. (1978) Alteration of basaltic rocks by hydrothermal activity at 100°-300°C. In: Developments in Sedimentology, M.M. Mortland, V.C. Farmer (Eds), Int'l Clay Conference (1978)

MACDONALD, G. A., and KATSURA, T. (1964) Chemical composition of Hawaiian lavas; J. Petrol., 5, pp 82-133

MARTIN, R.T. (1955) Reference chlorite characterization for chlorite identification in soil clays. Clays and Clay Minerals, Proc. 3rd, National Conference (1954)

MASON, B., and MOORE, C. B. (1982) Principles of Geochemistry; John Wiley and Sons, 4th ed, pp 344

MASTERSON, W.D., and KYLE, J.R. (1983) Geological, Geochemical, Stabe Isotope, and Fluid Inclusion Characteristics of Epithermal Gold Mineralization, Velvet District, Nevada; J. Geochem. Expl., 20, pp. 55-74.

MIYAZAWA, T.; TOKUNAGA, M.; OKAMURA, S.; and EJOJI, M. (1971) Formation Temperatures of Veins in Japan. Soc. Min. Geol. Japan, Spec. Issue 3, pp. 340-344.

MONGER, J. W. H., PRICE, R. A., and TEMPELMAN-KLUIT, D. J. (1982) Tectonic accretion and the origin of the two major metamorphic and plutonic welts in the Canadian Cordillera. Geology, 10, pp. 70-75.

MOORHOUSE, W. W. (1959) Study of rocks in thin section; Harper-Row Publ., pp 514

NASH, J.T. (1972) Fluid Inclusion Studies of Some Gold Deposits in Nevada, in U.S.G.S., Prof. paper 800-C, pp.15-19.

NESBITT, B.E., MUROWCHICK, J.B., and MEUHLENBACHS, K. (1986) Dual origins of lode gold deposits in the Canadian Cordillera. Geology, 14, pp 506-9.

NOCKOLDS, S. R. (1954) Average chemical compositions of some igneous rocks;Bull. Geol. Soc. Am., 65, p 1007-1032

OHMOTO, H. and RYE, R.O. (1979) Isotopes of Sulfur and Carbon. In: H.L. Barnes (Ed), Geochemistry of Hydrothermal Ore Deposits, 2nd Edition, Wiley-Interscience Publ., John Wiley and Sons, New York, pp 509-567.

O'NEIL, J.R. and SILBERMAN, M.L. (1974) Stable Isotope Relations in Epithermal Au-Ag Deposits. Econ. Geol. 69, pp 902-909.

O'NEIL, J.R., et al (1973) Stable Isotope and Chemical Relations During Mineralization in the Bodie Mining District, Mono County, California. Econ. Geol. 68, pp 765-784.

PEARCE, J. A., CANN, J. R. (1972) Ophiolitic origin investigated by discriminant analysis using Ti, Zr, and Y; Earth Planet. Sci. Lett., 12, pp 339

PEARCE, J. A., CANN, J. R. (1973) Tectonic Settings of basic volcanic rocks determined using trace element analyses; Earth Planet Sci. Lett., 19, pp 290-300

PETRUK, W. et al, 1974; Observations on Acanthite, Aguilarite and Naumannite; Can. Mineralogist, v. 12, pp 365-369.

PETRUK, W. and OWENS, D., 1974; Some Mineralogical Characteristics of the Silver Deposits in the Guanajuato Mining District, Mexico. Econ Geol, v. 69, pp 1078-1085

POTTER, R.W. II; CLYNNE, M.A. and BROWN, D.L. (1978) Freezing Point Depression of Acqueous Sodium Chloride Solutions, Econ. Geol., Vol. 73, pp. 284-285.

REEVE, A., RENNIE, D. (1985) The geology of the Blackdome gold-silver deposits, Clinton, B.C. Paper presented at the CIM meeting, Vancouver, April 1985.

ROEDDER, E. (1967) Fluid Inclusion as Samples of Ore Fluids, in Barnes, H.L., ed., Geochemistry of Hydrothermal Ore Deposits: John Wiley and Sons Inc. (Publ.) 1979, pp. 684-737.

ROEDDER, E. (1984) Fluid Inclusions. Reviews in Mineralogy, Vol. 12, Min. Soc. Am., 644 p.

ROEDDER, E.; and BODNAR, R.J. (1980) Geologic Pressure Determinations from Fluid Inclusion Studies. Ann. Rev. Earth Planet Sci., 8, pp. 263-301.

RYE, R.O. and OHMOTO, H. (1974) Sulfur and Carbon Isotopes and Ore Genesis: A Review. Econ. Geol. 69, pp 826-842.

SAWKINS, F.J.; O'NEIL, J.R.; and THOMPSON, J.M.f (1979) Fluid Inclusion and Geochemical Studies of Vein Gold Deposits, Baguio District, Philippines. Econ. Geol., Vol. 74, pp. 1420-1434.

SHILO, N.S.; SIDOROU, A.A.; GONCHAROU, V.I.; and NAIBORODIN, V.I. (1971) The Temperature Conditions and the Depths of Formation of Gold Ore Deposits. Soc. Min. Geol. Japan, Spec. Issue 3, pp. 356-359.

SHIMODA, S. and SUDO,T. (1960) An interstratified mixture of mica clay minerals: Am. Mineralogist, 45, pp 1069-1077

SMITH, D.M.; ALBINSON, T.; and SAWKINS, F.J. (1982) Geologic and Fluid Inclusion Studies of the Tayoltita Silver-Gold Vein District, Durango, Mexico. Econ. Geol., Vol. 77, pp. 1120-1145.

SMITH, R. E., and SMITH, S. E., (1976) Comments on the use of Ti, Zr, Y, Sr, K, P and Nb in the classification of basaltic magmas; Earth Planet Sci. Lett., 32, pp 114-120

SRODON, J. (1980) Precise Identification of Illite/Smectite Interstratifications by X-Ray Powder Diffraction. In: Clays and Clay Minerals, Vol. 28, No. 6, pp 401-411

SRODON, J. (1981) X-Ray identification of randomly interstratified illite/smectite in mixtures with discrete illite. In: Clays and Clay Minerals, Vol. 16, pp 297-304

SRODON, J. (1984) X-Ray powder diffraction identification of illitic materials. In: Clays and Clay Minerals, Vol. 32, No. 5, pp 337-349

STEINER, A. (1968) Clay Minerals in Hydrothermally Altered Rocks at Wairakei, New Zealand. In: Clays and Clay Minerals, Vol. 13, pp193-213

SUDO, T., HAYASHI, H. AND SHIMODA, S. (1962) Mineralogical problems of intermediate clay minerals. In: Clays and Clay Minerals, Vol. 9, pp 378-392

SUMI, K. (1969) Zonal distribution of clay minerals in the Matsukawa geothermal area, Japan. In: Int'l Clay Conf., pp 500-512

SUTHERLAND BROWN, A. (1986) Linkages between Geological Branch Studies, geological knowledge, and exploration success in British Columbia. Canadian Mining and Metallurgical Bulletin, vol. 79, No. 886, pp 51-62.

TAKENOUCHI, S.; and IMAI, H. (1971) Fluid Inclusion Study of

Some Tungsten-Quartz Veins in Japan. Soc. Min. Geol. Japan, Spec. Issue 3, pp 345-350.

TAYLOR, H.P. (1973) O^{18}/O^{16} Evidence for Meteoric-Hydrothermal Alteration and Ore Deposition in the Tonopah, Comstock Lode, and Goldfield Mining Districts, Nevada. Econ. Geol. 68, pp747-764.

TAYLOR, H.P. (1974) The Application of Oxygen and Hydrogen Isotope Studies to Problems of Hydrothermal Alteration and Ore Deposition. Econ. Geol. 69, pp 843-883.

TAYLOR, H.P.(1979) Oxygen and Hydrogen Isotope Relationships in Hydrothermal Mineral Deposits. In: H.L. Barnes (Ed), Geochemistry of Hydrothermal Ore Deposits, 2nd Edition, Wiley-Interscience Publ., John Wiley and Sons, New York, pp 236-277.

THOREZ, J. (1976) Practical Identification of Clay Minerals. Lelotte, Dison, Belgium, pp 90

VIKRE, P.G., 1985; Precious Metal Vein Systems in the National District, Humboldt County, Nevada. Econ Geol, v. 80, pp 360-393.

VIVIAN, G., MORTON, R.D., CHANGKAKOTI, A. and GRAY, J. (1987) Blackdome Eocene epithermal Ag-Au deposit, British Columbia, Canada- nature of ore fluids. In: Trans. Inst. Min. Met., Section B, Applied Earth Science, Vol. 96, pp 9-14.

WHITE, D.E. (1981) Active Geothermal Systems and Hydrothermal Ore Deposits. Econ. Geol. 75th Anniversary Vol., 1981, pp.392-423.

WHITE, J.L. (1962) X-Ray Diffraction Studies on Weathering of Muscovite. In: Soil Science, Vol. 93, pp 16-21

WHITEHEAD, R. E. S., GOODFELLOW, W. D. (1978); Geochemistry of volcanic rocks from the Tetagouche Group, Bathurst, N. B., Canada; Canadian Journal Earth Sciences, 15, pp 207-219

WINCHESTER, J. A., FLOYD, P. A. (1975) Geochemical magma type discrimination: Application to altered and metamorphosed basic igneous rocks. Earth Planet. Sci. Letters, 28, pp 459-469

WINCHESTER, J. A., FLOYD, P. A. (1977) Geochemical discrimination of different magma series and their differentiation products using immobile elements; Chem. Geol., 20, pp 325-343

YERMAKOV, N.P. (1971) Correlation of Stages of Veined Ore-Formation and Alterations of Host Rocks (as indicated by gas-liquid inclusions) Soc. Min. Geol. Japan, Special Issue 3, pp. 337-339.

VIII. APPENDICES

APPENDIX A

Experimental Techniqes for Clay Mineral Analyses

Bulk Sample

All samples were crushed to an average size of less than 0.1 mm and mounted on a "back-packed" disc to determine whole rock mineralogy.

Clay Size Fraction

Sample preparation and analytical procedures are described in detail by Ignasiak et al. (1983) anf Foscolo's et al. (1982).

Using the settling velocity, the <2 um, 2-5 um, and the 5-20 um size fractions were separated. After being shaken, the sample is allowed to settle a given time according to the temperature. The <2 um fraction is separated first followed by the latter two size fractions. For each fraction, 900 ml of the 1000 ml graduated cylinder is removed by siphoning after the given time for that size range. This procedure is repeated three times for each size fraction. After the three sizes are separated they are palced in a hot water bath for one day. Bleach is added before the bath in order to flocculate the clays. The water bath destroys any organics present in the sample.

Wash the samples after the water bath in order to rid the samples of the bleach. This is done by adding distilled water to the samples and centrifuging and then drawing off the excess water and repeating the step until there is no blrach left in the sample. Test for bleach by using $AgNO_3$ litmus paper.

Saturating the Samples

Separate the <2 um fraction into three portions. Label the three test tubes as Ca^{++}, K^+ and "as is". Introduce 10 ml of $CaCl_2.2H_2O$ into the Ca^{++} test tube and 10 ml of KCl into the K^+ test tube. Sonicate these samples, centrifuge and draw off supernatant. Wash these samples like before to ensure the Ca^{++} and K^+ cations are trapped within the interlayers of the clays.

Upon obtaining clean samples of the saturated samples, leave approximately 0.5 cm of water in the bottom of the test tubes. Place all prepared samples in the freeze dryer overnight. After freeze drying, obtain 50 milligrams of sample. Obtain ceramic discs, label and attach to a lab vacuum set-up. Place the prepared sample material in separate test tubes and about 5 ml of distilled water. Sonicate all samples to disperse material. Place all mareial on discs and allow vacuum to work for approximately for 2-3 hours.

Procedures prior to X-Ray Diffraction Analysis

i) For Ca^{++} disc:

a) Place disc in the 54% humidity chamber for 24 hours and X-Ray sample from $2^{\circ}20$ to $35^{\circ}20$

b) Place disc in glycolation chamber, evacuate and place in oven at $65^{\circ}C$ overnight. X-Ray sample from $2^{\circ}20$ to $60^{\circ}20$

ii) For K^{+} disc:

a) Place disc in the oven at $105^{\circ}C$ for 24 hours. X-Ray sample from $2^{\circ}20$ to $35^{\circ}20$ maintaining 0% humidity.

b) Place disc in the 54% humidity chamber for 24 hours and X-Ray sample from $2^{\circ}20$ to $22^{\circ}20$.

c) Place disc in oven at $300^{\circ}C$ for three hours and X-Ray from $2^{\circ}20$ to $22^{\circ}20$ maintaining 0% humidity.

d) Place disc in oven at $550^{\circ}C$ for two hours and X-Ray from $2^{\circ}20$ to $22^{\circ}20$ maintaining 0% humidity.

iii) For 2-5 um disc:

a) Place disc in X-Ray chamber and analyze from $2^{\circ}20$ to $60^{\circ}20$.

iv) For 5-20 um disc:

a) Place disc in X-Ray chamber and analyze from $2^{\circ}20$ to $60^{\circ}20$.

Properly identify and label all charts.

Calculation of Clay Abundances

The calculation of clay abundances is carried out in two fashions:

1) Peak height method

a) calculate the form factors

i) 10A mineral is the internal standard with form factor of 1.000

ii) smectite (17A)= height of 17A peak/ 4 x 10A peak

iii) chlorite (14A)= height of 14A peak/ 3 x 10A peak

iv) kaolin (7A)= height of 7A peak/ 2.5 x 10A peak

v) mixed layer = height of ML peak/ 2 x 10A peak

Sum the form factor values and calculate percentages.

Example of Peak Height Method

Peak	**Form Factor**	**% of Total Clay**
10A	1.000	1.000/2.5 = 40
17A	.250	.250/2.5 = 10
14A	.750	.750/2.5 = 30
.7A	.500	.500/2.5 = 20
	2.500	100

2) Peak Area Method

The peak area method is carried out by using a planimeter or counting squares. An estimation of the area is taken amd multiplied by a form factor. This form factor has been derived by doing numerous experiments and it has been found the calculations usually show too low of an abundance so the value is multiplied by a form factor.

a) Illite - area under the 10A peak x 4

b) Smectite - area under the 17A peak x 1

c) Kaolinite - area under the 7A peak x 2
d) Chlorite - area under the 14A peak x 3

e) Mixed-Layer - form factor has to be derived for each experiment.

Whether using the peak height or peak area method, a best fit background line has to be established along the X-Ray charts. All measurements are taken from the background base established. Either of these methods is semi-quantitative.

APPENDIX B

Photo - Micrographs of thin section work

PLATE 2.1 No. 1 Vein Blackdome Mine, DDH 06,

Specimen #06-7.5

An andesite showing a plagioclase phenocryst altered to sericite with Fe-stain (limonite or goethite). Groundmass shows minor trachytic texture of both glassy and fine-crystalline material (plag, k-spar, qtz and pyx). Note the .4 mm apatite crystal in extinction above the plagioclase. This section is in cross-polars with the field of view being dmass. The field of view is 4 mm and is in plane-polars.

PLATE 2.2 No. 1 Vein Blackdome Mine, DDH 06,

Specimen # 06-12.5

An andesite with an altered plagioclase phenocryst (sericite, minor K-spar). The two fractures indicate a later silicification and K-feldspar event. Groundmass has both a pilotaxitic and trachytic texture. Section 06-12.5 is in cross-polars and has a field of view of 4 mm.

THE QUALITY OF THIS MICROFICHE IS HEAVILY DEPENDENT UPON THE QUALITY OF THE THESIS SUBMITTED FOR MICROFILMING.

UNFORTUNATELY THE COLOURED ILLUSTRATIONS OF THIS THESIS CAN ONLY YIELD DIFFERENT TONES OF GREY.

LA QUALITE DE CETTE MICROFICHE DEPEND GRANDEMENT DE LA QUALITE DE LA THESE SOUMISE AU MICROFILMAGE.

MALHEUREUSEMENT, LES DIFFERENTES ILLUSTRATIONS EN COULEURS DE CETTE THESE NE PEUVENT DONNER QUE DES TEINTES DE GRIS.

2.1

2.2

PLATE 2.3 **No. 1 Vein Blackdome Mine, DDH 06, specimen #06-37.5**

An andesite with an open fracture. The pyroxene phenocryst above the fracture shows alteration to epidote and minor carbonate. Quartz and K-feldspar (adularia) replacement of the plagioclase phenocrysts. Very fine-grained kaolinite is seen in the lower right corner of the section on the plagioclase. Field of view is 4 mm and is in plane-polars.

PLATE 2.4 **No. 1 Vein Blackdome Mine, DDH 06, specimen #06-45.0**

This photo shows plagioclase crystals that have altered, fractured and fragmented. Most noteworthy is the clay alteration seen in the groundmass. The field of view is 4 mm and is in plane-polars.

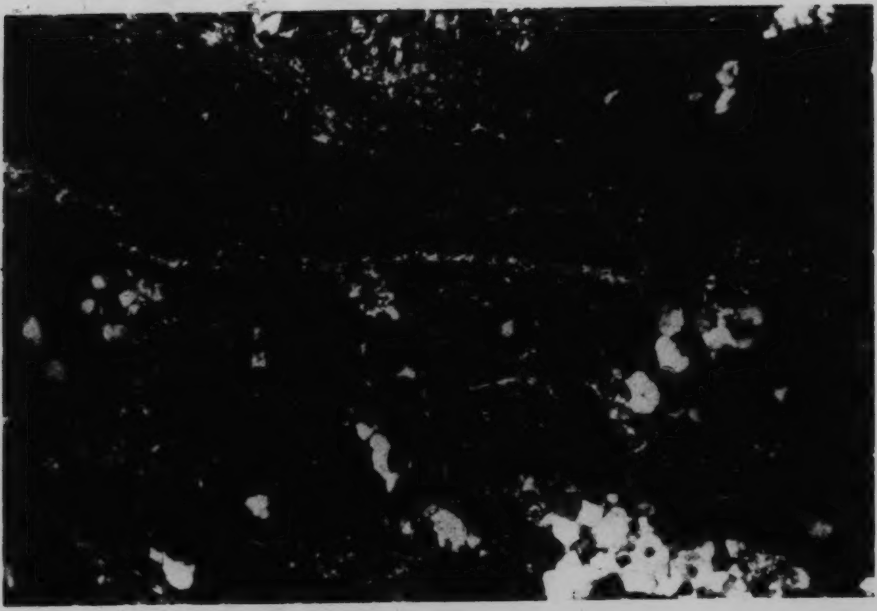

2.3

2.4

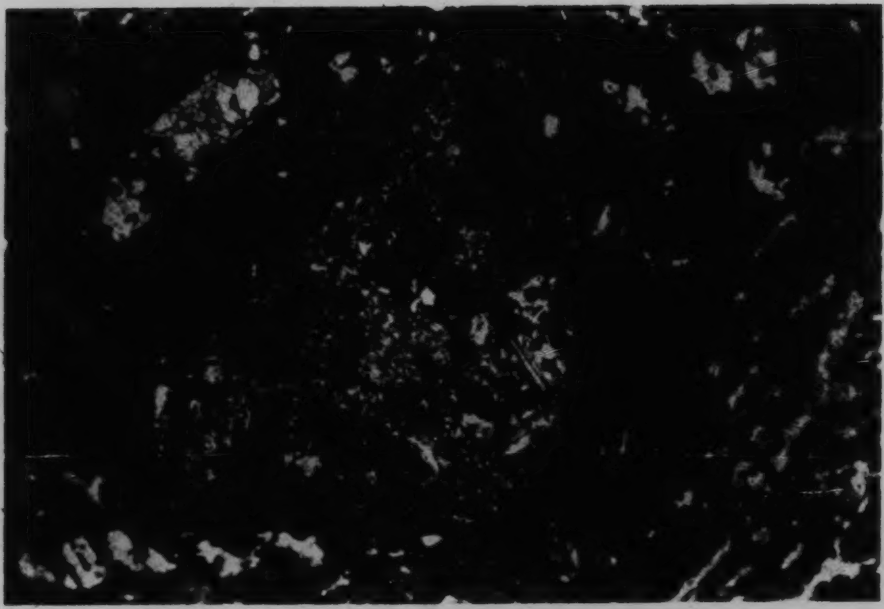

PLATE 2.5 No. 1 Vein Blackdome Mine, DDH 06

Specimen #06-45.0

Same as Plate 4 but in X-polars. Outstanding feature is the epidote, sericite and minor calcite alteration of the plagioclases. Field of view is 4 mm.

PLATE 2.6 No. 1 Vein Blackdome Mine, DDH 06

Specimen #06-50.0

A rhyolite showing autobrecciation, where the brecciated fragments are all devitrified glass. Interclast material shows sericite alteration with Fe-stain. Field of view is 4 mm XP.

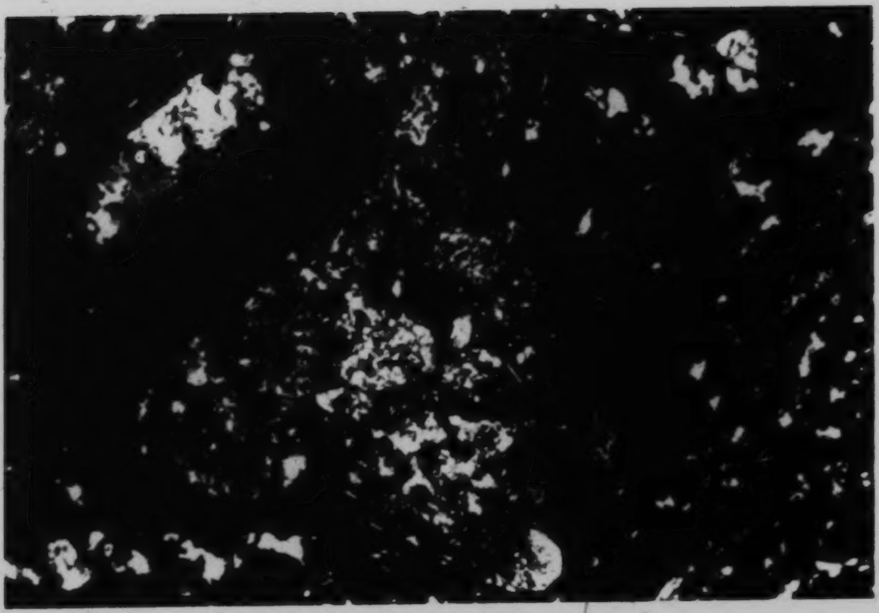

2.5

2.6

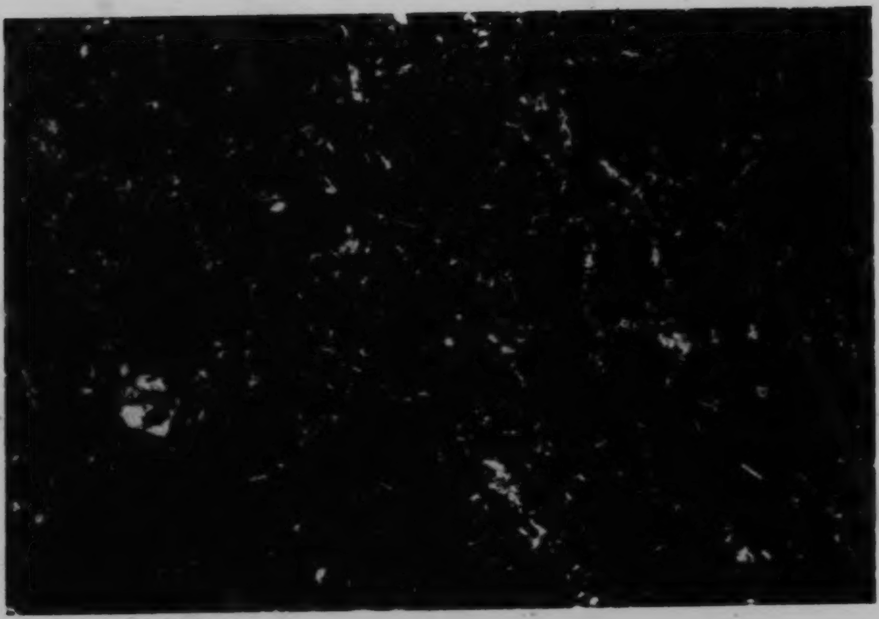

PLATE 2.7 No. 1 Vein Blackdome Mine, DDH 84
Specimen #84-15.0

An andesite containing an xenolith fragment of plagioclase crystals, totally replaced by carbonate and epidote. Characteristic amphibole cross-section is seen in the upper part of the photo. Field of view is 4 mm XP.

PLATE 2.8 No. 1 Vein Blackdome Mine, DDH 84
Specimen #84-70.0

A welded tuff of rhyolite composition. The clasts are mostly devitrified glass and are surrounded by essentially the same composition. Field of view is 4 mm XP.

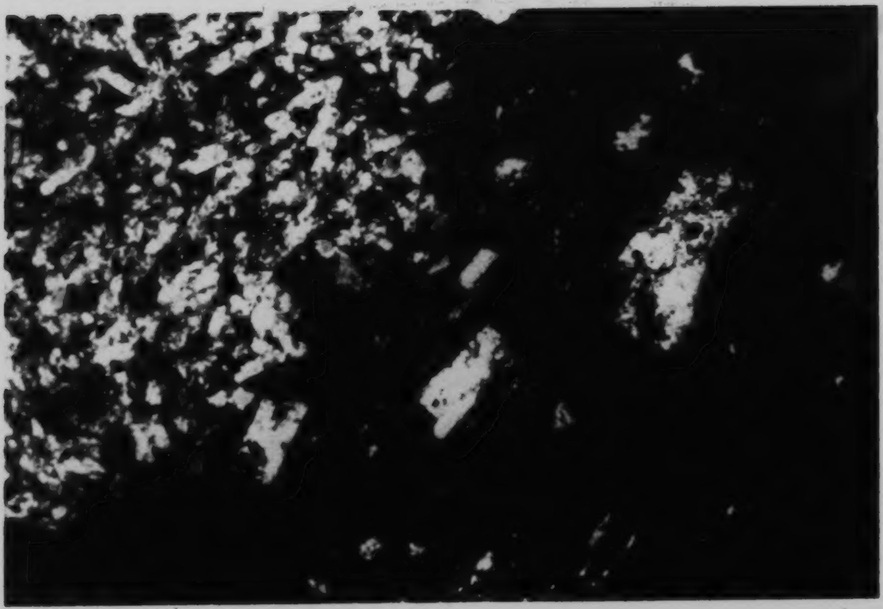

2.7

2.8

PLATE 2.9 **No. 1 Vein Blackdome Mine, DDH 84**

Specimen #84-120.0

A dacite in composition which is quite fine-grained with a glassy and crystalline groundmass. Later fracture with eipidote, quartz and kaolinite. Field of view is 4 mm XP.

PLATE 2.10 **No. 1 Vein Blackdome Mine, DDH 129**

Specimen #129-10.0

Basalt to andesite in composition that is mostly a crystalline mass. No large phenocrysts but shows smaller plagioclase laths in pilotaxitic groundmass that is altered to eipidote, chlorite, sericite and clay. Field of view is 4 mm XP.

2.9

2.10

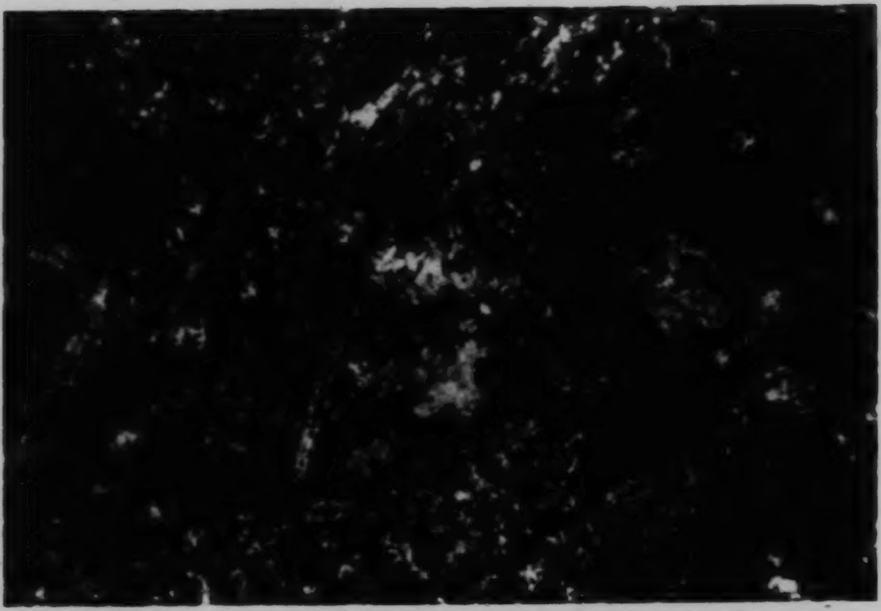

PLATE 2.11 No. 1 Vein Blackdome Mine, DDH 129

Specimen #129-40.0

Porphyritic andesite flow showing basitite (a pseudomorph of ortho-pyroxene, hypersthene, gone to serpentine). Also seen are some euhedral plagioclase laths that show epidote alteration.

Field of view is 4 mm XP.

PLATE 2.12 No. 1 Vein Blackdome Mine, DDH 137

Specimen #137-45.0

Autobrecciated andesite flow. Essentially same composition as Plate 15.

Field of view is 4 mm XP.

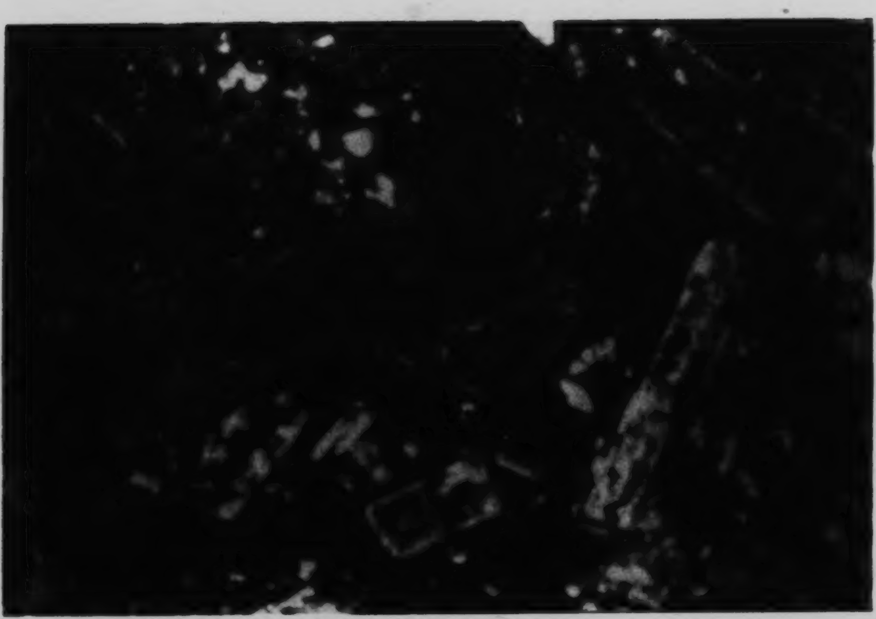

2.11

2.12

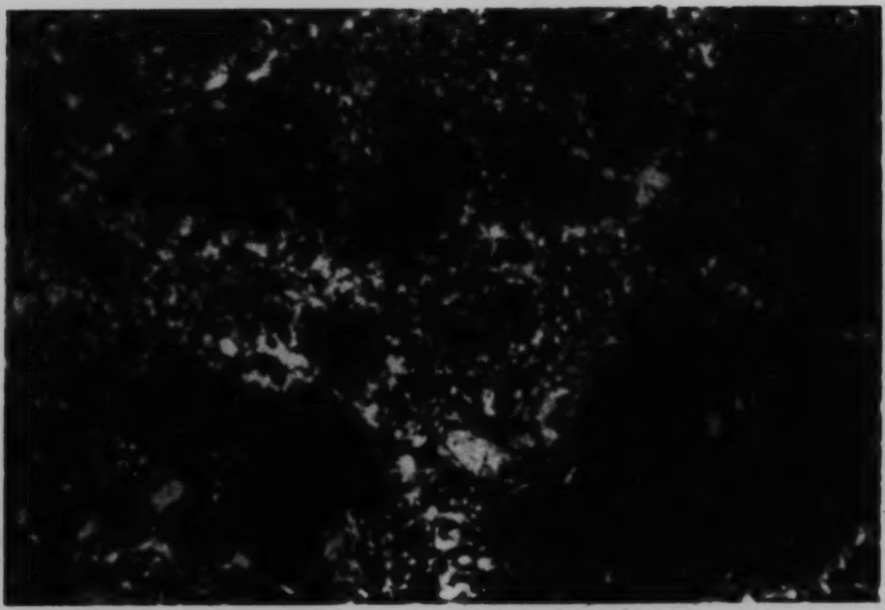

APPENDIX C

Photo - micrographs and EDA analyses of the clay components

PLATE 3.1,3.2 No. 1 Vein Blackdome Mine, DDH 84
Specimen #84-28.2

Photo-micrograph and an EDA analysis of the Smectite component within the ore zone of Blackdome.

PLATE 3.3,3.4 No. 1 Vein Blackdome Mine, DDH 139
Specimen #139-151.4

Photo-micrograph and an EDA analysis of the illite component within the ore zone of Blackdome.

PLATE 3.5,3.6 No. 1 Vein Blackdome Mine, DDH 84,
Specimen #84-30.5

Photo-micrograph and an EDA analysis of the illite component within the ore zone of Blackdome.

3.1

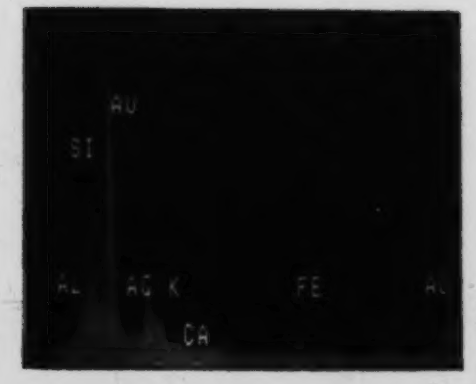

3.2

3.3

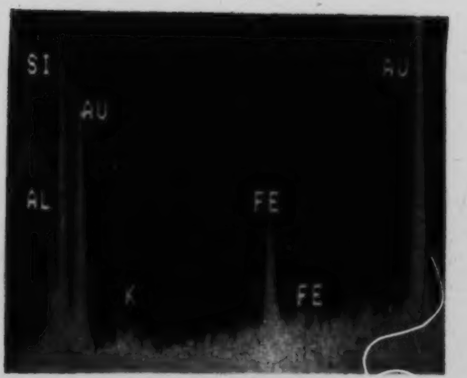

3.4

3.5

3.6

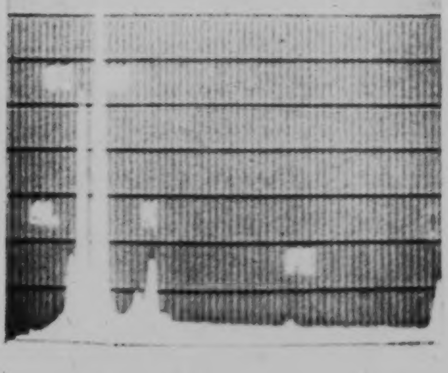

PLATE 3.7,3.8 No. 1 Vein Blackdome Mine, DDH 23
Specimen #23-23.1

Photo-micrograph and an EDA analysis of the kaolinite component within the ore zone of Blackdome.

PLATE 3.9,3.10 No. 1 Vein Blackdome Mine, DDH 84
Specimen #84-28.2

Photo-micrograph and an EDA analysis of the illite/smectite component within the ore zone of Blackdome.

3 7

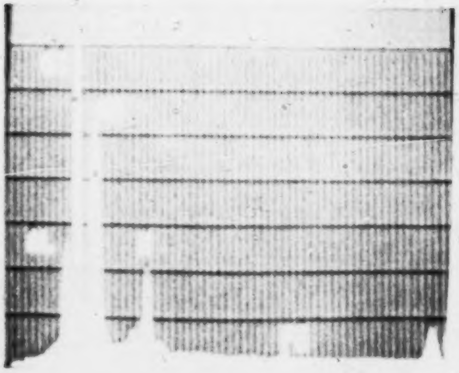

3 8

3 9

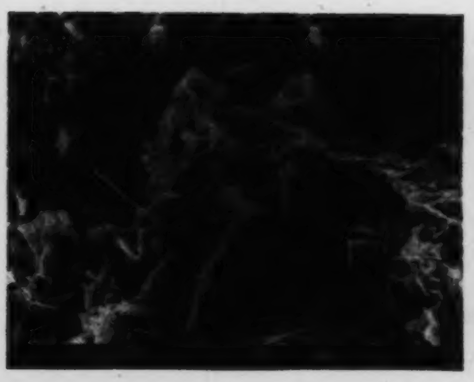

3 10

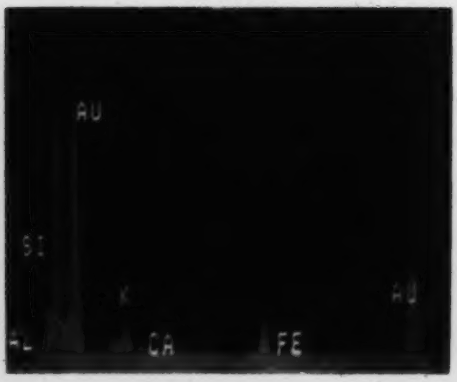

APPENDIX D

Photo - micrographs of the Fluid Inclusions

PLATE 4.1 No. 1 Vein Blackdome Mine, DDH 139

Specimen #139-158.0

Large primary, type 1 fluid inclusion, approximately 120 microns in length. Necking is visible in this inclusion. There are numerous secondary inclusions in the field of view. Fiew of view: 600 microns.

PLATE 4.2 No. 1 Vein Blackdome Mine, DDH 84

Specimen #84-31.8

In focus are two liquid-dominated inclusions, center of photo. There are numerous other liquid- and liquid-vapour-dominated inclusions slightly out of focus. Field of view: 200 microns.

41

42

PLATE 4.3 No. 1 Vein Blackdome Mine, DDH 06

Specimen #06-15.0

Primary, secondary and pseudo-secondary fluid inclusions. Field of view: 600 microns.

PLATE 4.4 No. 1 Vein Blackdome Mine, DDH 06

Specimen #06-15.0

Large liquid-dominated primary inclusion with a daughter crystal (Dawsonite?). An indication of necking is seen by the tail-type characteristic of this inclusion. There is another liquid-dominated inclusion below the inclusion with the daughter crystal. Field of view: 600 microns.

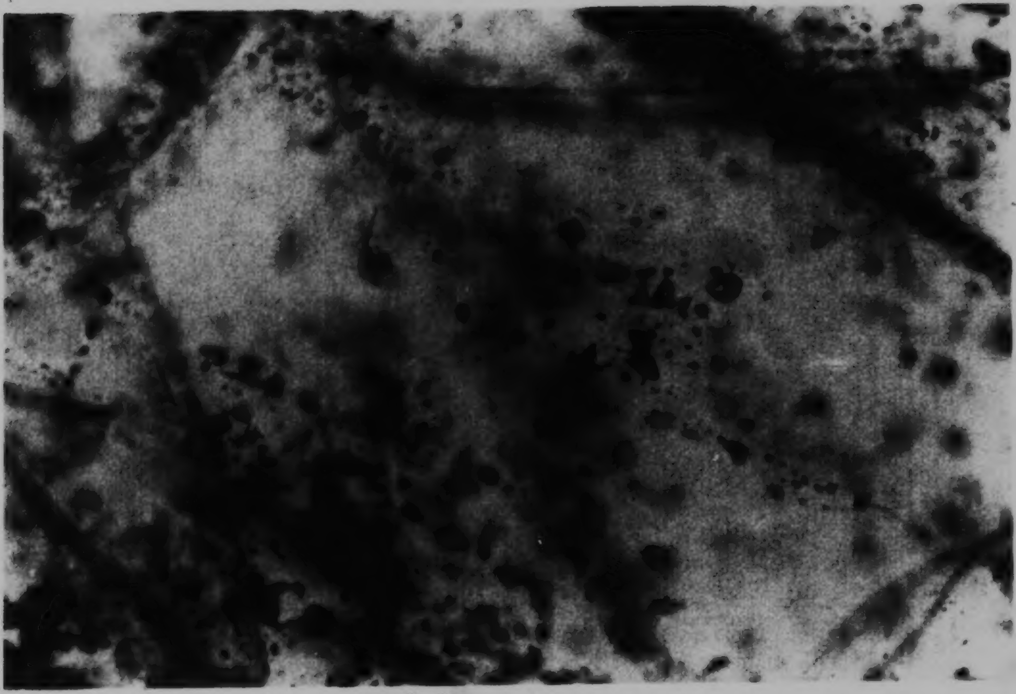

4 3

4 4

PLATE 4.5 No. 1 Vein Blackdome Mine, DDH 08

Specimen #08-32.2

Numerous type 1 fluid inclusions.

Field of view: 600 microns.

PLATE 4.6 No. 1 Vein Blackdome Mine, DDH 08

Specimen #08-32.2

Large, type 1, primary fluid inclusion with a length of 200 microns.

Field of view: 600 microns.

45

46

PLATE 4.7 No. 1 Vein Blackdome Mine, DDH 08

Specimen #08-32.2

Numerous primary fluid inclusions which have varying filling ratios.

Field of view: 1000 microns.

PLATE 4.8 No. 1 Vein Blackdome Mine, DDH 137

Specimen #137-51.6

A planar array of secondary fluid inclusions averaging 10-15 microns in length.

Field of view: 600 microns.

47

48

PLATE 4.9 No. 1 Vein Blackdome Mine, DDH 148

Specimen #148-165.0

Numerous pseudo-secondary inclusions within arcuate fractures which terminate over short distances. Field of view: 1000 microns.

PLATE 4.10 No. 1 Vein Blackdome Mine, DDH 148

Specimen #148-165.0

Numerous pseudo-secondary inclusions with some primary inclusions. Note pseudo-secondary inclusion planes do not cross grain boundaries. Field of view: 1000 microns.

4 9

4 10

PLATE 4.11 No. 1 Vein Blackdome Mine, DDH 136

Specimen #136-60.0

Large, primary fluid inclusion, type 3, with a daughter crystal in the right side of the inclusion. This inclusion is 115 microns in length. Field of view: 600 microns.

PLATE 4.12 No. 1 Vein Blackdome Mine, DDH 136

Specimen #136-60.0

Oriented secondary fluid inclusions, type 1, with one liquid-dominated inclusion and varying filling ratios. Field of view: 450 microns.

4 11

4 12

PLATE 4.13 No. 1 Vein Blackdome Mine, DDH 136

Specimen #136-60.0

Secondary and primary fluid inclusions. One liquid-dominated fluid inclusion is situated near the right hand side of the photo.

Field of view: 1000 microns.

PLATE 4.14 No. 1 Vein Blackdome Mine, DDH 01

Specimen #01-12.5

Secondary fluid inclusions.

Field of view: 1000 microns.

4 13

4 14

APPENDIX E

Photo - micrographs of the Ore Petrography

PLATE 6.1. No. 1 vein Blackdome mine, 20.5 m from surface, specimen #06-20.5

Photomicrograph of platey sheafs of marcasite replacing pyrite in a veinlet of quartz cutting andesite. Field of view is 1300 microns across.

PLATE 6.2. No. 1 vein Blackdome mine, 31.8 m from surface, specimen #84-31.8

Photomicrograph of a 400 micron electrum grain on the edge of acanthite-aguilarite. Open-space filling in a quartz vein. Field of view is 1800 microns across.

61

62

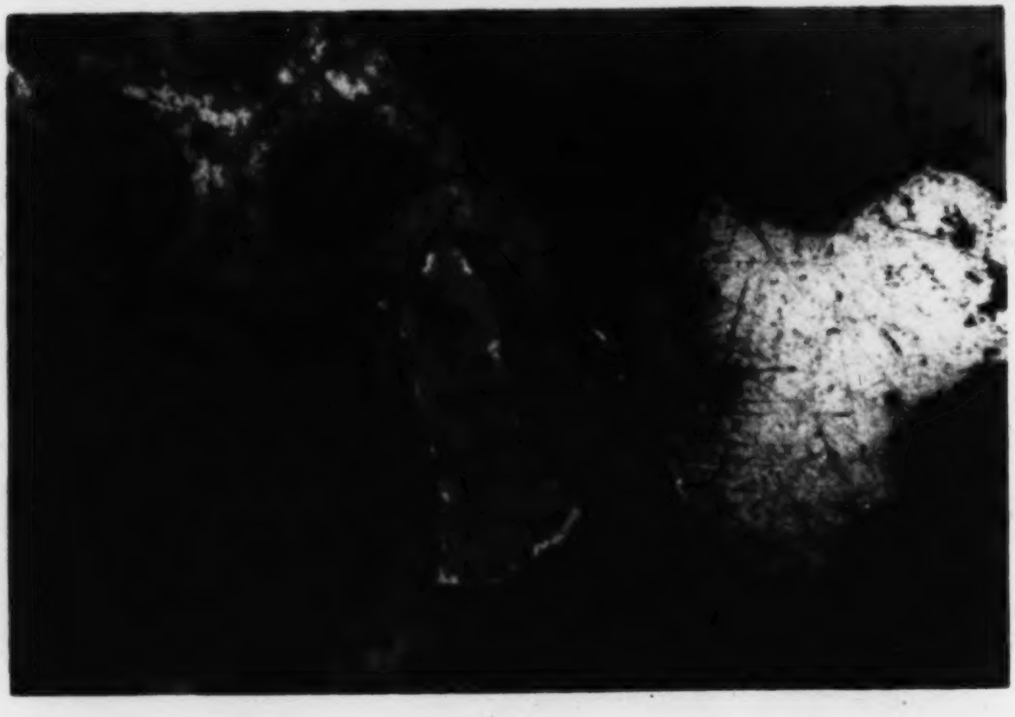

PLATE 6.3. **No. 1 vein Blackdome mine, level 1960, specimen #1960-12080**

Photomicrograph showing a 300 micron inclusion within pyrite. The large inclusion contains galena (blue), chalcopyrite (brownish), Ag-sulfosalt (greenish-gray grunge) and electrum (yellow). Numerous other galena inclusions with a few other Ag-sulfosalt inclusions. Field of view is 1300 microns across.

PLATE 6.4. **No. 1 vein Blackdome mine, 37.5 m from surface, specimen #08-37.5**

Photomicrograph of pyrite showing numerous inclusions of Ag-sulfosalt, ranging from 20-120 microns, and revealing galena inclusions of approximately 20 microns. Field of view is 1800 microns across.

6.3

6.4

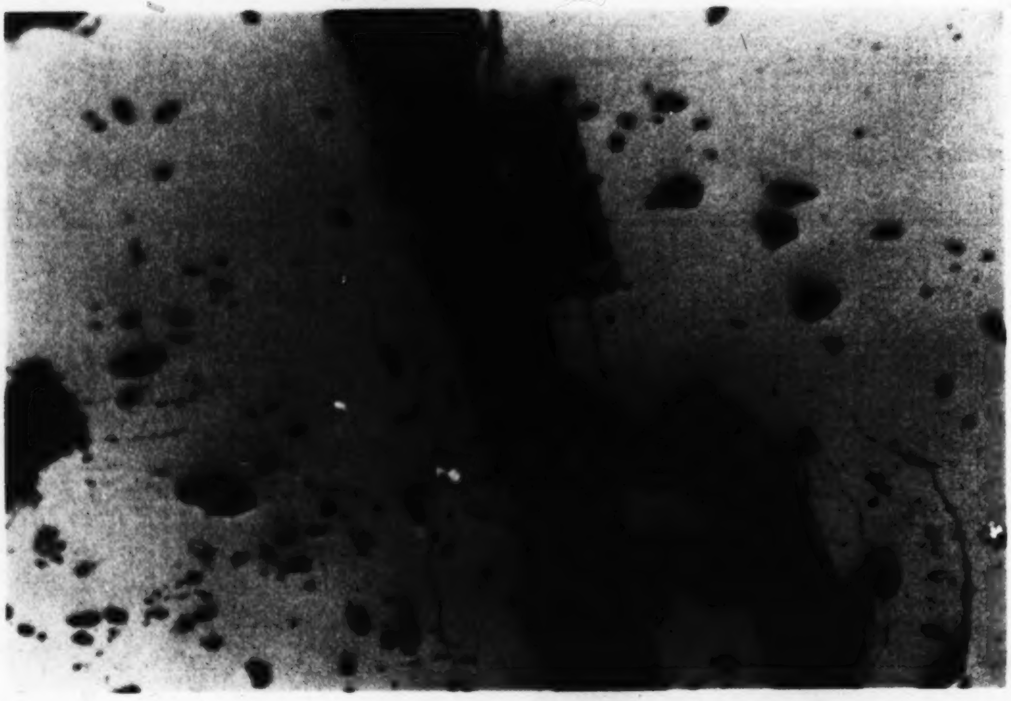

PLATE 6.5 **No. 1 vein Blackdome mine, 32.5 m from surface, specimen #84-32.5**

Photo-micrograph showing a crustified texture of the silver mineralization package. The brightest white material is compositionally almost all Ag, while the light gray material is acanthite and the darker gray material is acanthite-aguilarite composition. Field of view is 1800 microns across.

PLATE 6.6 **No. 1 vein Blackdome mine, level 1960, specimen #1960-12080 m N**

Photo-micrograph of pyrite (creamy white) surrounded by quartz (dark gray). Four electrum grains, ranging in size from 100-150 microns, and numerous Ag-sulfosalt inclusions, ranging in size from 20-150 microns in the pyrite, are most prominent. Field of view is 1800 microns across.

6 5

6 6

PLATE 6.7 No. 1 vein Blackdome mine, level 1970, specimen #1970-12080

Electrum within a package of acanthite and acanthite-aguilarite composition. Core of the open-space filling is acanthite (creamy white) and approaches acanthite-aguilarite composition (darker gray) as the edges are approached. Field of view is 1800 microns across.

PLATE 6.8 No. 1 vein Blackdome mine, level 1965, specimen #1955-12080

Photomicrograph of predominantly subhedral, mosaic-textured quartz with open space filling of electrum (yellow), acanthite (brighter white) and acanthite-aguilarite composition (very light gray). Field of view is 1800 microns across.

6 7

6 8

PLATE 6.9 No. 1 vein Blackdome mine, 22.5 m from surface, specimen #06-22.5

Photomicrograph showing open space filling in quartz. Electrum (yellow) and acanthite (creamy white). Field of view is 1800 microns across.

PLATE 6.10 No. 1 vein Blackdome mine, 15.2 m from surface, specimen #01-15.2

Native gold grain, 25 microns in size, within the field of view. Solid gray material is quartz whilst the remaining white material is acanthite and the grayer material is acanthite-aguilarite. Field of view is 1800 microns across.

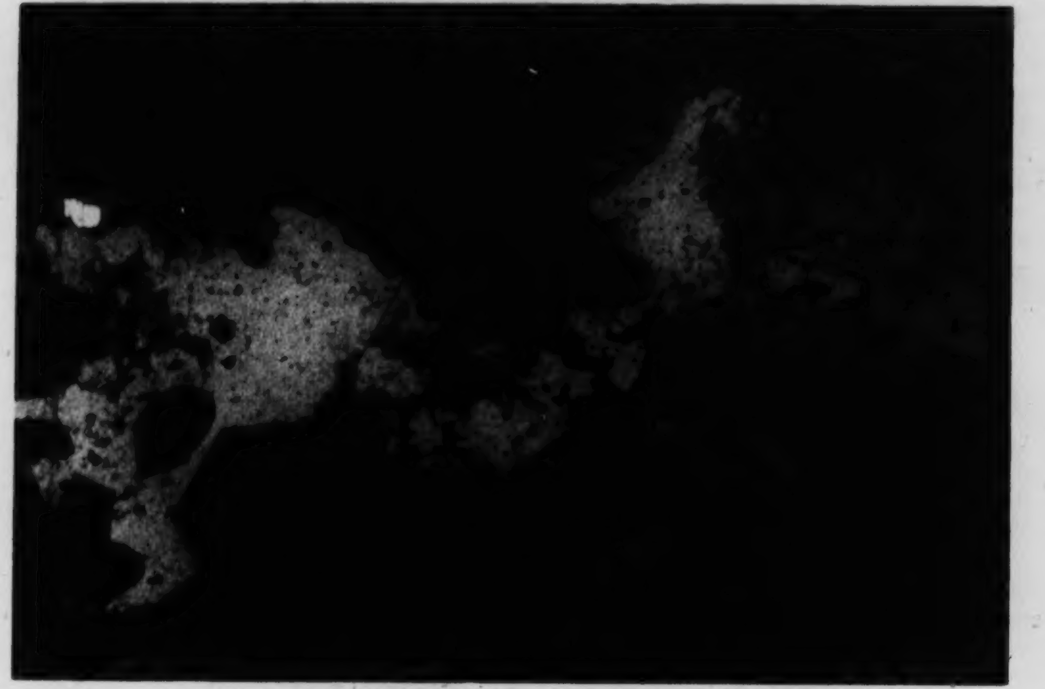

6 9

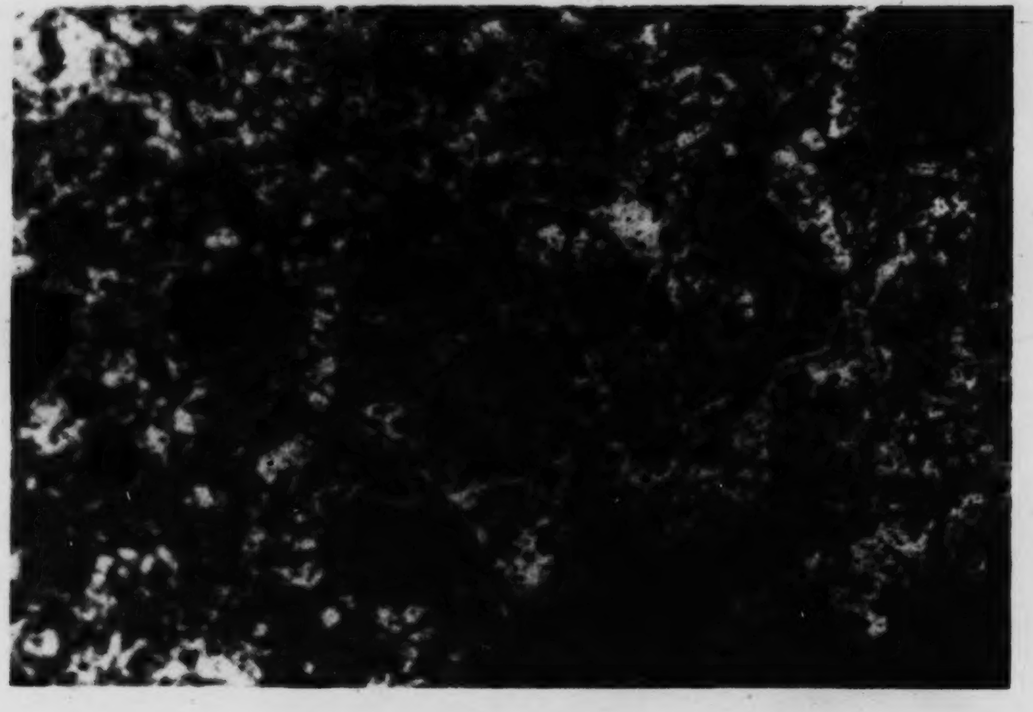6 10